



저작자표시-비영리-변경금지 2.0 대한민국

이용자는 아래의 조건을 따르는 경우에 한하여 자유롭게

- 이 저작물을 복제, 배포, 전송, 전시, 공연 및 방송할 수 있습니다.

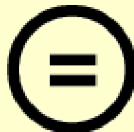
다음과 같은 조건을 따라야 합니다:



저작자표시. 귀하는 원저작자를 표시하여야 합니다.



비영리. 귀하는 이 저작물을 영리 목적으로 이용할 수 없습니다.



변경금지. 귀하는 이 저작물을 개작, 변형 또는 가공할 수 없습니다.

- 귀하는, 이 저작물의 재이용이나 배포의 경우, 이 저작물에 적용된 이용허락조건을 명확하게 나타내어야 합니다.
- 저작권자로부터 별도의 허가를 받으면 이러한 조건들은 적용되지 않습니다.

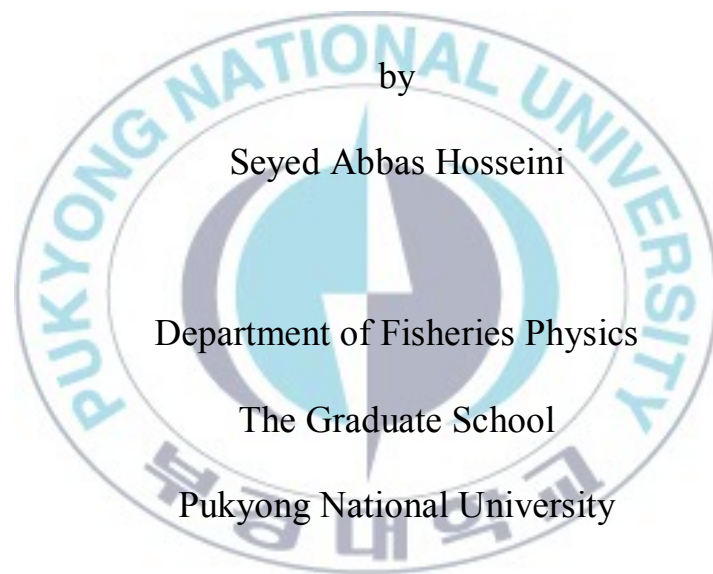
저작권법에 따른 이용자의 권리는 위의 내용에 의하여 영향을 받지 않습니다.

이것은 [이용허락규약\(Legal Code\)](#)을 이해하기 쉽게 요약한 것입니다.

[Disclaimer](#)

Thesis for the Degree of Doctor of Philosophy

**Dynamic simulation of tuna purse seine gear
verified by field experiments**



February 2011

Dynamic simulation of tuna purse seine gear
verified by field experiments

다랑어 선망어구의 동적 거동 시뮬레이션과
현장 실험 검증

Advisor: Prof. Chun Woo Lee

by
Seyed Abbas Hosseini

A thesis submitted in partial fulfillment of the requirements
for the degree of

Doctor of Philosophy

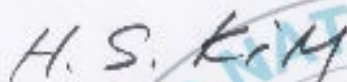
In Department of Fisheries Physics, The graduate School,
Pukyong National University

February 28, 2011

Dynamic simulation of tuna purse seine gear verified by field
experiments

A dissertation
by
Seyed Abbas Hosseini

Approved by:



(Chairman) Prof. Hyung Seok Kim



(Member) Prof. Ju Hoo Lee



(Member) Dr. Hyun Young Kim



(Member) Prof. Chun Woo Lee

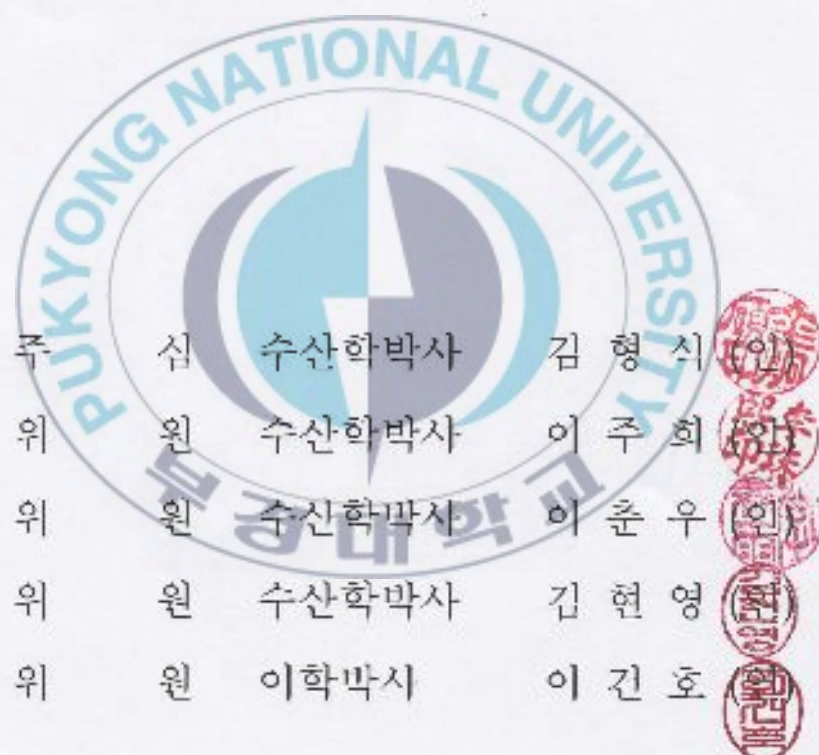


(Member) Dr. Gun Ho Lee

February 28, 2011

아바스의 수산학박사 학위논문을 인준함

2011년 2월 28일



주	심	수산학박사	김 형 식	(인)
위	원	수산학박사	이 주 희	(인)
위	원	수산학박사	이 춘 우	(인)
위	원	수산학박사	김 현 영	(인)
위	원	이학박사	이 건 호	(인)

Acknowledgement

First and foremost, I thank my wife and lovely daughter for their prayer, encouragement and patience. Particularly, I thank my parents, Mr and Mrs. Hosseini who greatly supported me morally during my study. I am deeply indebted to them for their prayer and encouragement.

I thank God who created the opportunity for me to embark on this academic pursuit and has been with me throughout the journey.

My special thanks go to my supervisor, Professor Chun Woo Lee whose encouragement, guidance and support from the initial to the final level enabled me to develop an understanding of the subject. This dissertation would not have been possible without his invaluable comments. I also thank Professor Hyung Seok Kim, Professor Ju Hee Lee, Dr. Gun Ho Lee, Dr. Hyun Young Kim and Dr. Jihoon Lee for their constructive criticism and invaluable comments during the preparation of the dissertation.

I am grateful to the President of Iranian Fisheries Research Organization Dr. Motalebi and the former and present Presidents of the Offshore Fisheries Research Center, Dr. Hafezieh and Engineer Azini for providing me with the facilities and supports for my study.

I thank the president of KTI Company, Iil Dae Seo, Captain Cab Young Kim, and all other the staff who extended their valuable assistance in the preparation and completion of this study.

Other members of my Lab that were helpful in this work include Moo Youl Choe, Dae Ho Song, Myoung Woo Lee, Po Hyoung Lee, He Jung Kim. They provided their assistance on how deal with my study conveniently.

Lastly, I offer my regards and blessings to all of those who supported me in any respect during the completion of the project.

Tables of contents

Acknowledgement-----	i
Tables of contents-----	ii
List of Figures-----	v
List of Tables-----	xi
Abstract-----	xii
Chapter 1. General Introduction-----	1
I. Principle and layout of the purse seine gear-----	1
II. Characteristics of some main components of purse seine gear-----	4
1. Introduction-----	4
2. Length of the purse seine -----	4
3. Hanging of the purse seine and the net depth-----	7
III. Literature review -----	13
Chapter 2. Modelling and numerical method of the fishing gear system-----	18
I. Introduction-----	18
II. Numerical modeling-----	21
1. Netting-----	22
1.1 Internal force-----	24
1.2 External forces-----	25
2. Purse line-----	31
3. Seiner-----	35
III. Numerical method-----	37

Chapter 3. Field experiments and verification of simulation-----	39
I. Introduction-----	39
II. Materials and methods-----	39
1. Hydrodynamic coefficients from model tests-----	39
2. Field experiments-----	44
2.1 Description of setting operation-----	44
2.2 Characteristics of the practical fishing gear-----	47
3. Simulation tools-----	55
III. Results-----	58
1. Field measurement at sinking depth of the purse seine-----	58
2. Simulation performance and verification-----	61
2.1 Visualization of the net shape-----	61
2.2 Sinking depth verification-----	61
IV. Discussion-----	66
Chapter 4. Application of numerical simulation for the gear designing-----	76
I. Advantages of numerical simulation-----	76
II. Effects of mesh size and netting material on the purse seine gear-----	77
1. Introduction-----	77
2. Materials and methods-----	78
3. Results-----	82
III. Effect of sinking weight on the sinking depth-----	90
IV. Effect of pursing speed on the purse seine gear performance-----	93
V. Discussion-----	96

Chapter 5. A preliminary research on behaviour of tuna fish schools to purse seining process-----	101
I. Introduction-----	101
II. Field observation-----	102
III. Discussion-----	107
References-----	111



List of Figures

Fig. 1. Schematic diagram of a purse seine gear with accessories-----	2
Fig. 2. Shape of the purse seine at the instant that setting is terminated. Front view (a), lateral view (b) -----	3
Fig. 3. Position of the center of the lead line of the purse seine and the seiner movement during pursing process -----	3
Fig. 4. Fishing pattern of purse seine for fast-swimming fish (after Fridman, 1973) -----	7
Fig. 5. Dependence of the depth increment of the purse seine during pursing versus hanging coefficient (after Fridman, 1973) -----	10
Fig. 6. Net loaded with a system of vertical forces uniformly distributed along the main line-----	12
Fig. 7. Dependence on function $z(E_1)$ on the hanging coefficient (after Fridman, 1973) -----	12
Fig. 8. Arrangement of the virtual mathematical mesh using mesh grouping method (a) and vector notation of the mesh bar (b) -----	23
Fig. 9. Hydrodynamic forces depending on twine orientation. F_D , drag force; F_L , lift force; V , flow velocity; α , attack angle -----	27
Fig. 10. Schematic diagram showing a webbing of virtual mathematical meshes of 1×1 positioned in two angles to the current velocity. Note how the attack angles of individual triangles to the current produce resultant attack angles for a plane of four triangles, as indicated by α . Solid circles represent knot mass points; hollow circles mesh bar mass points -----	28

Fig. 11. Schematic diagram of knot and its dimension specification -----	30
Fig. 12. Schematic diagram of forces applied to a vertical netting stripe of purse seine during setting (a) modeling of netting (b). W, weighting force; D, water resistance; p_z , weight of netting wall; T, friction force; F_x , the resistance force in the X-axis direction; F_y , the resistance force in the Y-axis direction -----	31
Fig. 13. Schematic diagram of the motion of purse seine during pursing. A strip AB in wide 1 m separated from the seine by two vertical planes (a) forces applied to the netting wall when the force is variable over the depth of the purse seine (b) -----	33
Fig. 14. A cross section of the seine along a part of the purse line (AB) and the diagram of the forces -----	34
Fig. 15. Schematic diagram of the purse line. Purse line runs through the purse rings during the operation (a) modeling of purse line and forces applied to mass points during pursing (b). W, the sinking force; D, the resistance of the mass point; R_r , the resultant force of the D and W forces; T, the tension of the winch -----	34
Fig. 16. Schematic diagram of tension forces on the main lines during pursing: T_{p1} and T_{p2} for purse line ends and T_{f1} and T_{f2} on the float line ends, F_{Ds} the drag of seiner -----	36
Fig. 17. Correlation of attack angle and Reynolds number with the drag coefficient (a) and lift force coefficient as a function of attack angle (b) for a specific model net -----	43
Fig. 18. Schematic diagram of the Alec MDS5 Data Processing and their dimensions -----	46
Fig.19. Current directions for three different layers applied to the simulation as the dominant difference values between the layer 1 (0-20m), layer 2 (20-60m) and layer 3 (60-120m)-----	47

Fig.20. Schematic diagram of the drawing plan of the tuna purse seine gear with the positions of the self-recording depth sensors for the field measurement. Numbers indicate the arrangement of the strips of netting. F denotes first position, M middle position and E end position on the lead line -----	50
Fig.21. Arrangement of floats on the float line of the experimental tuna purse seine gear-----	54
Fig.22. Arrangement of bridle chain of 7/16" and purse rings on the lead line of the experimental tuna purse seine gear. The numbers indicate the length in meter. The number of rings is scaled to around 1:11-----	54
Fig.23. Basic menu bar (up) and initial input windows (right) along with drawing of purse seine gear by the design program-----	56
Fig.24. Basic menu bar (up) and property window (down) along with simulation of purse seine gear by the simulation program -----	57
Fig. 25. The mean sinking depth of the four settings for the three positions of the lead line of the tuna purse seine gear obtained from the field measurements. The positions are similar to those used in Fig. 20 -----	59
Fig.26. Comparison of the sinking depth performance of the tuna purse seine gear at the three positions of the lead line, measured from the experimental operations-----	60
Fig.27. The sequential shape of the simulated purse seine gear from shooting to the end of pursing under a pursing speed of 1.3m-s and current speed velocities of 0.11, 0.40 and 0.38 m-s for the three layers. Note that the seiner pulled into the center of the enclosed net area-----	63

Fig.28. Comparative sinking depth of the lead line of the purse seine from the field operation and the numerical result, simulated under the same condition as in Fig. 27 -----	64
Fig.29. Comparison of sinking depth of the lead line of the purse seine at the three sections from one case of the field operation and the simulation result when simulated with a pursing speed of $1.3 \text{ m}^{-\text{s}}$ and current velocities of 0.2, 0.1 and $0.15 \text{ m}^{-\text{s}}$ for the three successive layers-----	65
Fig. 30. Mesh opening change (elliptical line) during shooting (a) and purse seining process (b) shown by the numerical simulation -----	70
Fig. 31. Schematic diagram of the forces applied to the purse line during pursing process-----	75
Fig.32. Schematic diagram of the new drawings of the tuna purse seine gear with different large-meshed panels and netting material; the different recording positions for sinking depth from the simulation are presented. The solid line indicates the range of the strip nettings changed under the new designs. PA and PES denote polyamide and polyester, respectively; the numbers attached to the characters indicate the different mesh sizes for four new designs-----	81
Fig.33. Comparison of the simulated sinking depth of the lead line for the prototype and the different new designs of the main body of the prototype at the same three positions (for detailed explanation, see text) -----	85
Fig.34. Simulation results for mean sinking speeds by time for the lead line of the purse seine for the prototype and the new designs at the same three positions as in Fig. 33 -----	86

Fig.35. Simulation results for mean sinking speeds by depth of the lead line of the purse seine for prototype and the new designs at the same three positions as in Fig. 33 with the same simulation conditions-----	87
Fig. 36. The trend of tension in the purse line at both ends for the prototype and the new designs, simulated at a pursing speed of $1.3 \text{ m}^{-\text{s}}$ -----	88
Fig.37. Average tension values of the purse line at both ends for the prototype and the new designs simulated by the same situation as in Fig. 36 -----	88
Fig.38. Netting material volume comparison for the prototype and new designs of the net----	89
Fig.39. Comparative analysis of the net construction costs of prototype and new designs of the net-----	89
Fig.40. The simulated sinking depth of the prototype gear rigged with different sinking weights of lead line for the same three positions as in Fig. 20 (for simulation conditions, see text) -----	91
Fig.41. Average sinking speed of the prototype gear rigged with different sinking weights as simulated with conditions in Fig. 42 -----	92
Fig.42. Positions in depth of the central part of the lead line (solid lines with filed symbols) and the float line (dotted lines with empty symbols) of the prototype when simulated under different pursing speeds -----	94
Fig.43. The trend of tension for the prototype gear recorded by the numerical method at different pursing speeds the same as in Fig. 42 -----	94

- Fig.44. Comparison of the average tension values for the prototype gear simulated under the conditions in Fig. 43 -----95
- Fig.45. Mean values of tension S in the purse line, speed of its movement V and power winch N during pursing. Measurements carried out at five times from a typical anchovy purse seine of 400×75 m (after Fridman, 1973) -----99
- Fig.46. Horizontal movement of skipjack as centers of school in purse seine capture situations. School of 30 t escape under the lead line (circle and dotted line) in relation to net setting (circle and solid line) during shooting (a). School of 50 t escape under lead line during pursing (b). Similar numbers refer to the track of the school and vessel simultaneously-----105
- Fig.47. Horizontal movement of skipjack as centers of school in purse seine capture situations when school of 50 t captured (circle and dotted line) in relation to net setting (circle and solid line) during pursing. Similar numbers refer to the track of the school and vessel simultaneously -----106

List of Tables

Table 1. Specifications and dimensions of the netting panels of the typical tuna purse seine gear used for experiments and simulation -----	51
Table 2. Arrangement and dimensions of the float line of the tuna purse seine gear-----	52
Table 3. Specifications of the floats used in the tuna purse seine gear-----	52
Table 4. Specifications of the materials of the lead line used in the experimental tuna purse seine--	53
Table 5. Arrangement and dimensions of the lead line of the tuna purse seine gear (from bunt to the wing part) -----	53
Table 6. Preliminary data on tuna catch of the Korean purse seiner during 2008 and 2010 from Elspeth vessel -----	80
Table 7. Twine parameters for net of different designs used in the simulation method-----	80
Table 8. Comparison of sinking depth of the prototype and the new designs of the purse seine gear with different mesh sizes in the main body for different measurement positions on the lead line as represented in Fig.32-----	84
Table 9: Characteristics of catch of the skipjack school as observed in capture and escape status (the catch size visually approximated by the fishing master) -----	104

Dynamic simulation of tuna purse seine gear verified by field experiments

Seyed Abbas Hosseini

Department of Fisheries Physics, The graduate School,

Pukyong National University

Abstract

The purse seine gear consists mainly of flexible components; nettings, ropes and purse line, which are considered a flexible structure. To describe the dynamic behaviour by the numerical method, mass-spring model, as the mechanics of flexible twine, was applied to the system including three main components: netting, purse line and purse seiner. The equations of motion of the mass points were adapted and integrated by the fourth-order Runge-Kutta method to qualify the displacements of the mass points for the net shape in 3-D under the flow condition. The present study removes the inadequacies of the last paper on mackerel purse seine by refining the calculation model to consider drag coefficient as a function of attack angle and Reynolds number applicable to the setting operation of the purse seine gear. An estimate of the validity of the numerical simulation is made by comparing the measured and calculated values for the sinking depth of the net. Discussions are made on the some adequacies of the modeling method along with suggestions for any improvement. The numerical simulation was used to examine the sinking performance of the different designs in which large meshed-panels and netting materials are used together in the main body section of the netting. The results indicate that the nets with larger mesh panels take more sinking depth with much more pronounced

operational depth at corresponding times of the fishing operation when heavier netting material is used as compared to the prototype net. Moreover, with the new designs, lower tensile forces were exerted on both ends of the pure wire during pursing. A preliminary analysis was made on the swimming behavior of skipjack school in responses to the purse seine operation. The new constructions of the nets with regard to the operational depth represent alternatives that may reduce the potential problem of frequent failed setting of the tuna purse seine gear.



다랑어 선망 어구의 역학적 거동 시뮬레이션과 해상실험에 관한 연구

Seyed Abbas Hosseini

부경대학교 대학원 수산물리학과

요약

선망어구는 주로 망지, 로프, 조임줄과 같은 유연 구조체로 구성된다. 수치해석을 적용함으로써 어구의 역학적 거동을 해석하기 위하여 질량-스프링 모델을 적용하였고, 망지, 조임줄, 선망 어선을 주된 구성요소로 고려하였다. 조류의 영향에 대한 그물 형상의 질점 변위를 3차원으로 구현하고 검증하기 위하여 질점의 운동 방정식과 4차 Runge-Kutta 법을 적용하였다.

다랑어 선망어구에 초점을 둔 본 연구는 레이놀즈수와 영각의 함수로 표현되는 항력계수를 고려한 수치모델을 개선함으로써 고등어 선망에 관한 이전 연구의 부적절성을 제거하였다. 수치 시뮬레이션을 검증하기 위해 그물의 침강수심에 대한 측정값과 계산값을 비교하였다. 고찰에서는 개선된 모델링 방법의 타당성을 다루었다.

기존의 몸그물에 대형 망목으로 이루어진 판넬과 다른 재질의 망지를 사용하여 다른 조건에 대한 그물의 침강 성능을 시뮬레이션하였다. 본 연구 결과, 몸그물 부분에 대형 망목을 사용한 그물에 대하여, 어획시간에 대한 그물의 침강 수심은 기존 재질을 사용한 그물에 비해 비중이 큰 재질의 망지를 사용한 그물에서 더 크게 나타났다. 또한, pursing 이 이루어지는 동안 조임줄의 양 끝단에 더 낮은 장력이 작용하였다. 연구에 앞서, 선망 조업 작업에 대한 가다랑어군의 유영행동 관련 연구가 개략적으로 수행되었다. 적용 수심과 제작 비용에 관한 그물의 새로운 구조개선은 다랑어 선망 어구의 높은 실패율 등 잠재적인 문제를 감소시키기 위한 대안이 될 수 있다.

Chapter 1

General Introduction

I. Principle and layout of the purse seine gear

Purse seine gear catches the pelagic fish, i.e., fish living in the upper water layers far from shores, in the high seas, often in great depths, with a special fishing method of powerful filtering performance. A method of fishing consists of circling the fish school with a high vertical net and of barring their escape from below by the use of a purse line at the bottom is the principle of purse seine.

An ordinary purse seine gear is built up by a large fine-meshed wall of the horizontal netting strips being laced together. The netting mesh sizes and twine diameters are different and are calculated to prevent gilling of the fish and to provide free access of the fish along the net into the bunt. The float line and lead line as main lines are usually different in length. With longer lead line the seine sinks more freely after shooting. The lead line of Japanese purse seine is 5-15% longer than the float line (Iitaka, 1964). As the net is hung, the hanging coefficient gradually increases towards the wing ends; this makes the wings to taper outward and less depth achieved at the ends rather than the middle section. The reduction in the height of the two ends is provided by using a denser hanging ratio on the side lines or by bevelling the outermost sections of the seine. Fig.1 depicts a general configuration of a purse seine gear with some information on the accessories.

The hanging of purse seine changes during the fishing process and the depth of the seine becomes asymmetric at the end of setting operation (Fig. 2). When the seine is pursed and the purse line is bunched up, the depth is increased by bending the lower part of the seine.

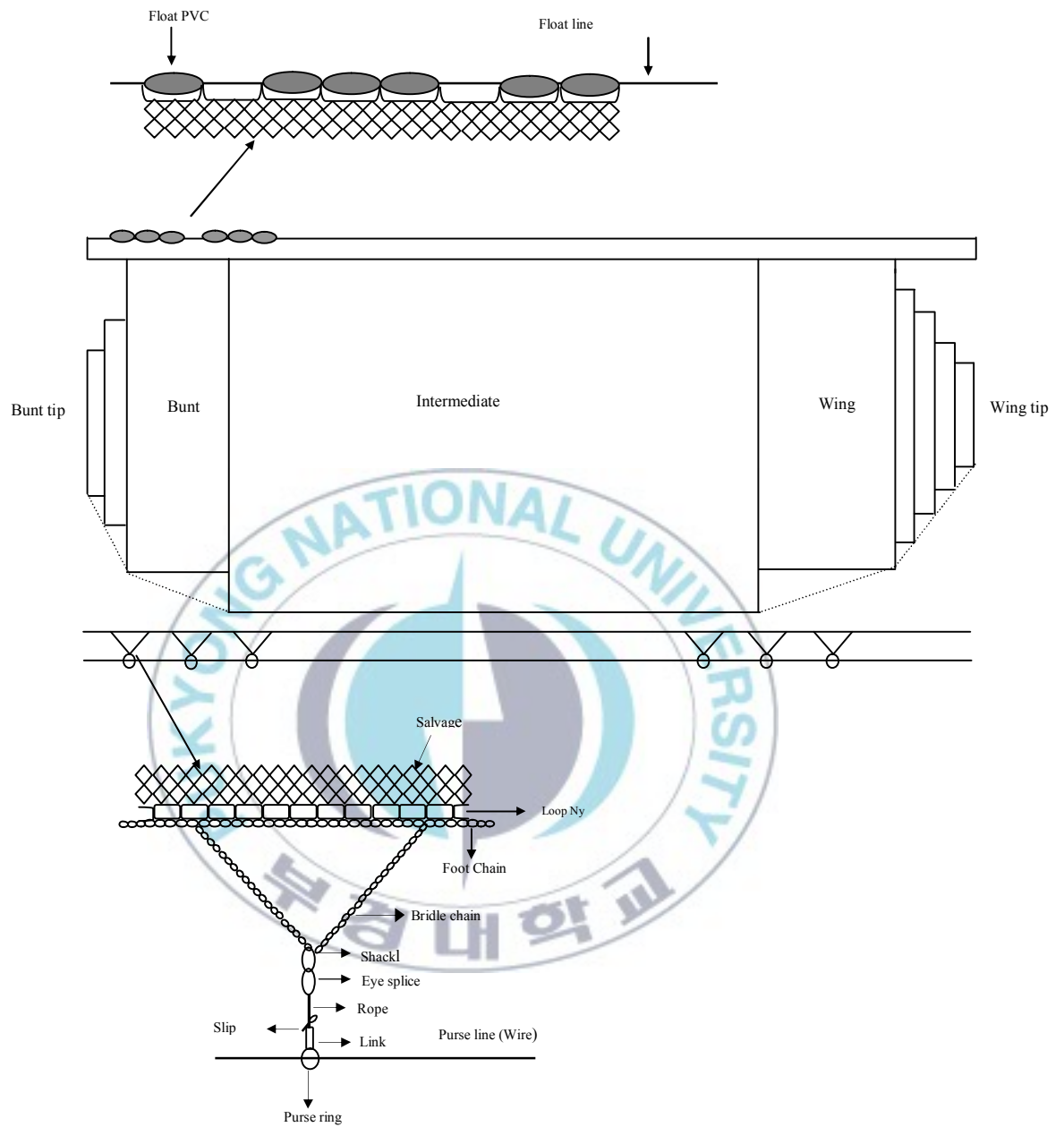


Fig. 1. Schematic diagram of a purse seine gear with accessories.

Fig. 3 shows position of the center of the lead line of the purse seine with seiner movement at different instances of pursing. Note that the seine sank to a depth of 30m before pursing begins.

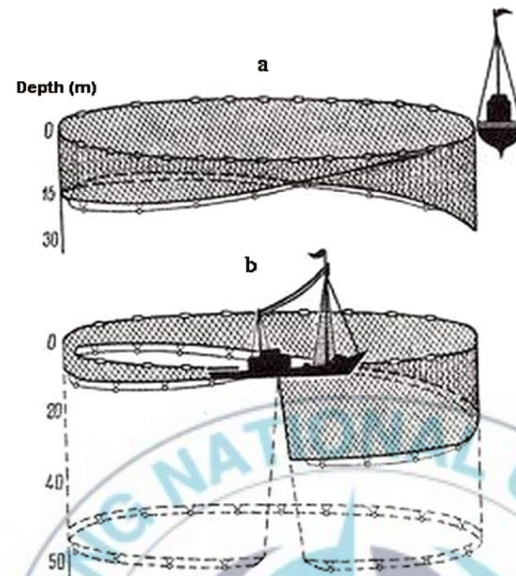


Fig. 2. Shape of the purse seine at the instant that setting is terminated. Front view (a) lateral view (b).

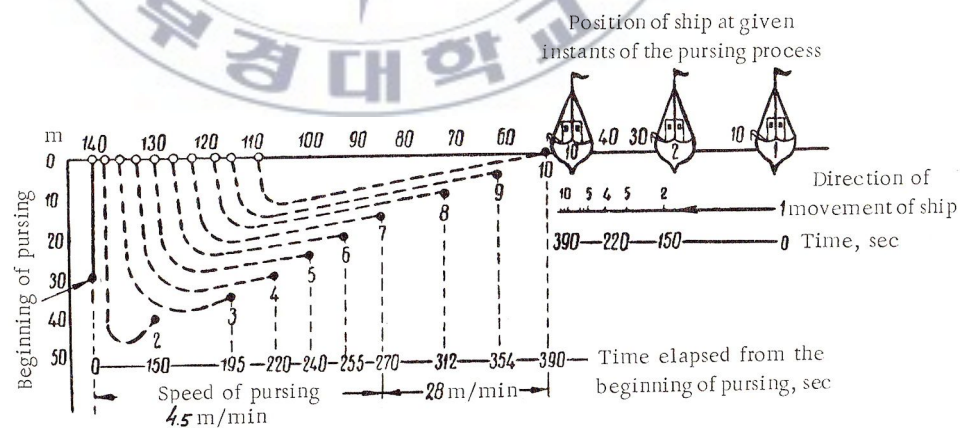


Fig. 3. Position of the center of the lead line of the purse seine and the seiner movement during pursing process.

II. Characteristics of some main components of purse seine gear

1. Introduction

The design of the net is influenced by the configuration of the seine shape and fish behaviour during fishing process. The main points for the successful catch is the sinking speed of the seine, the shape of the net wall during the operation course, the size of the fish school, the distance at which the fish can detect the purse seine wall under the fishing condition. The following issues only deals with the length, hanging ratio and depth features of the purse seine gear because of their great importance to the consequent shape of the gear which in turn affects the success of the fishing operation.

2. Length of the purse seine

The longer and deeper the seine the more probable is seining of a school of a given size. Two basic requirements must be fulfilled when designing of the purse seine: First, the school must be encircled by the seine in a time when the fish encounter with the closed net at the ends. Second, the school must be prevented by escaping under the net.

The efficiency of a purse seine is proportional to the water volume encircled by the net, which is calculated as

$$V = \left(\frac{F}{4\pi} \right) L \quad 1.1$$

From this it can be seen that for a given area of the seine F , the seine volume V is proportional to the length of the seine L . Consequently, it is serviceable to increase the length of the seine in comparison to its depth.

The purse seine length here is estimated based on the theory of purse seining strategy for fast-swimming fish school (Fridman, 1973) as shown in Fig. 4. The pattern is based on the assumption that the net is thrown upon a circle and the school when encountering the seine wall keeps moving parallel to the wall as the seine is being shot and attempts to escape under the lead line. The seine is shot at the point C on a circular course at a minimum distance x from the head of the school in order to intercept the direction of movement of the school at point D with one quarter of the seine is paid out. At the same time the fish school moves from point A to point B.

The distance must be such that the school is not alarmed by its normal swimming behaviour and is not scared away by the seiner and the descending seine when the seiner approaches it. Therefore, the ratio of the speeds of the seiner and fish is

$$\varepsilon = \frac{CD}{AB} = \frac{\pi R}{2\sqrt{2}(R-x-r)} \quad 1.2$$

where R is the radius of the set net and r the radius of the school.

Thus, the setting radius is given as

$$R = \frac{\varepsilon(x+r)}{\varepsilon - \frac{\pi}{2\sqrt{2}}} \quad 1.3$$

While the length of the seine based on the perimeter taken by the circle is

$$L = \frac{2\pi\varepsilon}{\varepsilon - \frac{\pi}{2\sqrt{2}}}(x+r) = b(x+r) \quad 1.4$$

Coefficient b depends on the ratio of the vessel and fish speeds ε during setting. As the ratio increases the coefficient decreases and the minimum seine length is also reduced.

To prevent escaping of the fish school under the lead line, x must be sufficient that the school must encounter a wall deeper than the maximum diving depth, h , when the fish reach the seine.

In this case x must be at least

$$x = v_f t_0 \quad 1.5$$

where t_0 is the time the fish dive to depth h and v_f is the horizontal swimming speed of the fish school. And the length of the seine is formularized simply as

$$L = b(v_f t_0 + r) \quad 1.6$$

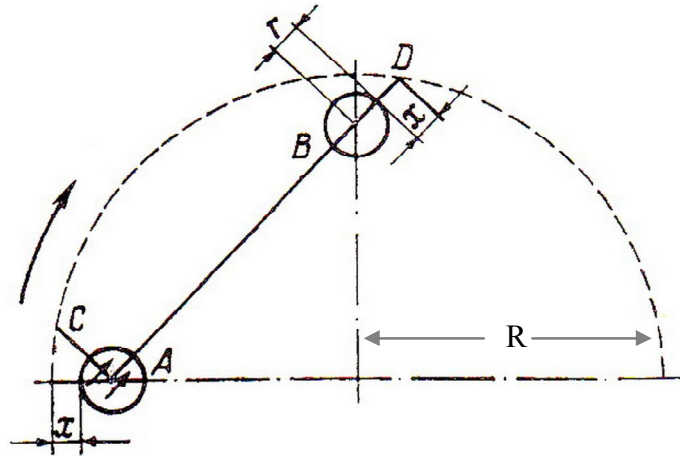


Fig. 4. Fishing pattern of purse seine for fast-swimming fish (after Fridman, 1973).

3. Hanging of the purse seine and the net depth

The proper distribution of tension, the fishing depth, and the shape of the seine in operation are all involved in the value of the hanging coefficient.

The stretched depth of a purse seine H is described in terms of the netting hung on it

$$\begin{aligned} H &= \sqrt{1 - E_1^2} \cdot H_0 \\ &= E_2 \cdot H_0 \end{aligned} \quad 1.7$$

where E_1 and E_2 are, respectively, the primary (horizontal) and secondary (vertical) hanging ratios of the netting and H_0 is the extended depth of the netting. The pressure from the external forces applied to the vertical netting will be increased by a hanging coefficient of 0.5/0.87 (E_1/E_2), causing submersion of the wall considerably (Baranov, 1976).

The depth of a seine is selected by taking into account both the biological features of the target species and the design features of the gear.

The features of fish species can be considered as the depth to which the fish are capable of descending, their maximum swimming depth and their speed at that time. Accordingly, the seine depth can be selected as 20% to 30% deeper than the dominant swimming depth of the fish school (Fridman, 1986). When thermophilic fish species such as tuna are sought, the thermocline depth is the bases on which the seine depth is determined because the fish usually do not dive below it.

To ensure normal operation of the purse seine process and to preserve a desired shape of the net during pursing, its depth-to-length (H/L) must be designed properly. The average and normal ratio of the length of a purse seine to its depth is $L = 10 H$ (Baranov, 1976). According to this, the radius of the setting circle is

$$R = \frac{L}{2\pi} \approx 1.5 H \quad 1.8$$

The height of the purse seine at the wing ends can be reduced by 30% to 50% of the depth of the central part and even less than 2 meter at the running end which is set last (Fridman, 1973).

The depth of seine during pursing H_1 will be (Baranov, 1976)

$$H_1 = H_0 \left(\frac{E'_1 - E_1}{\text{arc sin } E'_1 - \text{arc sin } E_1} \right) \quad 1.9$$

where the angle arc sin is in degree and should be converted as radians.

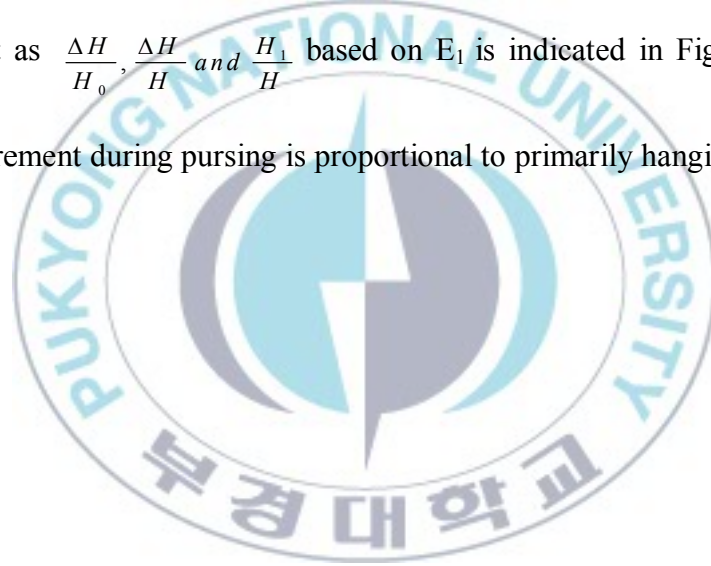
After pursing, when hanging along the lead line E'_1 is equal zero, the depth of the seine is

$$H_1 = H_0 \frac{E_1}{\arcsin E_1} \quad 1.10$$

The increment in the depth during pursing is

$$\Delta H = H_1 - H = H_0 \left(\frac{E_1}{\arcsin E_1} - \sqrt{1 - E_1^2} \right) \quad 1.11$$

Depth increment as $\frac{\Delta H}{H_0}$, $\frac{\Delta H}{H}$ and $\frac{H_1}{H}$ based on E_1 is indicated in Fig. 5. According to this figure, depth increment during pursing is proportional to primarily hanging ratio E_1 .



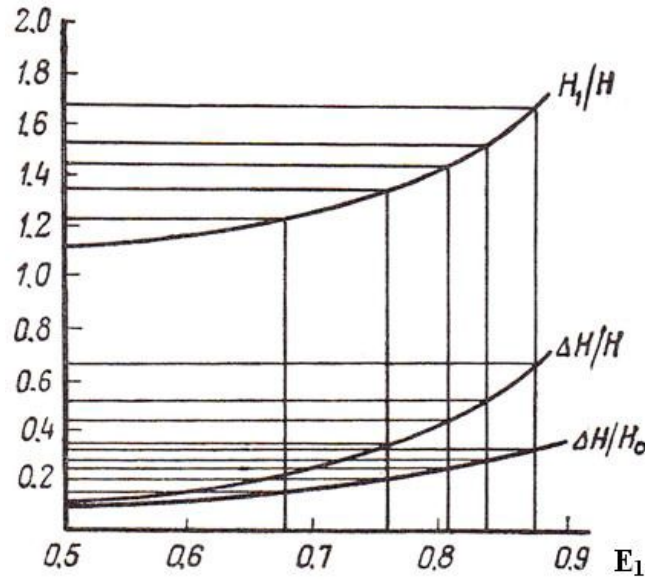


Fig. 5. Dependence of the depth increment of the purse seine during pursing versus hanging coefficient (after Fridman, 1973).

In some cases fish descend to the full depth of the seine and can escape underneath the lead line during pursing process, and it is profitable to use a seine of larger hanging ratio because of attaining more increment in operating depth during pursing.

From the relation $F_{se} = L \cdot H_1$ for the area of the netting after pursing, the nominal area (F_{nom}) of the seine would be (Fridman, 1973)

$$F_{nom} = \frac{\arcsin E_1}{E_1^2} F_{se} \quad 1.12$$

The value of E_1 for which F_{nom} will be minimal is

$$\frac{dF_{nom}}{dE_1} = \frac{\left(E_1^2 \frac{1}{\sqrt{1-E_1^2}} - 2E_1 \arcsin E_1 \right) F_{se}}{E_1^4} = 0 \quad 1.13$$

$$\frac{E_1}{\sqrt{1-E_1^2}} = 2 \arcsin E_1$$

The relation is true for $E_1 = 0.92$. As a practical consequence, when the hanging coefficient lies within the range of $0.707 < E_1 < 0.92$ the seine will cove the maximum water volume at the end of pursing and the net is used in the most efficient way.

The vertical force σ_y (Fig. 6) as an internal stress applied to the netting of the seine during pursing is governed by the condition

$$\sigma_y = PR \frac{1-E_1^2}{E_1^2} = z(E_1)PR \quad 1.14$$

where the p is the external pressure and R the radius of the seine.

As σ_y is determined by the function $z(E_1)$, with increasing E_1 , therefore, the vertical forces (current and pressure of fish) attempting to submerge the float line during the pursing operation is decreased (Fig. 7). However, E_1 should not exceed the range 0.87-0.90, owing to the fact that any further increase in the hanging coefficient ensures an unfavourable shape of seine and a slight elongation of the main lines would stretch the net edges which leads the net to be torn.

As a practical application, hanging ratios of $E_1 = 0.7$ to 0.8 can be used on the float line, provided that there are no special requirement of the seine. In the case of the lead line, the ratios increase to 0.8 to 0.9 (Iitaka, 1971). The higher coefficient on the bottom gives the net an

advantage of not being entangled frequently during pursing due to reduction in the excessive netting.

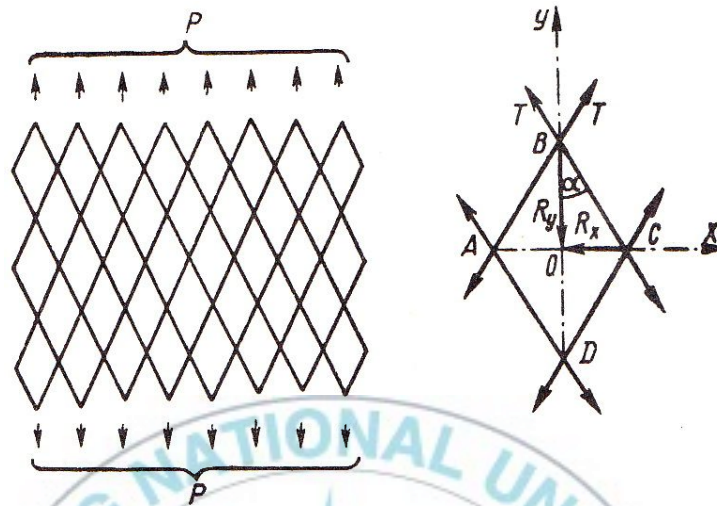


Fig. 6. Net loaded with a system of vertical forces uniformly distributed along the main line.

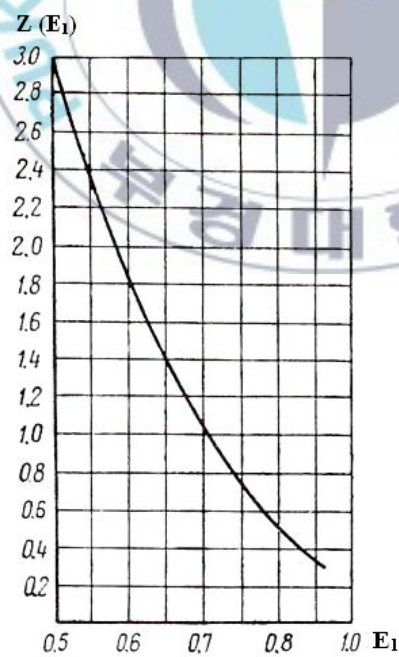


Fig. 7. Dependence on function $z(E_1)$ on the hanging coefficient (after Fridman, 1973).

III. Literature review

The mostly studies to date conducted with purse seine involve experimental and model tests. Iitaka (1964) made research on the mechanical behaviours of the purse seine in action along with some model experiments to introduce the theoretical analysis of sinking movement of the lead line. To verify the results of the 1/250 and 1/10 model experiments in terms of sinking depth a test with the actual fishing gear of a two-boat type sardine and pilchard purse seine was conducted. The results of the sinking speed proved that a 1/10 full-scale model was close to that of actual fishing gear, indicating an appropriate scale for model experiments.

Beltestad (1981) conducted experiments at sea to examine the performance of two types of purse seines made of H-net (Hexagonal meshes) and F-net (rhombic meshes). The H-net was characterized by the dimensions of 643×165m, a type of netting of 17% lighter with the same thickness in all bars, mesh opening of 60mm, a hanging-in ratio (slack or looseness) of 25% and a total sinking weight of 1242 kg. The comparable F-net was constructed as 865× 170m, the same mesh opening as H-net, a hanging -in ratio of 45% and a total of 3000 kg lead. The results were shown some superior achievements for H-net as follows:

- The average sinking speed of H-net was the same as that of F-net.
- Giving time to sink, the H-net achieved maximum stretched depth whereas the F-net only reached about 80-85% of stretched depth.
- Tension in the purse line during pursing for the H-net was about 30% lower than for the seine with F-net.
- The H-net was not pulled down by the fish, even when great catches were taken.
- The H-net kept its original round shape throughout the operation without the float line curling in any way.

The differences in their performance were explained by the lesser water resistance for the H-net as the netting stretches vertically. Also, the H-net can be produced with less material bars, at least saving 25-30% in net materials

Examples of model tests done by the authors include Kim (2000) for the 3-D geometry shape of the net during pursing and hauling operations. In the test, an offshore mackerel purse seine of 1/77 scale model with 12.62 m float line was used. The geometry of the model in time and space during hauling represented as a ratio of shooting diameter or maximum net depth and a ratio of hauling operation time. After shooting, the horizontal shape of the float line changed from a circle to an ellipse during the pursing process. The lateral shape of the purse lines was described as a shape of water drop and the enclosed volume in time described to be changed as a function of sine or polynomial curves.

Kim (2004) made model tests to analysis the sinking resistance for the purse seine with different netting materials and sinkers. In the flume tank under the static water condition, three groups of models of 420cm for the float line and 85 cm for the depth, constructed from the knotless netting materials of polyester (PES), polyamide (PA) and polypropylene (PP), and rigged 25, 45 and 60g, respectively, with the same weight in water, were examined. The results showed a faster sinking speed as 12.2 cm/sec for the PES case, followed by the PA and PP seines.

Kim *et al.* (1995) described the sinking behaviour of the three model purse seines with the same netting characteristics as above. The netting bundle of the PP seine was shown to be on the surface of water, spreading out as the net sinks vertically. Netting bundle of the PES seine lay out in the middle of float line and lead line.

Konagaya (1971a) during model test found that the resistance of lead line had little effect on the sinking speed of the bottom margin of the seine. The seine configuration affected by the sinker weight so that larger sinkers lessened the concavity of the scooping net wall during pursing.

Mechanical properties of a rectangular purse seine in special and ideal conditions were studied in static water condition by a geometric method and their relevant equations (Machii and Nose 1990a, 1992). The shape of purse seine during pursing and hauling stages was mentioned under the equilibrium condition by the factors such as tension and drag as forces (kgw), pursing velocity (m/s) and pursing distance (s).

In contrast to above work, simulating the purse seine process requires the solution of a large time dependent. Because of the complicity of the purse seine system and its laborious work required, little attempts made on the numerical simulation. Despite this, some attention has been paid to the numerical simulation of purse seine to describe the dynamic behaviour of the fishing net shape. To our knowledge, Delmer and Stephens (1981) were the first investigators who developed a constructive numerical formulation for simulation of purse seining process, but no visual results represented due to the lack of availability of capable computer. In their theory, the net behaviour was described by a large macromesh at which the equation of motions integrated by the numerical formulation using the method of lines. And also, the purse line, as a cable, and the seiner, as a rigid body, were considered as the two other components to describe the behaviour of the system.

Kim *et al.* (2007) described the dynamic behavior of the typical mackerel purse seine by mass-spring model. In their study, drag coefficient was treated as a function of the attack angle.

Kim and Park (2009) used some empirical formula to show 3-D geometry of skipjack purse seine during the fishing operation from shooting to the end of pursing. In the model used, the current profile by depth was applied to the fishing gear system from surface to the middle depth at right angle to the flow direction. They used finite element methods, as resultant force vector from current drag, buoyancy and sinking force, and tension of pursing exerted on the webbing wall along with the drift of purse seiner into the circled area for the model.

Many researches have been conducted using mathematical models to describe the dynamic behaviour of the fishing gears, as flexible systems, in three-dimensions. The mathematical description depends on the formulation skills, numerical calculation methods, and the capabilities of the computer programming systems. Hue *et al.* (1995) explained mathematically the trawl system by applying lumped mass method and solved the problem by using Lagrange equation. Niedzwiedz and Hopp (1998) indicated mathematically the trawl system by applying numerous meshes to the system and dynamically simulated it. Bessonneau and Marichal (1998) modeled mass points for important elements such as trawl doors, floats and sinkers and the meshes of the net for the purpose of dynamic simulation.

The numerical bars used to describe dynamically the behaviour of the fishing gear, in which a large numbers of the numerical bars exerted by external forces including drag from current and the weight and buoyancy of the twine (Lader *et al.*, 2003; Lee *et al.*, 2005a; Vincent, 1999). She (1994) calculated tension and configuration of the gill net on the assumption that the net can be considered as a completely flexible thin membrane.

Different numerical methods have been applied to calculate the mathematical models of the fishing gear with the purpose of preserving the accuracy, stability and time efficiency.

Takagi *et al.* (2004), Yun-pong and Yu-cheng (2007) and Lee *et al.* (2008) used the higher orders of Runge-Kutta method to solve the non-linear of the equations of motion to determine the configuration of the fishing gears under studied.

Wan *et al.* (2004) adopted the Newton-Raphson method on the numerical model to find the solution of the problem for gillnet configuration.

Lee *et al.* (2005a, 2005b) and Tsukrov *et al.* (2003) applied the solution technique of Newmark's β method, as an implicit method, to solve the mathematical model of the fishing gear.



Chapter 2

Modelling and numerical method of the fishing gear system

I. Introduction

This chapter deals with describing qualitatively the mechanical behaviour of purse seine gear and adapting quantitatively a simplified model applied to the numerical simulation.

A model is a numerical representation of the mathematics describing the behaviour of an idealized physical system. Simulation based on a computer-aided method can only work with numerical model. The key points related to the modelling and numerical method are

- Modeling procedure
- Accuracy of the model
- Selection of numerical method
- Potential problems

Commercial fishing gear differs considerably from the majority of the engineering equipment due to its special purpose and operating conditions. Fishing gear is a system that possesses unique technical and design parameters. The substantial difference between the fishing gear and rigid engineering structures lies in the requirement for fishing gear to interact with living objects that show self-dependent behaviour. This requirement necessitates special design features of the structure in terms of material, shape, size, and mobility, and these design features depend on the target species. Another considerable difference of fishing gear arises from its mechanical properties, which is flexible, permeable and anisotropic- the same element can acquire various shapes and occupy a different area, depending on the hanging coefficients.

Under the action of even small external loads it suffers a substantial deformability which is different from that of most of the rigid engineering structures.

The change in shape and position of the fishing gear is frequently important for the success of the catch, depending on the ability to acquire the suitable shape allowing for the behaviour of the fish to be caught. Under the action of external forces, the fishing gear, as an ideal elastic shell, changes the shape as the loads on the individual elements are redistributed and concentrated on the frame elements of the gear, as elastic twines. Such a characteristic makes it complex for the beneficial application of the material from which the net is constructed.

The net is subjected to unsteady motion whose magnitude is controlled by the equilibrium of the external static and dynamic forces in terms of velocity and direction during fishing course, so as the solution becomes complicated quantitatively as the complexity in the relationship between the loads and the shape of fishing gear.

Analytical study on the behaviour of a dynamic problem such as purse seine is one of the most difficult problems. The nonuniform motion of the gear, in which all forces are time-dependent, is expressed by the reasons of

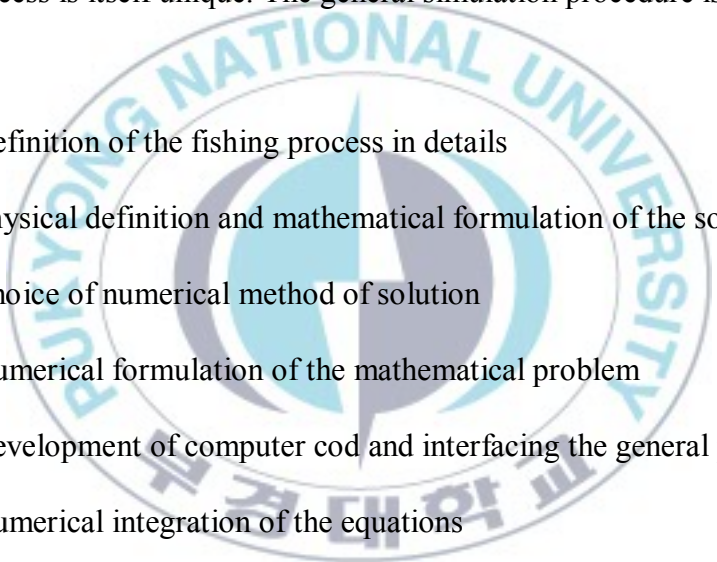
- Hanging and subsequently mesh opening change during the fishing process
- Nonuniform distribution of the external loads over the depth
- The attack angle of net against the water differs during the fishing course

The method of simulation is particularly valuable, because it enables such problems to be solved without complicated mathematical calculations as long as the outcome of the simulation performance can be verified by the experimental data.

The calculation of the shape and the magnitude of the forces by simulation on and in the gear, like other engineering structures, are based on deductions of geometry and mechanics.

On the other hand, mechanics function with the forces act along geometric lines without mass and applied to geometric points possess mass.

An essential prerequisite for successful simulation involves in observing the seining process, breaking the circumstances into separate time and equipment components, applying a simple and easily realized modeling to the various pieces of equipment and recombining the pieces in the proper time series. However, the simulation requires a unique modeling as the purse seining process is itself unique. The general simulation procedure is summarized as

- 
- Definition of the fishing process in details
 - Physical definition and mathematical formulation of the solution (modeling)
 - Choice of numerical method of solution
 - Numerical formulation of the mathematical problem
 - Development of computer code and interfacing the general process
 - Numerical integration of the equations

The purse seining process is a series of different components. A package routine prepared here explains roughly from setting to pursing, as an applied configuration in the numerical method.

The phases of the process considered as separate problems and the qualitative features are as

Phase/Transition	Features
Transition to setting	Skiff boat keeps the bunt end and the net in position
Setting	Net is set upon the circle at a specified rate
Transition to pursing	The purse line at two ends retrieved and connected to the seiner
Pursing	Purse line length lessened orders of magnitude in sequential time

II. Numerical modeling

The purse seine gear consists mainly of flexible components: nettings, ropes and lead line, which are considered a flexible structure. The net itself comprising the main elements of the mechanical system in which the calculation of the shape of the gear and that of the loads subjected to it is based on the mechanics of flexible twine.

For the sake of simplicity in the modeling procedure, three distinct components can be distinguished in the system. In order of importance they include

- Netting
- Purse line
- Seiner

1. Netting

In order to apply mathematical description for calculating the forces acting on the structural materials of the net, we simplified its physical properties, i.e., a mass–spring model was adopted. The model describes a physical system is composed of a finite number of mass points which are interconnected by springs without mass and which offers no resistance to bending.

In applying the mathematical model to the purse seine net to describe the dynamic behaviour of the system, we modeled the net by considering the mesh bars as springs and the knots of the mesh as mass points. Here, the float line is divided into finite elements and the floats tighten on it, as rigid bodies, are considered as mass points.

When all the knots at the mesh and at the bar are considered as mass points, there would be several million mass points for the purse seine net, which requires too long a calculation time for practical simulations. In order to reduce the computational effort for such a flexible structure consists of numerous numbers of mass points, a mesh grouping method is used; approximately 5000 actual meshes are bundled up as a virtual mathematical mesh having the same physical properties such as mass, specific gravity, weight, projected area, hydrodynamic coefficients (Lee *et al.*, 2005a). In fact, the scaling required by the net is unique so that the numerous numbers of the knots and the bars in a net is modeled and scaled in the same manner rather than modeling every bar as can be done in some structures. One additional mass point is also placed between two adjacent knots to represent the bending characteristic of the bar (Fig. 8a).

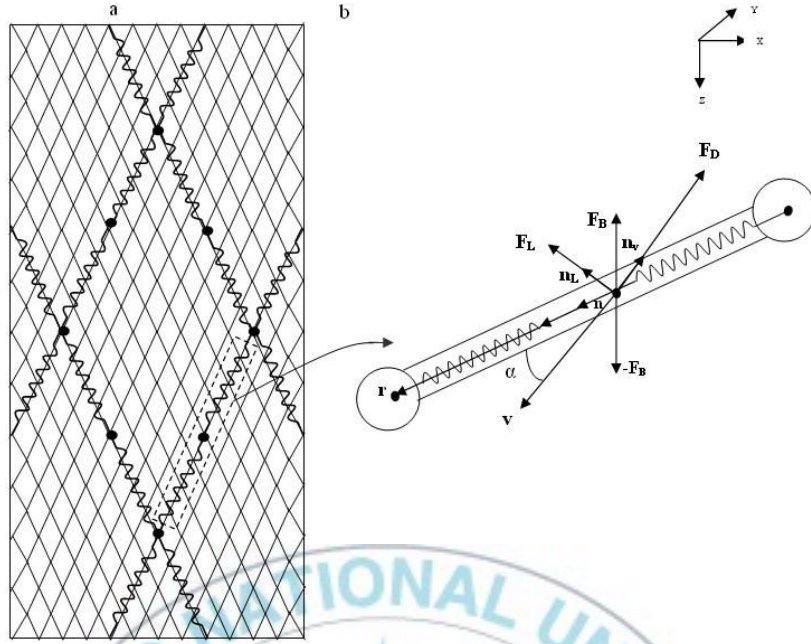


Fig. 8. Arrangement of the virtual mathematical mesh using mesh grouping method (a) and vector notation of the mesh bar (b).

All the external forces applied on the elements are just concentrated on the mass points. The springs are not subjected to the external forces, but offer internal forces resulted from their elasticity properties.

The equation governing the motion of each mass point can be described as follows:

$$(m + \Delta m)\ddot{\mathbf{q}} = \mathbf{F}_{\text{int}} + \mathbf{F}_{\text{ext}} \quad 2.1$$

where m is mass, Δm is the added mass, $\ddot{\mathbf{q}}$ is the acceleration vector, \mathbf{F}_{int} is the internal force acting on the mass point and \mathbf{F}_{ext} is the external force applied to the mass point. The added mass of the mass points is given by

$$\Delta m = \rho_w V_n C_m \quad 2.2$$

where ρ_w is the density of seawater, V_n is the volume of the mass points, and C_m is the added mass coefficient, which is set to be constant at 1.5 because the mass points at knots are assumed to be spheres. For mass points at bars and ropes, C_m is calculated is given by

$$C_m = 1 + \sin \alpha \quad 2.3$$

where α is the angle of attack.

1.1 Internal force

The internal force describes the force exerted on the springs connecting mass points. The force is generally a function of the fractional extension of the material extending along the line of the spring for each element of the bars and ropes, that is, along the vector extending from the knot under consideration to the next knot. In fact, these forces reacted by tension in the netting and are transmitted from the adjacent parts of the net. For this, the knot positions must be known to describe it. The internal force for each mass point due to tension is given as

$$\mathbf{F}_{\text{int}} = -k\mathbf{n}(|\mathbf{r}| - l^0) \quad 2.4$$

where k is the stiffness of the spring for the structural material, \mathbf{n} is the unit vector along the line of the spring; $|\mathbf{r}|$ is the magnitude of the position vector between the neighbouring mass points, and l^0 is the initial length of the spring.

The stiffness for each material is calculated using the following formula

$$K_t = \frac{EA}{l^0} \quad 2.5$$

where E is the Young modulus and A is the effective area of the material. The effective area of the mesh bar, rope and purse line is considered to be 60% of the apparent cross-sectional area, and also the effective modulus of the structures is assumed to be 60% of the original modulus of the materials (Lee *et al.*, 2008).

1. 2 External forces

The most important external forces, F_{ext} , acting on the fishing gear are hydrodynamic forces from the reaction of the water. The external forces limit the sinking rate, the pursing rate, and all other motion of the purse seine gear.

These forces applied to each mass point consists of the drag force (F_D), lift force (F_L), and buoyancy and sinking force (F_B), as follows (see Fig. 8b):

$$\mathbf{F}_{ext} = \mathbf{F}_D + \mathbf{F}_L + \mathbf{F}_B \quad 2.6$$

The total force \mathbf{F} may conveniently be expressed as the resultant of two components i.e., F_D parallel to flow and lift force or sheering force F_L perpendicular to the flow, as shown in Fig. 9. The current is assumed to be steady and uniform so as inertial force is neglected. The drag and lift forces are given in the following formula

$$\mathbf{F}_D = -\frac{1}{2} C_D \rho_w S V^2 \mathbf{n}_V \quad 2.7$$

$$\mathbf{F}_L = \frac{1}{2} C_L \rho_w S V^2 \mathbf{n}_L \quad 2.8$$

where C_D is the drag force coefficient, S is the projected area of the mass point, ρ_w is the density of sea water, V is the magnitude of the resultant velocity vector, \mathbf{n}_V is the unit vector of the resultant velocity vector, C_L is the lift force coefficient, and \mathbf{n}_L is the direction of the lift force and, as a silent factor, is very important in determining the shape of the seine in space as affects on the spread and height of the net.

Lift force at a right angle to the drag, calculated as follows:

$$\mathbf{n}_L = \frac{(\mathbf{V} \times \mathbf{r}) \times \mathbf{V}}{|(\mathbf{V} \times \mathbf{r}) \times \mathbf{V}|} \quad 2.9$$

where \mathbf{V} is the resultant velocity vector. The resultant velocity vector \mathbf{V} is composed of the motion velocity vector of the mass point \mathbf{V}_m and the current velocity vector \mathbf{V}_c , as follows:

$$\mathbf{V} = \mathbf{V}_m - \mathbf{V}_c \quad 2.10$$

The attack angle for each bar is estimated as the angle between the bar and the resultant velocity vector which is obtained as

$$\alpha = \cos^{-1} \left[\frac{\mathbf{V} \cdot \mathbf{r}}{|\mathbf{V}| \cdot |\mathbf{r}|} \right] \quad 2.11$$

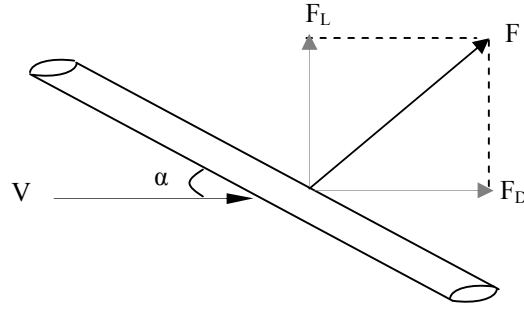


Fig. 9. Hydrodynamic forces depending on twine orientation. F_D , drag force; F_L , lift force; V , flow velocity; α , attack angle.

In the numerical modeling, the attack angle is considered as a resultant value for a single small plane comprising four triangles derived from the attack angle of the individual triangles (Fig. 10). This method of attack angle reflects adequately the real situation of the netting strips subjected to the water current during the purse seine process. The angle for ropes is treated the same as the single mesh bar (see Fig. 8b).

The buoyancy and sinking force, F_B , can be written as follows:

$$F_B = (\rho_i - \rho_w)V_n g \quad 2.12$$

where ρ_i is the density of the material, g is the gravitational acceleration and V_n is the volume of the material.

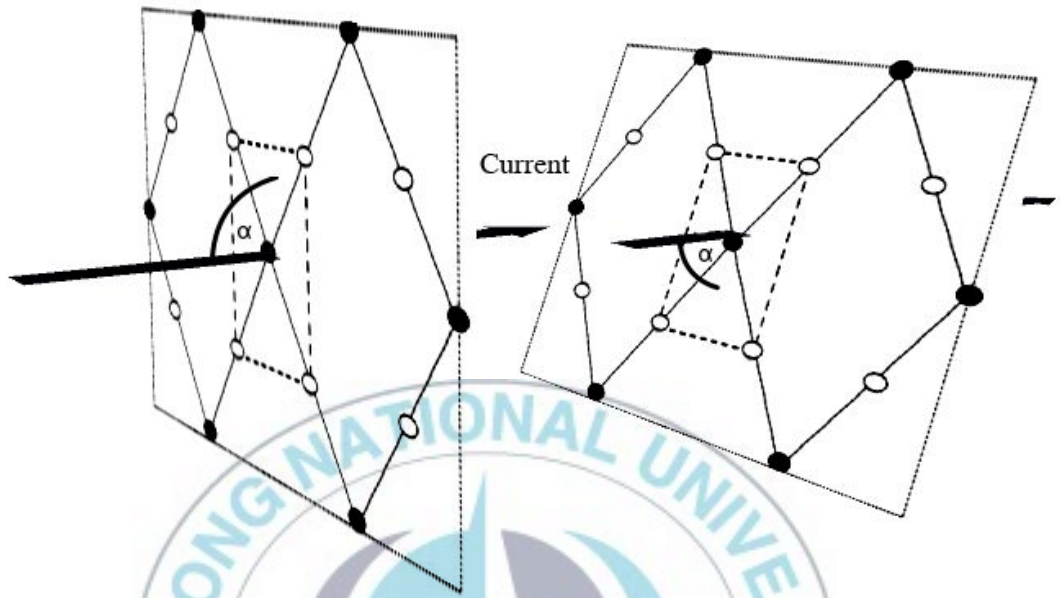


Fig. 10. Schematic diagram showing a webbing of virtual mathematical meshes of 1×1 positioned in two angles to the current velocity. Note how the attack angles of individual triangles to the current produce resultant attack angles for a plane of four triangles, as indicated by α . Solid circles represent knot mass points; hollow circles mesh bar mass points.

In the model, the diameter of the mesh knot d , as a sphere, needs to reflect the physical properties of the net. The effect of knots of the net resistance is small and comparable to the effect of the points of intersection of the twines in knotless nets (Baranov, 1976). To assess the effect of the mesh knots on the weight forces acting on the net, we consider the knot as a twine over which a second twine is wound (Fig. 11). The volume of the knot can be considered equal to the volume of a sphere with diameter of $3d$, three times the diameter of twine, and its

effective volume is considered to be $9d^3$ (Fridman, 1973). For the cylindrical structure like bars and ropes the volume is given as

$$V_N = \frac{1}{4}\pi ld^2 \quad 2.13$$

where l is the length of the mesh bar and d is the diameter of the structure.

With regard to projected area of a mass point, the area for the bar knot and mesh knot, due to the various physical structures, can be estimated differently to give the total projected area (TPA) of the net as

$$TPA = \sum_{i=1}^j (4d_i l_i) + \Upsilon \sum_{i=1}^j d_i^2 \quad 2.14$$

where j is the number of meshes and Υ is knot constant. As each knot length is $3d$, Υ is considered at 9 for the knotted netting. For the knotless netting, the area intersected by the netting is taken as the square of the netting thickness; therefore, the knot constant is considered 1.

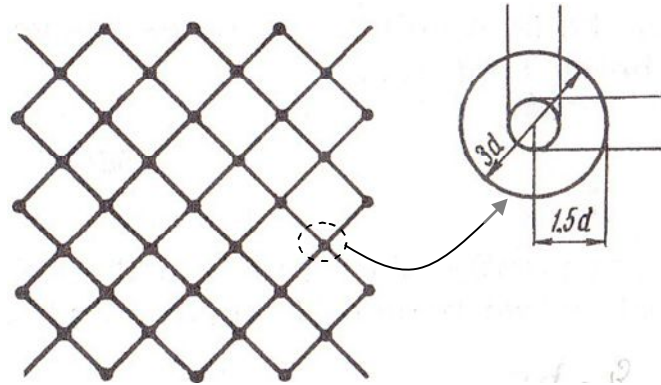


Fig. 11. Schematic diagram of knot and its dimension specification.

As to the setting process, the schematic diagram of the forces acting on a vertical netting strip is shown in Fig. 12, in which the sinking speed of the lead line is variable. When the seine is submerged and the area of the unfolding netting gradually increases the sinking speed becomes progressively smaller because of increasing in resistance force D from the water. Ideally, the resistance must not exceed the constant sinking forces of the sinkers. When the net is shot, the netting strip gradually begins to sink due to the sinking force from the total ballast w and the weight of the netting wall itself P_z . During sinking the net, the friction force T from netting bundle hinders the opening of the net.

To make a simple mathematical model of these forces, we conveniently apply the external forces to the each mass point as shown in Fig. 12b. During shooting, the resistance force of the mass point, D , acts in the opposite direction of the sinking force W and can be resolved into two components: F_x , the resistance force in the X-axis direction; F_y , the resistance force in the Y-axis direction.

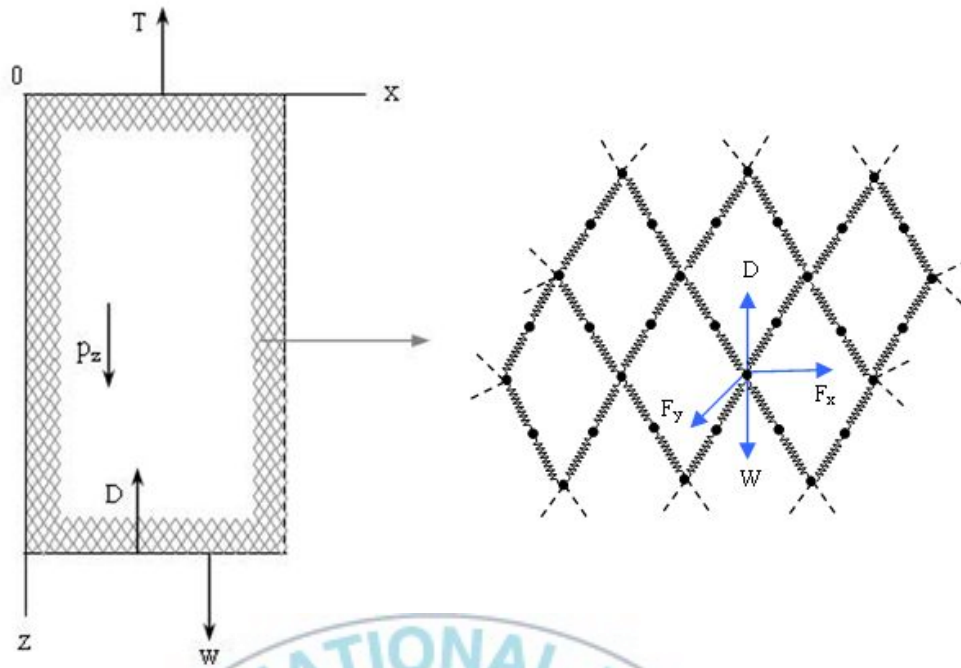


Fig. 12. Schematic diagram of forces applied to a vertical netting stripe of purse seine during setting (a) and modeling of netting (b). w , weighting force; D , water resistance; p_z , weight of netting wall; T , friction force; F_x , the resistance force in the X-axis direction; F_y , the resistance force in the Y-axis direction.

2. Purse line

The shape of the seine walls during the pursing process influenced by the movement of the purse line. Fig. 13 shows a simplified scheme of design of motion of the seine during pursing. A nonuniform distribution of the external forces over the depth of the net is shown by a strip AB in 1 m wide which separated from the seine. A cross section of the seine along the purse line is shown in Fig.14. In the figure, the dashed line AB represents a part of the purse line. The tensile forces are equilibrated with the resistance forces of the purse seine and the friction

of the line against the rings. The motion of the purse line is forced to follow the net in the direction perpendicular to the length of the purse line but free to move in direction parallel to its length due to presence of rings (Fig. 15a). In other words, the purse line is tied to the net transversely but free longitudinally. The constraining force between the purse line and ring is unknown and must be a result of the calculation. There is also free hanging purse line between the net and a specified point on the purse line, in which the force on the net representing rings moving on the purse line is zero.

To determine analytically the forces during pursing, we consider a simple scheme of the design, independent the complicated scheme explained above. The purse line is assumed to be totally flexible that undergoes fractional extension. Here, the purse line is modeled by the mass points imposed on it. These mass points are extracted from the physical properties of lead line, purse rings and bridle. The external forces applied to the mass points are: the sinking force W , the resistance of the mass point D resulted from the drag force F_D and lift force F_L , the resultant force R_r derived from the D and W forces, and the tension of the winch T (Fig. 15b). The internal forces exerted on the mass points are derived from the elasticity characteristics of the pure line, which are calculated from the same equation as Eq. 2.4. In the simulation, when the retrieval speed from the velocity of the winch winding is applied and the length of the purse line changes orders of magnitude from one time to another time, the space between the mass points are shortened owing to the displacement of the mass point i in position. The radial velocity v_1 of the space is defined as (Fridman, 1973)

$$V_1 = \frac{v_2}{\pi} \quad 2.15$$

where v_2 is the hauling speed (at one end) of the purse line.

With this modeling, at the beginning of the pursing the length of the purse line intersects with the net over a length of purse line greater than two thousands meters. At the time when the pursing is completed, the length of the purse line intersects with the net is around 10 meters.

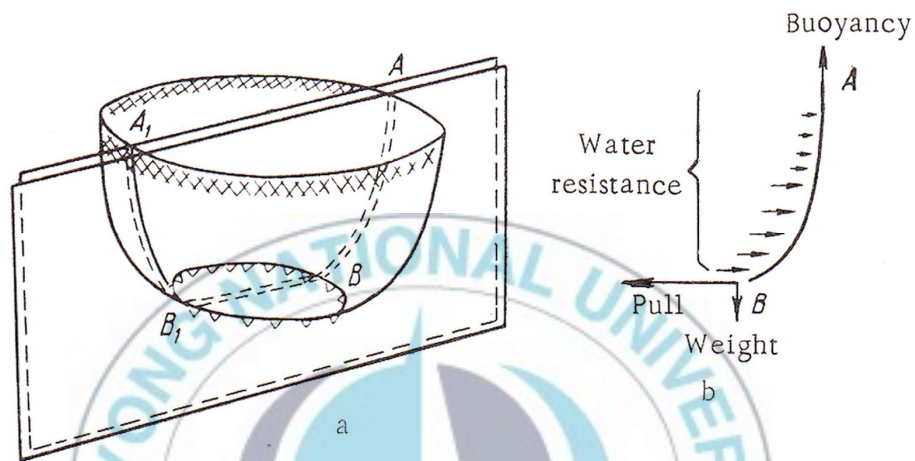


Fig. 13. Schematic diagram of the motion of purse seine during pursing. A strip AB in wide 1 m separated from the seine by two vertical planes (a) forces applied to the netting wall when the force is variable over the depth of the purse seine (b).

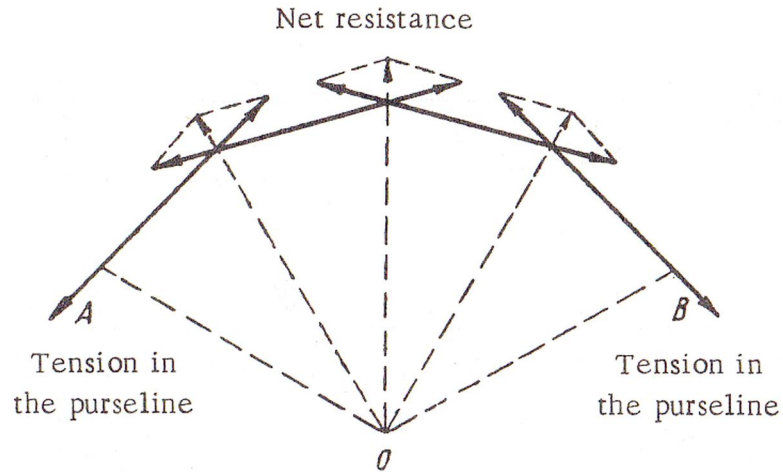


Fig. 14. A cross section of the seine along a part of the purse line (AB) and the diagram of the forces.

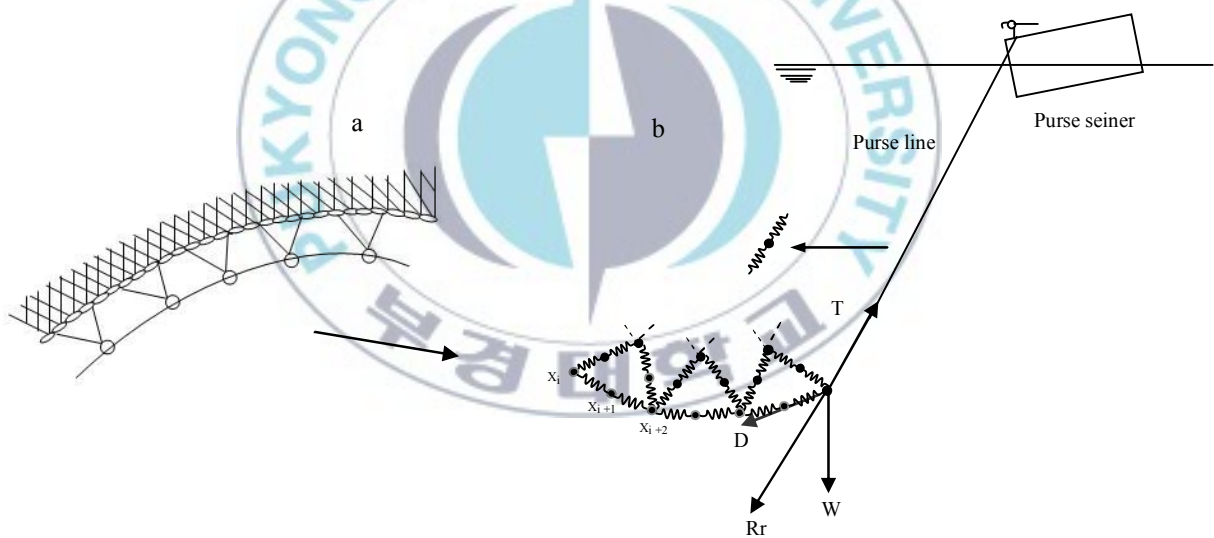


Fig. 15. Schematic diagram of the purse line. Purse line runs through the purse rings during the operation (a) and modeling of purse line and forces applied to mass points during pursing (b). W , the sinking force; D , the resistance of the mass point; R_r , the resultant force of the D and W forces; T , the tension of the winch.

3. Seiner

Two phases can be distinguished for the seiner motion. First one is high speed when the net is being set and second is the low speed that follows. In the first phase, the seiner is free to manoeuvre as long as it closes the path at the skiff boat when the net is pulled off the seiner. Inversely, in the second phase the seiner is linked to the net and no longer free to manoeuvre. During the first phase, the net is constrained to move with seiner; its setting speed is that of the seiner, and the route of the seiner is prescribed because its motion is not significantly influenced by the net. The route is predetermined by a forward speed and specified angular velocity, which should be in accordance with the speed and manoeuvrability of the vessel.

During the second phase the motions of the seiner and the net is closely tied, so as the shape of the net and the closing time are determined during the phase.

During the second phase the motion of the seiner is governed by the four forces from the tensions of purse line and float line ends, and also from the drag of seiner as shown schematically in Fig. 16. The tensions are occurred from the netting resistance which are propagated to the main lines.

To simplify the formulation of the drag of the seiner during the second phase, as a rigid body, the drag force is calculated on the assumption that the seiner speed is negligible in comparison to the current speed and it moves just along its broadside to the cross current during pursing process. The drag of the seiner equivalent to current force is calculated as

$$\mathbf{F}_{Ds} = \frac{1}{2} C_{Ds} \rho_w A_s \mathbf{V}^2 \quad 2.16$$

where C_{Ds} is the drag coefficient of the seiner. Because the seiner is considered as a circular cylinder, the coefficient is taken to be 1.2 with due consideration of the lateral movement. A_s is

the lateral area of the submerged part of the seiner, equals 595 m^2 (its length is of 85 m with a draft of 7 m), and V is the velocity.

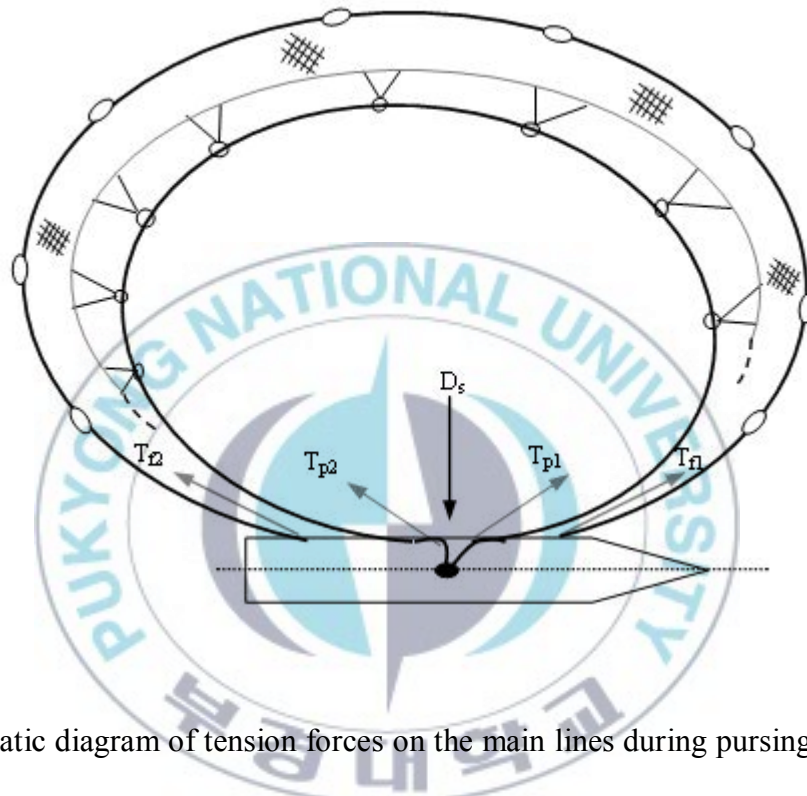


Fig. 16. Schematic diagram of tension forces on the main lines during pursing: T_{p1} and T_{p2} for purse line ends and T_{f1} and T_{f2} for the float line ends, F_{Ds} the drag of seiner.

III. Numerical method

Modeling procedure gives a set of time dependent coupled differential equations. A numerical method chosen to integrate these equations and the method depends on the characteristics of the equations. The salient feature of the set of the differential equations describing the pursing process is that they are stiff. The feature is described by the fact that certain things, such as a change in the extension of a purse line or the net twine, would relax in a very short time. However, the motion of the purse line and the net are rather smooth and continuous and take place over a long time. Another feature of the problem is that the quantitative unknowns such as the knot positions and velocities do not interact with many other quantities directly. For example, most knots directly influence the four surrounding knots only and influence distant knots indirectly.

The numerical method for solving the equations describing the fishing course keeps record of how one part of the component acts on another part, that is, the model realizes the effect moving one part has on another parts. An excellent example of this incidence is that the purse line acts on a mass point, which acts on the part of the net, which acts on another part of the net, etc. In general, any part of the net is coupled directly to any other parts of the net.

The net as described is a well-defined entity with bars of their own properties. The purse line is considered as a flexible structure attached to the netting with the purse line changing orders of magnitude in sequential time in the problem.

Substituting the internal and external forces into the Eq. 2.1, we obtain a second-order nonlinear ordinary differential equation in the time domain as follows:

$$M\ddot{\mathbf{q}}(t) = \mathbf{F}_{\text{int}}(t) + \mathbf{F}_D(t) + \mathbf{F}_L(t) + \mathbf{F}_B(t) \quad 2.17$$

where M is mass point including added mass and $\ddot{\mathbf{q}}(t)$ is the acceleration.

We integrated the equations of motion adopted for each mass point, numerically given an initial net configuration. To solve the equation numerically, we used the fourth-order Runge-Kutta method (Steven and Raymond, 1998).

Eq. 2.17 can be transferred into first-order differential equations,

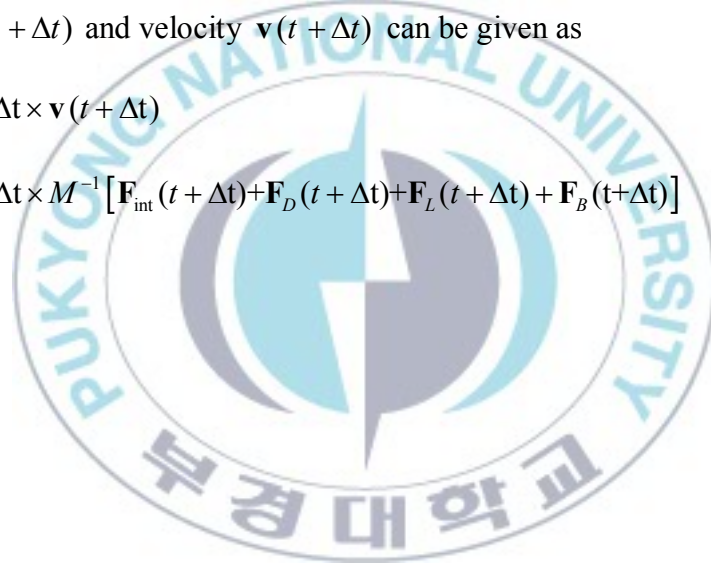
$$\dot{\mathbf{q}}(t) = \mathbf{v}_m(t) \quad 2.18$$

$$\dot{\mathbf{v}}_m(t) = M^{-1} [\mathbf{F}_{\text{int}}(t) + \mathbf{F}_D(t) + \mathbf{F}_L(t) + \mathbf{F}_B(t)] \quad 2.19$$

The position $\mathbf{q}(t + \Delta t)$ and velocity $\mathbf{v}(t + \Delta t)$ can be given as

$$\mathbf{q}(t + \Delta t) = \mathbf{q}(t) + \Delta t \times \mathbf{v}(t + \Delta t) \quad 2.20$$

$$\mathbf{v}(t + \Delta t) = \mathbf{v}(t) + \Delta t \times M^{-1} [\mathbf{F}_{\text{int}}(t + \Delta t) + \mathbf{F}_D(t + \Delta t) + \mathbf{F}_L(t + \Delta t) + \mathbf{F}_B(t + \Delta t)] \quad 2.21$$



Chapter 3

Field experiments and verification of simulation

I. Introduction

During fishing process, the three dimensional geometry of the purse seine gear can be presented by some variables. At the hauling process, it can be done by the factors such as the ratio of shooting diameter of float line or sinking net depth from the lead line to the ratio of the operation time. Sinking depth of lead line according to the elapsed time of the operation can be used as a pattern to make confirmation with the numerical simulation, as used in the study. In the following chapter, the context deals with describing the dynamic behaviour of purse seine shape through numerical simulation and its consistent with the experimental results.

II. Materials and methods

1. Hydrodynamic coefficients from model tests

The non-dimensional coefficients reveals the influence of the physical properties of the netting, such as twine size, mesh size, material, hanging ratio, etc., subjected to the magnitude of the hydrodynamic forces acting on the netting. The only prerequisite in using these coefficients is that the physical condition of design interest must be similar to that of hydrodynamic coefficients measured. In other words, the resistance coefficients are given as a function of the shape of the body, orientation of the body with respect to the direction of motion and the character of the flow past the given body.

Numerous studies have been conducted for hydrodynamic coefficients (Lee *et al.*, 2005a; Kim, 1995; Imai, 1986; Paschen and Winkel, 2002), but no versatile method was adopted for determining the hydrodynamic coefficient due to the involvement of numerous factors.

Likewise, because of difficulties in encoding the program, studies rarely allow two decisive parameters in the drag coefficient when making a simulation. In a more realistic situation, the values of the drag coefficient are suitable for calculating the resistance of the netting system moving in the fluid, provided the Reynolds number is satisfied.

The Reynolds number is a dimensionless number that gives a measure of the ratio of the

inertial forces $\frac{\rho V^2}{L}$ to viscous forces $\frac{\mu V}{L^2}$ as follows:

$$\text{Re} = \frac{VL}{\nu} \quad 3.1$$

where V is the relative velocity (m/s) between the fluid and the body, L is a characteristic linear dimension (m) of the body as selected or agreed for the given series of experiments in which it is considered as diameter d for spheres and cylinders, and ν is the kinematic viscosity of the fluid medium as $\nu = \frac{\mu}{\rho}$ m²/sec, which is given to be 1.01×10^{-6} .

The Reynolds numbers usually arise when performing analysis of fluid dynamic problems and as such can be used to determine dynamic similitude between different experimental cases. They are also used to characterize different flow regimes, such as laminar or turbulent flow. Laminar flow occurs at low Reynolds numbers in which viscous force are dominant, while turbulent flow occurs at high Reynolds numbers and is determined by the inertial forces.

In the previous paper on the mackerel purse seine (Kim *et al.*, 2007), the drag coefficient of the single bars was given only as a function of the attack angle. In present study, experiments conducted by the model tests at the flume tank in order to analyze and compare the

hydrodynamic coefficients. To do this, the results from the three kinds of netting planes composing diameters of 1.45, 4.35 and 7.25mm each with a hanging ratio of 80% were used as a basis data for the analysis. The model tests carried out in a situation in which they were subjected to the current velocities of 0.3 to 0.8 m/s at an interval of 0.1 m/s, and also to the attack angle of 0 to 90 degree at an interval of 10 degree.

Fig. 17 depicts the correlation of attack angle and Reynolds number with the drag coefficient and the lift force coefficient as a function of attack angle used in the study. For the drag coefficient, the values fall within the range of approximately 0.6 to 1.1.

As can be seen from the figure, within the Reynolds numbers range of 430 to 4700, at a specific value of the dimensionless number the drag coefficient C_D increased from the attack angle of 0 to 90 degree, but the increasing trend was higher for the lower values of Reynolds numbers, which is in agreement to the basic idea. On the other hand, the figure also shows the dependence of C_D on the Reynolds number; the coefficient decreases as the Reynolds number increases and it reaches at slightly states for the highest values of the Reynolds number when the comparison is made at a given value of the attack angle. For the nets positioned parallel to the velocity vector, at 0 angle, the dependency of C_D on the Reynolds number is slight.

With regard to the lift force coefficient, there is an direct relationship between the coefficient and the attack angle until the angle of 30 degree, but the trend shows a reduction for the angles over 40 degree.

Because the knot mass point, floats and sinkers modeled as spheres, no lift force is exerted and the drag coefficient is set at 1.5 (Fredheim and Faltinsen, 2003).

The equations describing the relationships given in Fig .17 for C_L and C_D are

$$C_D = (-1.3894 \sin \alpha^2 + 3.2198 \sin \alpha + 1.0896) 1.7887 \text{Re}^{-0.2591} \quad 3.2$$

$$CL = -0.6696 \sin \alpha^3 + 0.1323 \sin \alpha^2 + 0.5325 \sin \alpha + 0.0089 \quad 3.3$$

As it follows from the equation, the drag coefficient is treated as a function of two variants: Reynolds number, based on the diameter of single bar as the length scale, and the attack angle i.e., $C_D = f(\text{Re}, \alpha)$. For the lift force coefficient, the equation is only described by the attack angle.



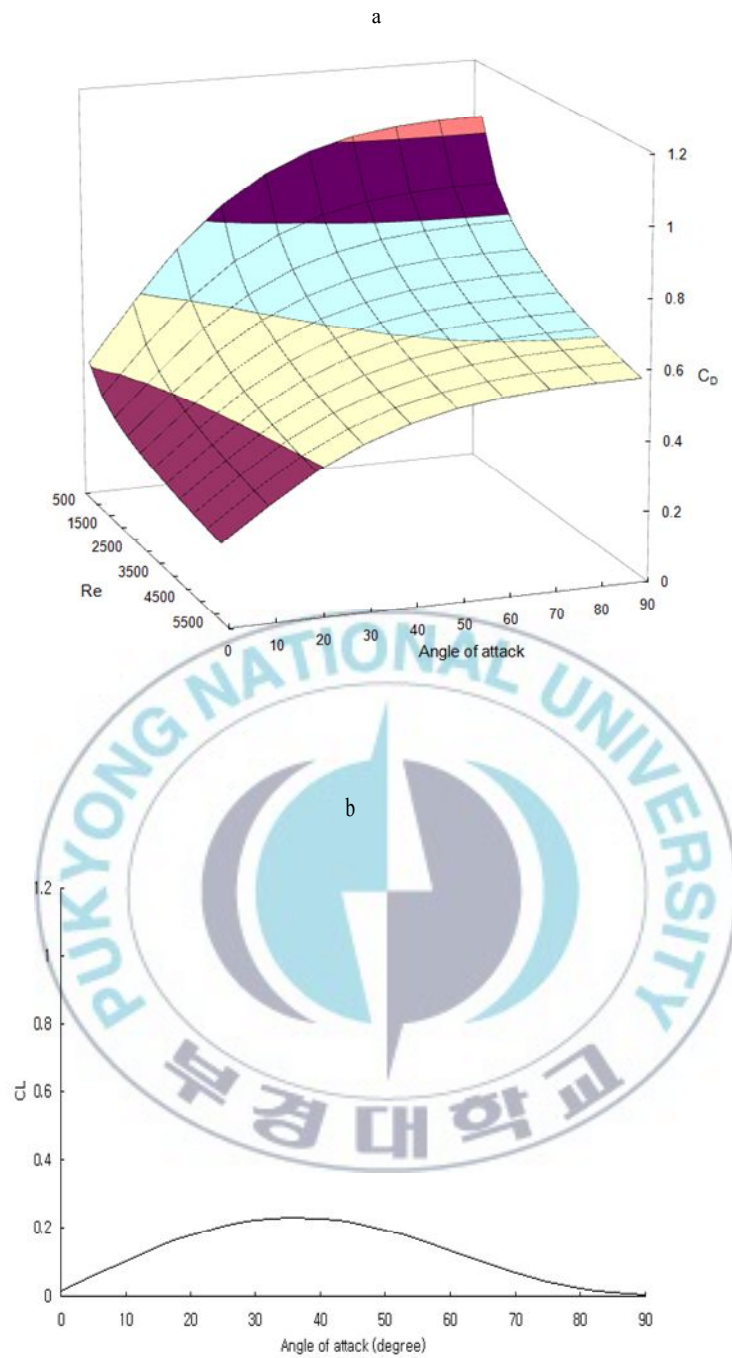


Fig. 17. Correlation of attack angle and Reynolds number with the drag coefficient (a) and lift force coefficient as a function of attack angle (b) for a specific model net.

2. Field experiments

2.1 Description of setting operation

Trial experiments were conducted on board the M/V ELS (Elspeth) with carrying capacity of 1500G/T during the period 15- 31 January 2009 in the Southwest Pacific Ocean at the northern part of Solomon Island to determine the timely sinking depth of the typical tuna purse seine. The vessel is characterized by LOA 85m, draft 7m and maximum speed around 19 kt belonging to Dongwon Ocean Master Company. The vessel is also occupied by the very accurate dynamic positioning system and colour scanning sonar (Furuno-FSV24) to record any data from the track of different setting operations of the net and also of the fish school swimming. Totally 20 net settings were carried out at sea. The sinking depth of the net was recorded by three underwater self-recording depth sensors attached to the lead line at three different positions of the purse seine gear (see Fig. 20) from the bunt to the wing length at an approximately equal distance apart. With this manner of attaching the sensors, sequential data of sinking depth of the whole net is gained as the net is submerged in an order of shooting. The self-recording depth sensors (Alec MDS5 Data Processing, Alec Electronic Co., Japan) can operate at a maximum water depth of 200m with a resolution of 0.05m and an accuracy of $\pm 1\%$ FS (1% of actual depth error). Its dimensions are 18mm wide, 93 mm length and 40 g weight in water (Fig. 18).

Before shooting started, the sensors were set to record the data at every second from the time they were submerged at the shooting operation until complete net retrieval at pursing end.

The recorded data from the sensors for each shooting operation were then transferred to the computer to retrieve the measurements.

The duration of the entire process varied with fishing condition; an average of 6 min was required to set the seine and 22 min to haul in the purse line completely.

Tidal currents in horizontal direction were recorded with Doppler Sonar Current Indicator (FURUNO CI-68) as speed and direction at three depths of 20, 60 and 120 m for each setting; these were used as input data for the simulation operation. With regard to direction, the data was applied to each layer as the dominant difference in the values between the layers, as shown in Figure 19.





Fig. 18. Schematic diagram of the Alec MDS5 Data Processing and their dimensions.

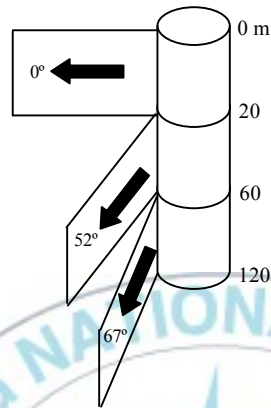


Fig.19. Current directions for three different layers applied to the simulation as the dominant difference values between the layer 1 (0-20m), layer 2 (20-60m) and layer 3 (60-120m).

2.2 Characteristics of the practical fishing gear

The gear used in the study is shown in Fig. 20, which is a typical tuna purse seine operated in Korea with a total length of 1786 m along the floatline and of 2249 m along the leadline. The full stretched depth measures at 220m. The gear is only made of nylon braided knotted netting with mesh sizes ranging from 89 to 254mm. The stronger twine number in the bunt, adjacent panels and salvages, which are typical for the purse seine, is used in the net structure. The gear specifications and dimensions are tabulated in Table 1.

A hanging ratio of 71 to 73% is used for the middle part of the net. Bunt and wings are hung with a ratio of about 90% .Table 2 lists these data in details.

The nettings on the lead line are hung with a higher hanging ratio of 91%. The difference length between the lead line and the float line is too much and, therefore, the lead line sinks faster during shooting.

On each meter of the float line, 2 to 3 E.V.A floats of oval-shaped with holes, made by Wthylene Vinyl Acetate, are fastened. This kind of float has a very high tensile strength which allows continuous use over long periods of time.

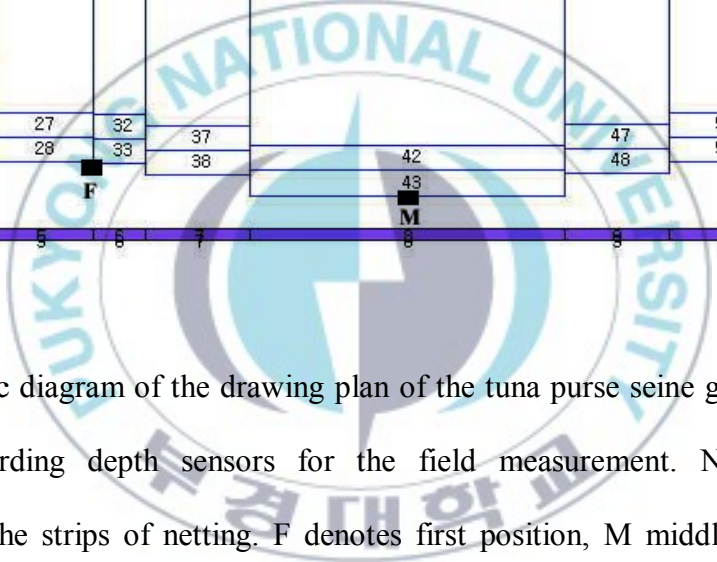
At two ends and some length of the middle part of the float line, however, bigger floats of SHE-85 type are fastened, each having a buoyancy of 8.5 kg. The weigh in air for the float amounts to 1.3 kg. Another type of float, SHE-70, with a buoyancy of 7 kg and weight in air of 1 kg each is also deployed by the gear. The floats are strung on a 40 or 44 diameter twisted polyamide rope (Fig. 21). The ropes are rigged with an average buoyancy of 25 kgm⁻¹ to support a total buoyancy of 44994 kg for the net. The specifications of the floats and their buoyancy are tabulated in Table 3.

The lead line is heavily weighted with the chain 5/8" or 1/2" type, each meter normally weighing 4.75 kg and 3.25 kg in water, respectively, by these kinds of chains (Table 4). The usage of the chain type varies alternately as the lead line position changes (Table 5).

The bridle is constructed by chain 7/16" weighing 2.7kg m⁻¹.The arrangement of the bridle is different depending on the places they are tied. At two ends at the bunt and wing parts, to some extend towards the middle part of the net, the bridles are arranged with higher length, amounting to 5.4m, and the length becomes smaller up to 4.5m at the middle of net. The distance between two rings is 17m (Fig. 22).

At two ends of the lead line, Samson rope of 2 1/2" diameter and weighing 0.21kgm^{-1} in water was used for a length of 27 m. A total of 129 galvanized snap rings consisting 5.8 kg sinking weight in water each, are attached to the purse line with 26mm in diameter. An average sinking weight of $6.5\text{ kg}^{-\text{m}}$ in water was used on the lower edge of the net to support a total sinking weight of 14723 kg for the net





of netting. F denotes first position,

Table 1. Specifications and dimensions of the netting panels of the typical tuna purse seine gear used for experiments and simulation.

Number	Mesh size (mm)	Hanging ratio	Length (m)	Vertical mesh number	D (mm)
1	89	90	36.6	244	4.2
2	89	90	36.6	122	4.6
3	89	90	36.6	122	4.2
4	89	90	36.6	366	3.8
5	89	90	36.6	366	3.5
6	89	90	36.6	366	3.2
7	89	90	36.6	488	3
8	89	90	36.6	366	2.6
9	89	77	73.1	244	4.2
10	89	77	73.1	122	4.6
11	89	77	73.1	122	4.2
12	89	77	73.1	366	3.8
13	89	77	73.1	366	3.5
14	89	77	73.1	366	3.2
15	89	77	73.1	488	3
16	89	77	73.1	366	2.6
17	108	76	91.4	300	3.2
18	108	76	91.4	1000	2.8
19	108	76	91.4	900	2.6
20	108	74	91.4	100	3.2
21	108	74	91.4	200	3
22	108	74	91.4	2100	2.2
23	108	74	219.5	100	3.2
24	108	74	219.5	100	3
25	108	74	219.5	1500	2.1
26	203	74	219.5	500	2.2
27	203	74	219.5	50	2.6
28	203	74	219.5	50	3.2
29	108	74	109.7	100	3.2
30	108	74	109.7	100	3
31	203	74	109.7	1300	2.2
32	203	74	109.7	50	2.6
33	203	74	109.7	50	3.2
34	108	73	219.4	100	3.2
35	203	73	219.4	100	3
36	254	73	219.4	1300	2.2
37	203	73	219.4	50	2.6
38	203	73	219.4	50	3.2
39	108	71	658.3	100	3.2
40	203	71	658.3	50	3.2
41	254	71	658.3	1040	2.2
42	203	71	658.3	50	2.6
43	203	71	658.3	50	3.2
44	108	73	219.4	100	3.2
45	203	73	219.4	50	3.2
46	254	73	219.4	1040	2.2
47	203	73	219.4	50	2.6
48	203	73	219.4	50	3.2
49	108	74	219.4	100	3.2
50	203	74	219.4	50	3.2
51	254	74	219.4	1040	2.2
52	203	74	219.4	50	2.6
53	203	74	219.4	50	3.2
54	108	75	219.4	100	3.2
55	203	75	219.4	50	3.2
56	254	75	219.4	1040	2.2
57	203	75	219.4	50	2.6
58	203	75	219.4	50	3.2
59	108	76	219.4	100	3.2
60	203	76	219.4	50	3.2
61	254	76	219.4	880	2.2
62	203	76	219.4	50	2.6
63	203	76	219.4	50	3.2

Table 2. Arrangement and dimensions of the float line of the tuna purse seine gear.

Float line (m)	160 (SHE-85 [*])		629 (SHE-70 [*])					312 (SHE-85 [*])		489 (SHE-70 [*])			196 (SHE-85 [*])		Total
Section	1 (Bunt)	2	3	4	5	6	7	8	9	10	11	12	13		
Slack	10% 23%	24%	26% 26% 26% 27% 29%			29% 29%			27% 26% 25%			24% 8%	26.1%		
Hung (m)	33 57	70	68 163 81 161 156			156 156			161 163 165			167 29	1786		
Stretched (m)	37 73	92	92 220 110 220 220			220 220			220 220 220			220 33	2417		

* Type of float

Table 3. Specifications of the floats used in the tuna purse seine gear.

Type	Length (mm)	Diameter (mm)	Hole diameter (mm)	Weight in air (kg)	Buoyancy (kg/ea)	Total quantities (5964)	Total buoyancy (44994 kg)
SHE-85	265	248	48	1.3	8.5	2162	18375
SHE-70	250	220	42	1	7	3802	26619

Table 4. Specifications of the materials of the lead line used in the experimental tuna purse seine.

Type	Size	Weight in water (kgf/m)	Length (mm)	Diameter (mm)	Total weight (kg)
Lead line chain	5/8"	4.75	80	16	5795
	1/2"	3.25	65	13	3149
Bridle chain	7/16"	2.7	55	11	5020
Purse ring	Model B-1X	5.8	356	76.2	748
Sinker SS. Rope ¹	2 1/2"	0.21		64	11
Total					14723

¹-SS. rope: Samson rope.

Table 5. Arrangement and dimensions of the lead line of the tuna purse seine gear (from bunt to the wing part).

Chain size	2 1/2" (SS .Rope)	1/2"	5/8"	1/2"	5/8"	1/2"	5/8"	1/2"	2 1/2" (SS .Rope)	Total
Hung (m)	27	123	425	485	275	489	275	123	27	2249

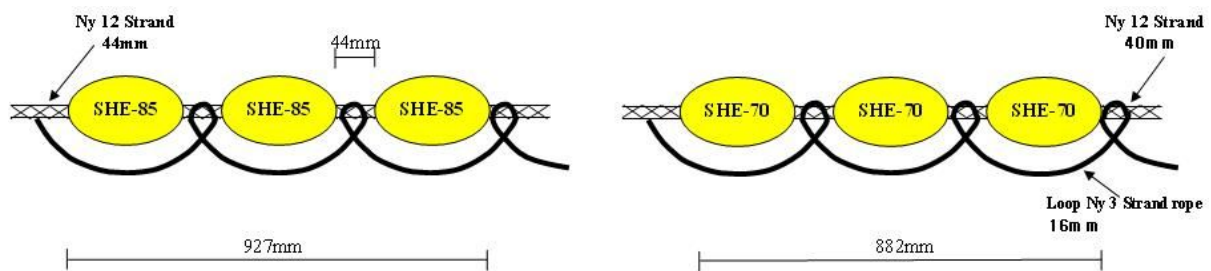


Fig.21. Arrangement of floats on the float line of the experimental tuna purse seine gear.

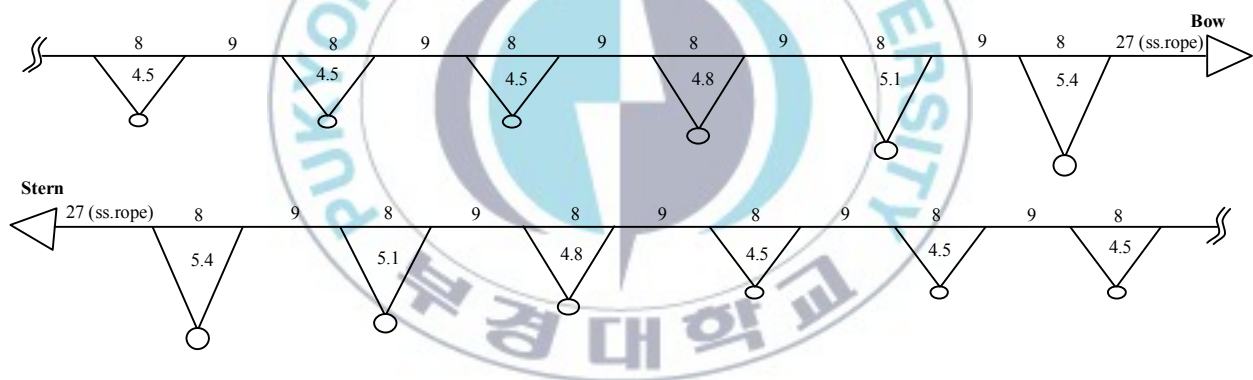


Fig.22. Arrangement of bridle chain of 7/16" and purse rings on the lead line of the experimental tuna purse seine gear. The numbers indicate the length in meter. The number of rings is scaled to around 1:11.

3. Simulation tools

Simulation procedure is followed by drawing a design of the gear with webbing, rope and riggings as developed by the design program. Because purse seine is not made up a unified material of rope or net, construction and arrangement of the complicated structure into the proper order require a special function. In this program, a mechanized system adopted to acquire a completed mathematical model of the gear once the drawing plan of the gear is achieved. The physical properties such as, projected area, mass, volume, weight of the gear corresponding to each mass point, are automatically derived from a database set in the program and then saved to file. The equations of motion of the mass points along with the parameters included in the equations are then formed. When the drawing process comes to an end, the preparations for simulation are completed by selecting an approximation ratio to make automatically virtual mathematical meshes as a mesh grouping process. In order to reflect the physical properties of the fishing gear, the mass points of the purse seine net is simplified to around 4400 in the simulation. Figs. 23 and 24 give a general view of the design and simulation tools.

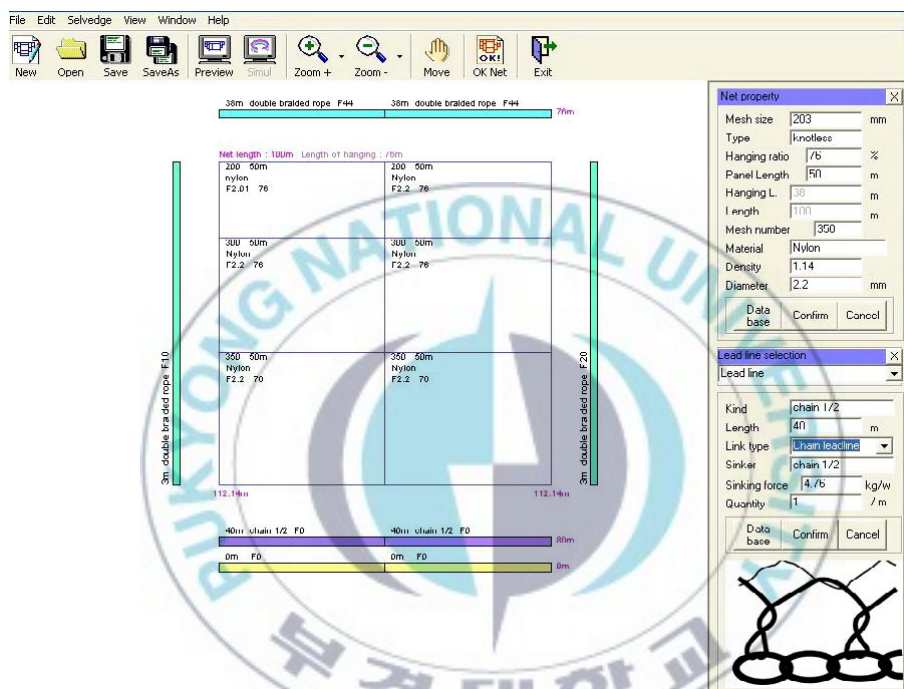


Fig.23. Basic menu bar (up) and initial input windows (right) along with drawing of purse seine gear by the design program.

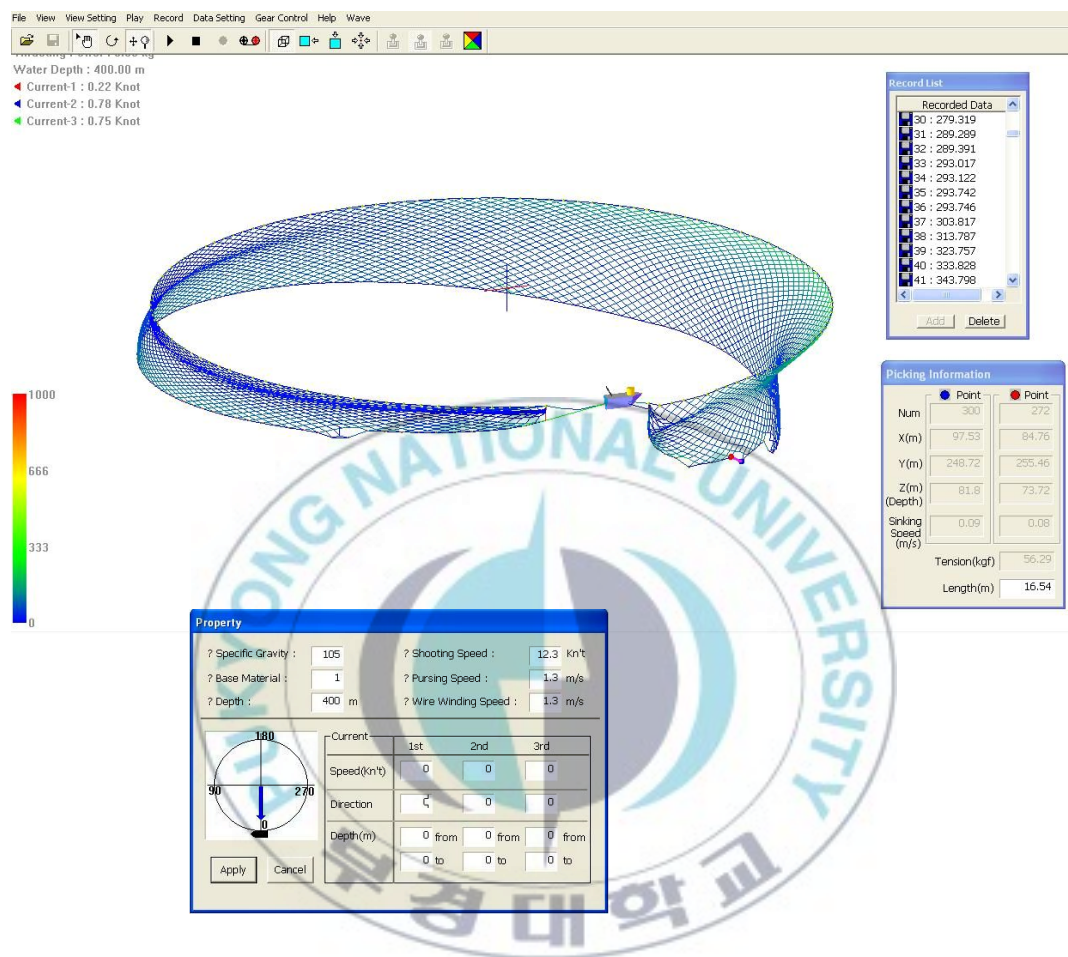


Fig.24. Basic menu bar (up) and property window (down) along with simulation of purse seine gear by the simulation program.

III. Results

1. Field measurement at sinking depth of the purse seine

In order to provide a whole picture of sinking behaviour of the net for the three positions, the measurements taken from the four selected settings out of 20 settings pooled together to show as an average trend of each section, as shown in Fig. 25. The figure shows the depth from the time of entry into the water until the time of purse line retrieval. As expected and apparent from the trajectory of the lead line, the sinking speed is rapid at the beginning and becomes slower towards its operating depth. Such a decreasing in sinking speed is due to the fact that the resistance of the webbing wall increases as the straight part spreads to the depth of water and the area of bundle part decreases.

If these measurements are converted to the corresponding stage of the fishing course, it can be seen from the figure that during setting process, the seine sinks at average speeds of 0.26, 0.31 and 0.29 m/s, respectively, for the First, F, Middle, M, and end, E, portions. The sinking speed trends of the lead line are due to the positions in which the depth is recorded. That is to say that the lowest sinking speed of the first position, F, involves using the horizontal netting panels of smaller mesh size of 108 mm (see Fig. 20 and Table 1) and, in opposite, the usage of larger mesh size of 254 mm in the entire middle part, except for the salvages, makes the section to sink at the higher sinking speed. Maximum operable depth is measured at 153 m which equals around 80% of the full stretched depth of the net. As shown in Fig. 25, the whole fishing process takes about 29 min from shooting to pursing end.

The measurements of sinking depth of the net from the four settings at field along with the average values are shown in Fig. 26 for the three positions. The trajectory of the lead line at

the middle, M, position shows no great variation among the settings, but a deviation from the average value recorded for the settings at the first, F, and last, E, positions with more variation for the former position. It is thought to contribute to either entanglement of the gear at the sections or some other fishing operation conditions such as skiff boat operations, especially for the first position.

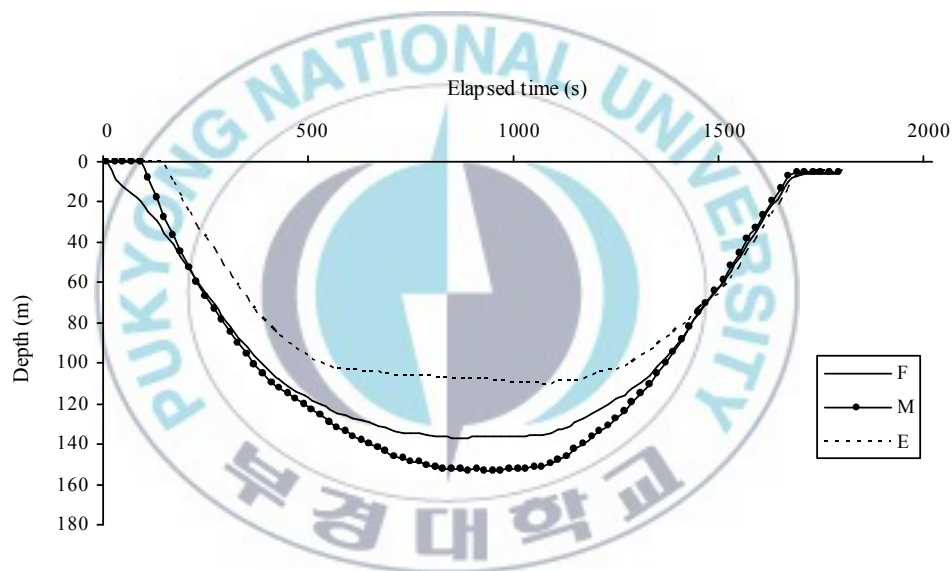


Fig. 25. The mean sinking depth of the four settings for the three positions of the lead line of the tuna purse seine gear obtained from the field measurements. The positions are similar to those used in Fig. 20.

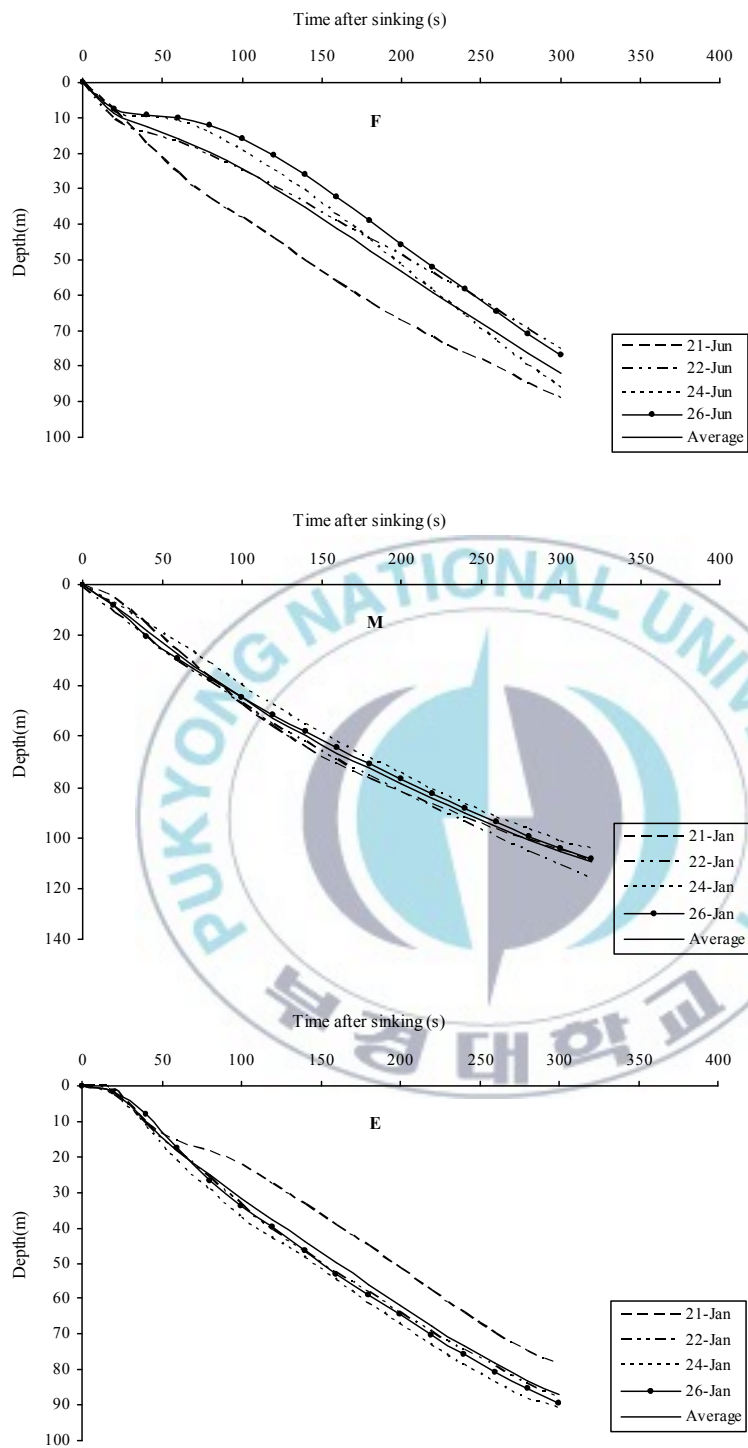


Fig.26. Comparison of the sinking depth performance of the tuna purse seine gear at the three positions of the lead line, measured from the experimental operations.

2. Simulation performance and verification

2.1 Visualization of the net shape

The field data required for simulation of each set, used as input, includes shooting and pursuing speeds and current velocities in magnitude and direction for three layers. As in the actual fishing condition the shooting and pursuing speeds vary with the operation course; the data obtained from knowledge of the field used as different values in the appropriate time of the simulation process. When the seine was simulated under the current velocities of 0.11, 0.4 and 0.38 m^s for the three layers, respectively, as mentioned before, and a pursuing speed of 1.3 m^s, the sequential 3-D visualization of the net shape from shooting to pursuing end shown in Fig. 27. The net is set uniformly in circle based on the assumption inherent in the simulation and deformed from the circle during the pursuing process as the seiner pulled transversely into the circled space, because the resistance of the seine is much greater than that of the seiner moving forward to it.

2.2 Sinking depth verification

Judging from a comparison of the average measured sinking depth results with the simulated results derived from the average operational condition at field (the same as applied to those in Fig. 27), the coincidence of the observed and calculated values is satisfactory as discrepancies due to the assumptions made in the numerical method are to be expected (Fig. 28). This deference is more pronounced for the first part, F, of the net where it is first submerged during setting.

A more closely comparison between the cases of numerical and measured results is given in Fig. 29, for which the results were simulated using current velocities of 0.2, 0.1 and 0.15 m s⁻¹ for the successive layers and a pursing speed of 1.3 m s⁻¹. As in Fig. 28, the sinking speed of the simulated net is greater than that of the experimental one and is generally in accord with the field results.



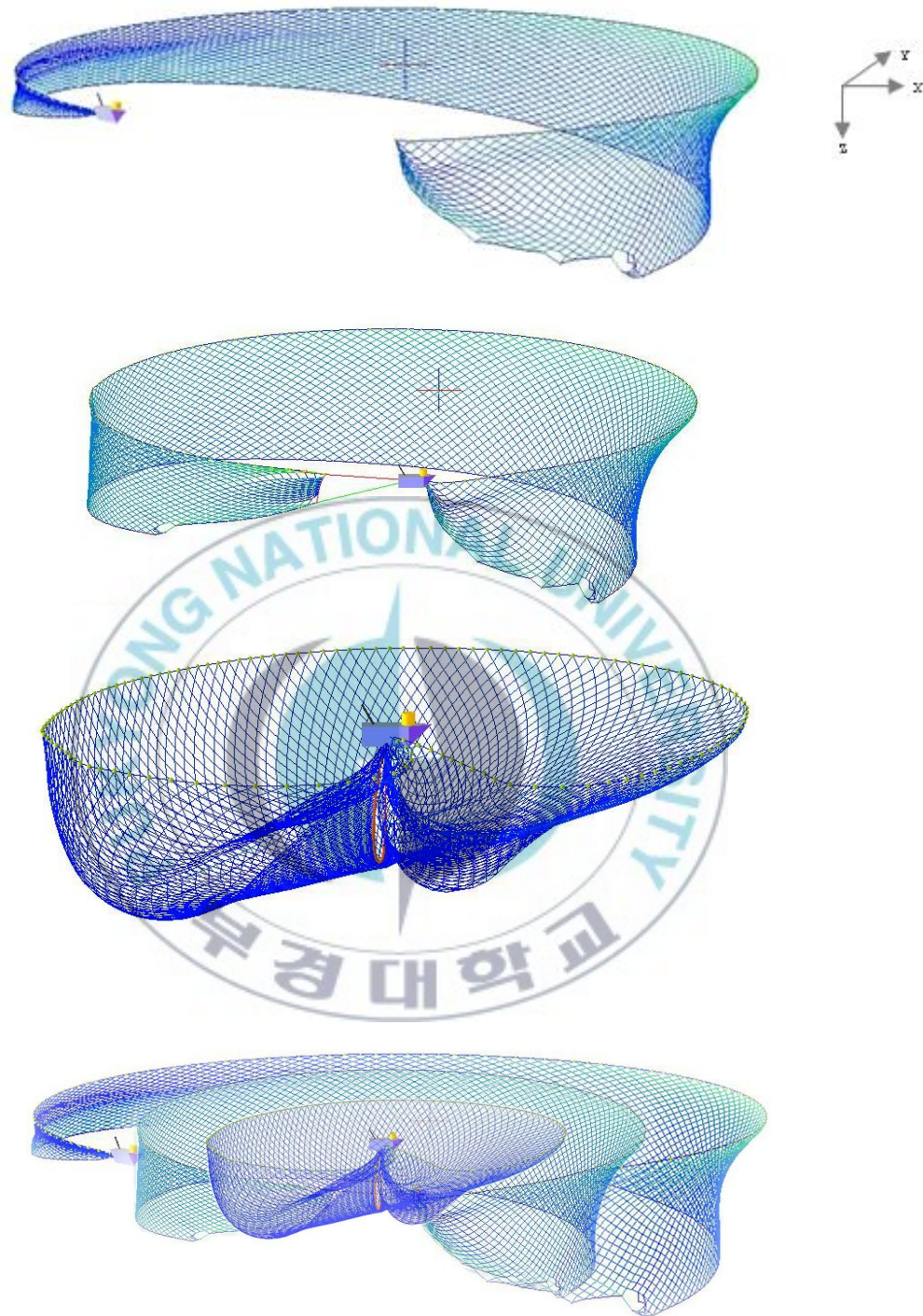


Fig.27. The sequential shape of the simulated purse seine gear from shooting to the end of pursing under a pursing speed of $1.3\text{m}^{-\text{s}}$ and current speed velocities of 0.11 , 0.40 and $0.38\text{ m}^{-\text{s}}$ for the three layers. Note that the seiner pulled into the center of the enclosed net area.

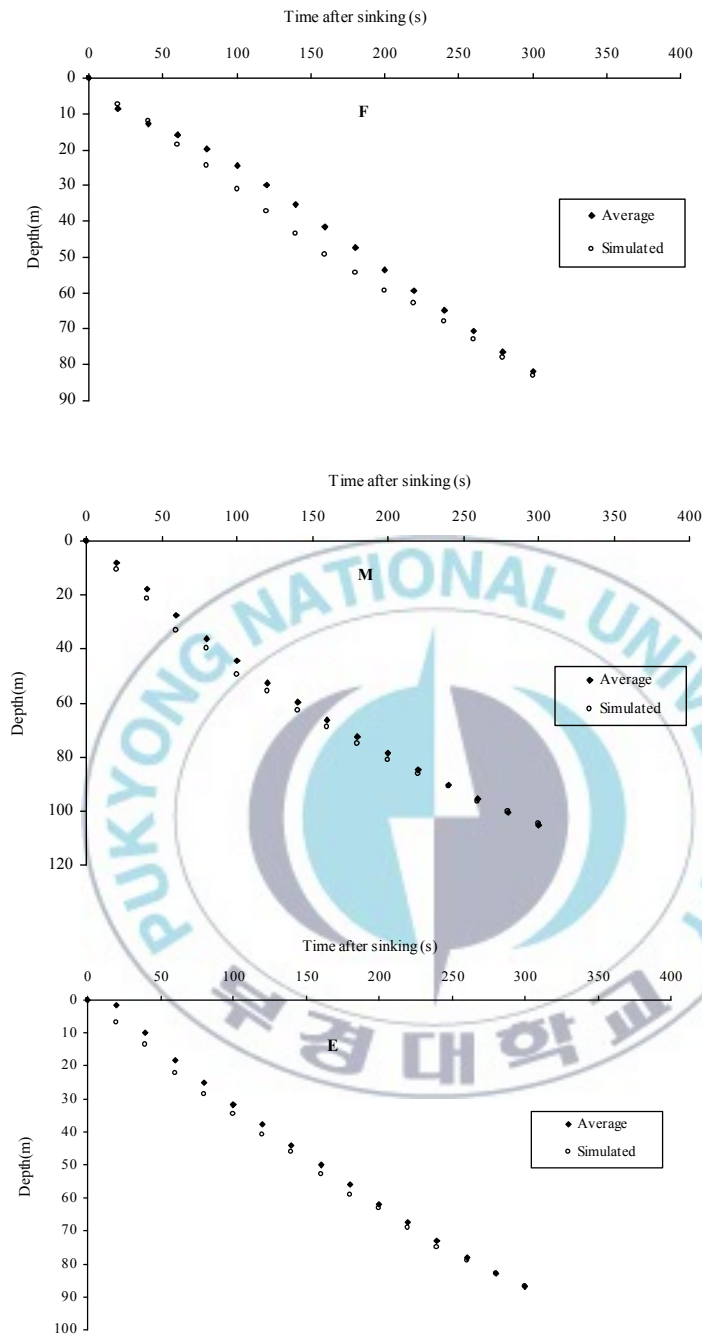


Fig.28. Comparative sinking depth of the lead line of the purse seine from the field operation and the numerical result, simulated under the same condition as in Fig. 27.

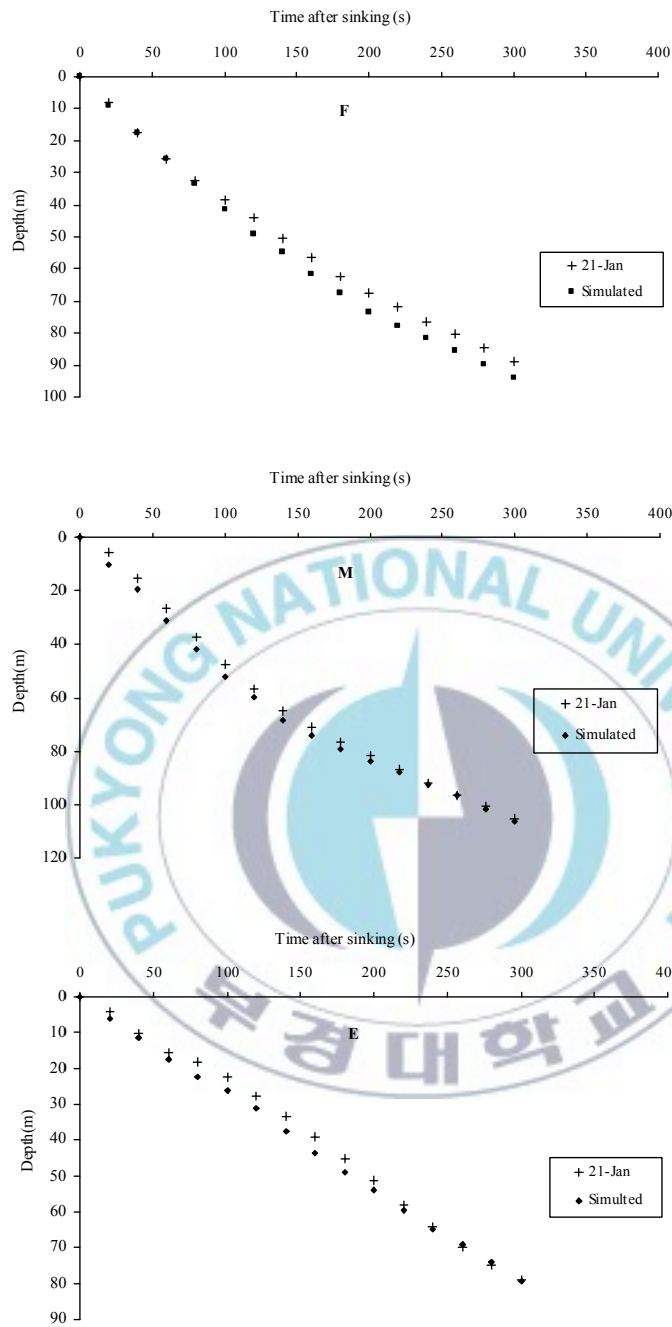


Fig.29. Comparison of sinking depth of the lead line of the purse seine at the three sections from one case of the field operation and the simulation result when simulated with a pursing speed of $1.3 \text{ m}^{-\text{s}}$ and current velocities of 0.2, 0.1 and $0.15 \text{ m}^{-\text{s}}$ for the three successive layers.

IV. Discussion

The calculated results quantitatively are in agreement with the measured values. Some potential quantitative differences, however, can be noticed due to deficiencies of the numerical simulation, which are given in details in the following.

Drag coefficients

The improved numerical model described here, which estimates the drag coefficient as a function of the Reynolds number and provides a realistic value for the attack angle of the netting wall, adequately represents the influence of the drag force as a decisive factor in the net configuration. The advantage of incorporating the Reynolds effect is that the net may function at low Reynolds number and, therefore, the drag coefficient is not considered to be constant for the velocity range. The numerical results arrived at by consideration of actual fishing conditions were verified by the field measurements.

The sinking depth calculations of the fishing gear, especially of the purse seine, based on the numerical method are not expected to give the precise results derived from the actual measurements, because it is extremely difficult to apply the precise fishing operation conditions as input data to the fishing gear system to simulate the purse seine process of the corresponding net. We reduced the difference between the measured and calculated values by improving in the numerical modeling used to include the effective drag coefficient for the netting during the setting operation. In the actual setting process, the bundle part of the webbing placed in the water body, varied in position depending on the netting material (Kim *et al.*, 1995), spreads out vertically as the net is set due to the sinking force. The current forces

influence on the straight part of the net according to the criteria mentioned in the present paper. As for the bundle part, only the outermost section of the netting is completely influenced by the current forces, and the inside of the wrapped webbing where a large number of meshes are gathered together, particularly the center, is much less affected by the current. This was considered in the calculation process by the optimizing the drag coefficient values ranging from 0.6 to 1.1 for the relevant parts.

Misund *et al.* (1992) approximated the sinking speed of the purse seine during shooting by considering the netting as the straight and snake parts separately. The snake part was divided into sections, each with its own speed. The empirical equations used by Kim and Park (2009) are only approximate and do not adequately describe the effect of the loads on the purse seine shape because in these equations, the drag force has no logical relationship to the Reynolds number. Moreover, in that study, no verified model was applied to the netting system because the resulting comparative analysis of the numerical values and field data was qualitative rather than quantitative.

In the current study, some erroneous outcomes of the numerical simulation probably arise due to the slight inadequacy in the determination of the drag coefficient as the coefficient is given as a function of Reynolds number for a higher range of 430 to 4700. Usually, the Reynolds number dependency of C_D for fishing gear, in which the frictional resistance is the prevailing factor, is in the range of smaller than 2×10^2 to 6×10^2 (Fridman, 1973). For the numbers exceeding this range, the coefficient changes independently of the Reynolds number; in this case, the resistance of the shape is the predominating factor and the resistance function

is considered to be nearly quadratic. The data in our new experiment shows a different pattern from the above case in terms of Reynolds number.

As calculated by Schlichting (1968) and Newman (1977), in the given Reynolds number ranging 10^2 to 10^4 , the drag coefficient for a cylinder C_{db} (positioned normal to the current) covers approximately the range of 1.0 to 1.8, indicating a variation from the present study as measured 0.6 to 1.1 according to the relevant Reynolds numbers.

Special studies showed that the drag coefficient of the nets depends on how it is hung, and also the dependence of C_D on the hanging ratios, E_1 and E_2 , is not the same for all the nets: it becomes weaker with increasing mesh size (Fridman, 1973). In the numerical method, the drag coefficients calculated by the relevant equation is just based on the hanging ratio of 80%, while variation of mesh opening in purse seine during fishing course is one of the notable features of the net performance. Such a case can be seen at the setting operation in which the mesh opening of the webbing gradually increases as the netting wall descends to the water (Fig. 30a). It is also more evident since pursing starts as the mesh opening further increases, attaining to its largest value in the normal direction (N) of the net as the process comes to an end (Fig. 30b). Therefore, some additional discrepancies likely arose from the hanging ratio.

The equation for the drag does not consider the shadowing effect of each row of bars behind the row in the front, where reduction in the water velocity by the term $\sqrt{d/a}$ appears (Dickson, 1980). According to the study, by the introduction of such a term in the shadow, the laminar flow was considered by the Reynolds numbers well below 1000 to turbulent flow at the Reynolds number of 2000 to 5000 to twines on trawls. Misund *et al.* (1992) applied the

shadow coefficient, taken as 1, along with the above term to the drag coefficient for meshes at zero angle of attack to the water when studied on the sinking depth.

Also, the depth profile of the current speed is left out of the consideration; the speed is assumed to be spatially uniform at each depth range, leading to some difference between the measured and calculated results.

Another factor that might result in differences between the measured and calculated values is the mesh-grouping process; we chose 18-mesh grouping. Finding a balance between the computational effort and accuracy of simulation is a major problem that needs to be solved. In a model test conducted in a flume tank, a 4-mesh grouping was reported to be the most effective, whereas increase in the number led to reduction in the accuracy of the results (Takagi *et al.*, 2004). The mesh-grouping ratio has also been discussed by Tsukrov *et al.* (2003). Based on their calculations, when 2×2 , 3×3 and 16×16 meshes of the plan net modeled to a factious equivalent mesh, similar predicted hydrodynamic forces were concluded from the given cases. Lee *et al.* (2007) mentioned some miner difference between the various mesh-grouping ratios of the net for the drag and lift coefficients during model tests in flume tank. They found lower values of the coefficients when the ratio increased.

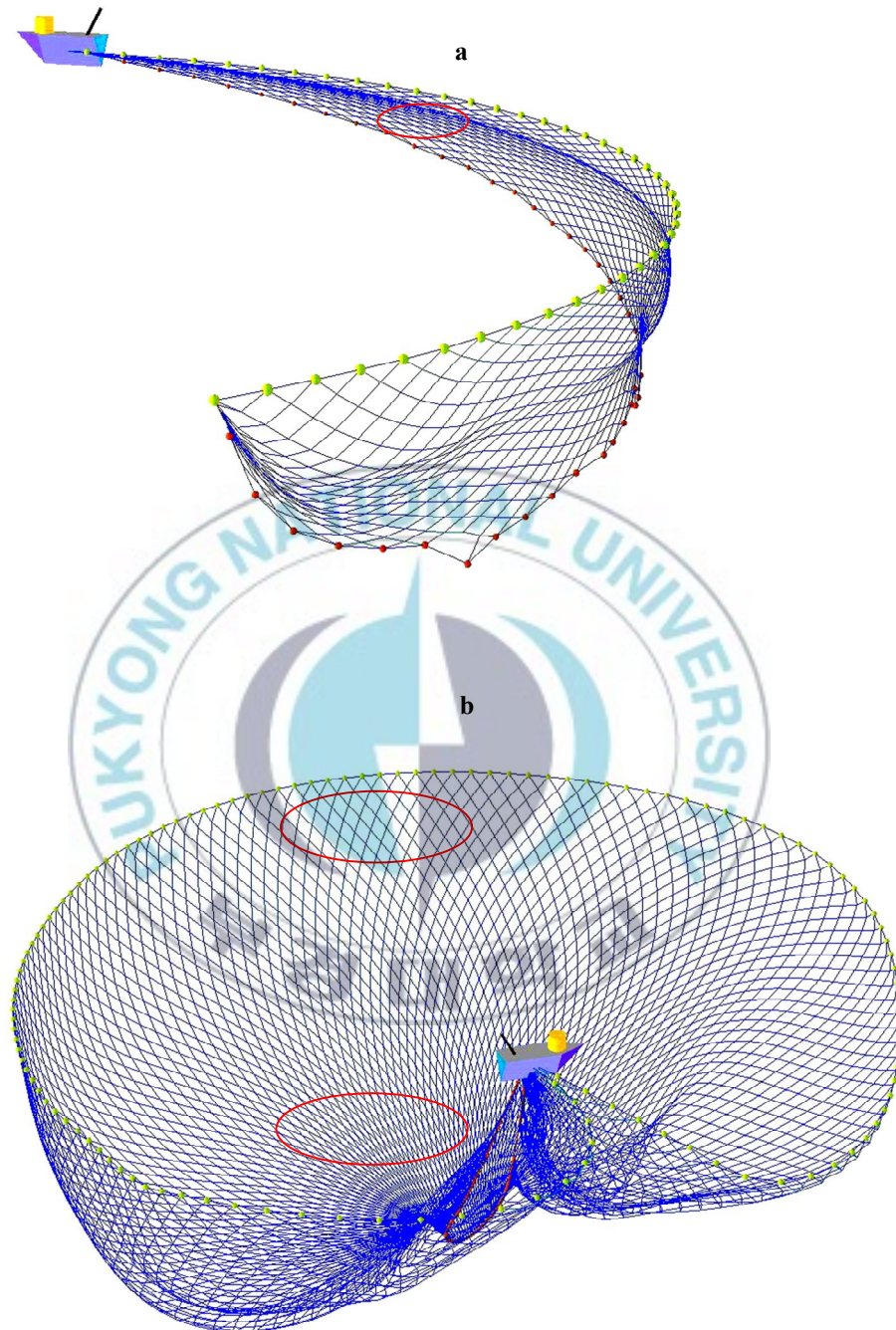


Fig. 30. Mesh opening change (elliptical line) during shooting (a) and purse seining process (b) shown by the numerical simulation.

In purse seine, floats of oval-shaped are enclosed in the netting nearly in groups (see Fig. 24). The experiments in the wind tunnel indicated that the drag coefficient for a 150-mm diameter free glass float was $C_D = 0.55$ in comparison with the case when a number of the floats enclosed in the netting which was $C_D = 0.93$ (Fridman, 1973). It was also concluded that a considerable lift force acted on the netting enclosing floats of close to cylindrical shapes. The consideration made by the numerical method for the mesh-grouping may cause reduction in resistance magnitude with a difference between the calculated and measured shape of the fishing gear.

The current speed as a depth profile is left out of the consideration in the simulation and it is spatially uniform at each depth range, leading to some difference between the measured and calculated results in the purse seine gear configuration and sinking speed. In our numerical simulation, however, we applied a current direction by depth profile at a difference of 67 degree between the upper and lower layers. The available data indicates that current speed by depth increase from an average of $0.1 \text{ m}^{-\text{s}}$ at upper layer to $0.4 \text{ m}^{-\text{s}}$ at the lower layer. Kim and park (2009) applied a sigmoid function to consider the flow speed and direction as depth profile into the numerical simulation of the purse seine for two layers, between the upper and middle depth of water. By applying this along with the drift of seiner into the center of the circled area, they described a heart-like float line at the end of pursing.

Shooting

The purse seine net is not always shot in a circle. The shape of the net depends on the way the fish are moving and how fast. Sometimes we might have to shoot half the length of the net

in a straight course just to get down past the school. In numerical simulation, the motion of the seine is simplified as the net is set uniformly in circle. This kind of motion does not certainly identify the shape of the actual net.

The greater difference in sinking depth between the numerical and measured results for the first position, F, of the net in our results can be explained by the fact that in the real fishing operation the beginning of the net, known as the bunt, is pulled back by the skiff boat to hold it in its own shooting position while the rest of the seine is pulled off the platform of the seiner. The forces caused by the pulling of the bunt region are distributed to the other parts in front of the bunt, leading to a lower sinking speed of the lead line. Moreover, a tight setting of the net, which can occur under actual fishing conditions, can affect the net's sinking performance. The incidence of entanglement of the net during setting by gathering of the webbing around the lead line located on the net space of the seiner can be considered an effect of reduced sinking speed. In the simulation, a bundle of webbing lies over the surface and the net sinks under the influence of the resultant force vector during shooting without any entanglement, resulting in a higher sinking speed than occurs in the actual experimental results. Additionally, the numerical simulation does not take into consideration of factors, such as the tension in the purse line during setting that may tend to reduce the sinking depth of the lead line at the moment and the depth of movement during pursing.

The maximum operable depth of purse seine gear is dependent upon the operating condition; in normal use, the seine rarely achieves its full stretched depth. This low incidence of achieving the full stretched depth of the seine can be explained by the combined effects of vessel maneuvers, tension of the purse line during setting, current velocity and other variable

factors of the pursing operation including pursing speed and time. In the latter case, the delay in the starting time of pursing after setting ends is the factor that determines the ratio of operating depth to the stretched depth of the net. During experiments with coalfish purse seines, a full operating depth of 150 m recorded when pursing started 14 min after setting was completed, as opposed to 100 m for 4 min of the holding time (Beltestad, 1981). Moreover, setting a purse seine in a fishing ground with a stronger underwater current results in a slower sinking speed of the net. Sinking speed can be reduced by one-third to one-half at a current velocity of 0.2-0.3 m/sec (Fridman, 1973). Inada *et al.* (1997) found less sinking speed for the tuna purse seine where higher current velocities were observed in the mid layer of water, which influenced on the tuna catch and its failure ratio of the sets.

Variation in sinking depth of the experimental purse seine in different settings, especially in the first section, F, as shown in Figure 26, is thought to contribute to entanglement of the gear, although other fishing operation conditions such as skiff boat operation can also contribute to such variation.

Pursing

By introducing the seiner drag force to the model, the simulation method enables to perform the mechanism of the transverse movement of the vessel progressively into the enclosed area of the net during pursing process, and the shape of the float line develops an elliptical appearance at the end of the process as the actual gear performs in the field (Baranov, 1976). No data from field observation was available to compare with the simulation performance.

Despite the drag equation of the seiner proposed here, more accurately consideration can be made on the motion of vessel in both directions; longitudinally, along the axis of the vessel, and transversely, perpendicular to the axis as explained by Delmer and Stephens (1981). In their modeling, two directions of motion resulted from the drag force by the current velocity and the propulsion which produce third component of force as torque around the vertical line assumed at the center of gravity of the vessel.

The tensions calculated by the numerical method describe the values without allowing for the friction between the rings and purse line. It is advisable to calculate the total tension properly as a reaction of purse line to the resistance of water and the frictional forces corresponding to the pull of the winch. Baranov (1976) proposed a solution for the total tension during pursing by considering the purse line as the shape of a regular polygon in the plane whose apexes lie the purse rings (Fig. 31). The tension at any point of the polygon-shaped purse line is calculated based on the angular distance between the middle part of the purse line and that point. Moreover, the pursing speed, as an effective factor in the seine shape and depth during the process, is not the same as the course goes forward (see Fig. 44 in chapter 4). On the other hand, almost no measurements are available for the pursing speed by each step of the process, becoming a problematic parameter as the entry data for the simulation when the comparison with field observation is intended. Therefore, an inherent difference between the two results can be expected by the pursing speed problem.

Towing the purse seiner by the skiff boat during pursing can not be considered as a parameter affecting on the purse seine shape. This force, as an additional drag applied to the seiner, was not considered in the numerical method.

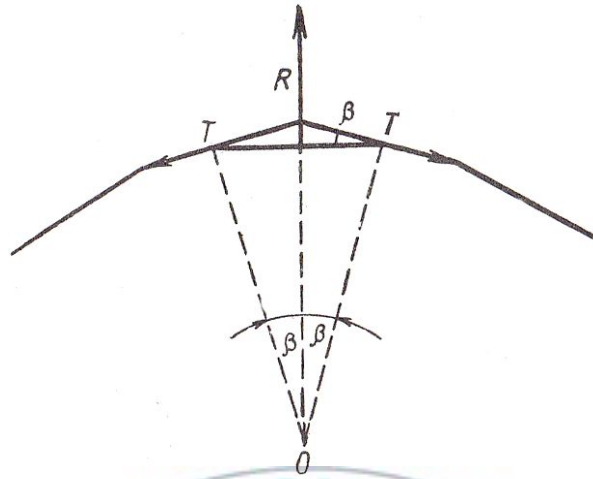
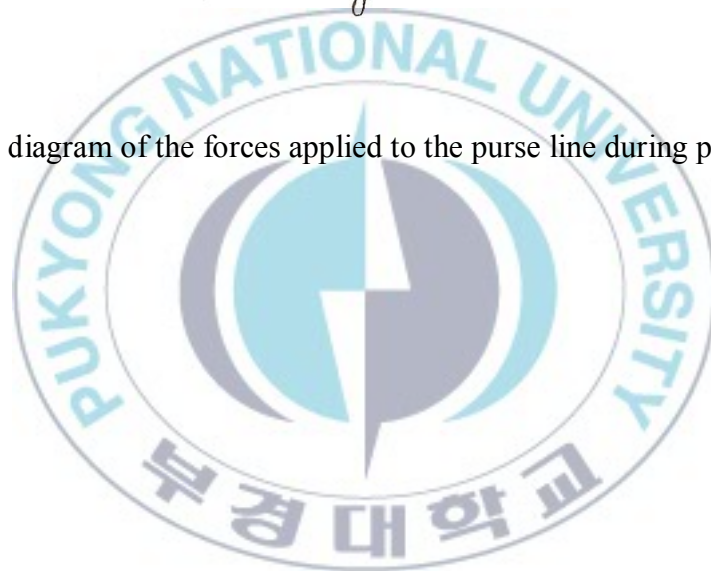


Fig. 31. Schematic diagram of the forces applied to the purse line during pursing process.



Chapter 4

Application of numerical simulation for the gear designing

I. Advantages of numerical simulation

A simplified computer-simulation system for designing and simulation of the fishing gear is required to reduce the costs, save time, and avoid the labor of the experimental observation and flume tank tests.

Applying the experimental method for studying the net behaviour has the disadvantage of highly operation expense. It is also difficult to control and measure ocean parameters and modification of the gear with new configuration requires great deal and is time-consuming, while the results from the experiments are real and undeniable.

Model tests are economical and time-saving and experimental conditions are easy to control as tests are done indoors as compared to the full-scale tests, but it necessitates building expensive experimental facilities like flume tank etc. and the models for the tests even if there are small changes in the design. Model experiment has the problem of rigidity because of its small size, as the webbing and other ropes are assumed to be flexible in the actual gear. For this reason, tests with small scale models may be inadequate to observe the exact and detailed mechanical behaviour of the net. On the other hand, the discrepancies can be aroused more with taking into account the scale effect, as the difference between full-scale and model tests results for the variables derived from the unsatisfied similarity criteria. Moreover, reliable information can not be obtained as it is difficult to do measurements under water with desired accuracy for both field experiments and model tests, for instance, the mesh opening and the tension distribution of fishing gear in detail.

Data from the analytical method, such as numerical simulation, lead to undesirable results and can be questionable. This disadvantage can be eliminated by comparing the results of the analysis with some experimental measurements. If the experimental verification is made the adequacy of the analytical method can be realized by low cost, and control of ocean and net parameters.

In the following, examples of capabilities and applications of the numerical simulation are given and the results can be advised for any practical purposes.

II. Effects of mesh size and netting material on the purse seine gear

1. Introduction

The success of fishing operation in purse seine largely influenced by the proficiency in surrounding the fish school as well as by the sinking speed of the net. The sinking speed in turn is dependent upon the weight in water, the type of knot, mesh size, twine thickness, hanging ratio, mesh geometry, method of setting, and the current profile (Beltestad, 1981).

The available data on tuna catches by the Korean purse seiners indicates variation in success according to the vessel size. The bigger purse seiners of about 2000 G/T, which operate nets of around 2600 m in length and 32 strips in depth, result in higher successful settings as compared with the smaller and medium-sized vessels carrying nets of 2300-2500 m in length and 29-31 strips in depth (Kim, K Y, pers. comm., 2010). The great variation in the positive incidences of the settings can be explained by the larger nets and bigger vessels, and also probably by the greater sinking loads rigged on the bigger nets as adapted properly to the size of the purse seiners. This favorable catch compelled the designers of these nets to

establish their goals of improving tuna purse seines in terms of building costs and standardization of net construction appropriate for rapidly swimming fish schools. Specific data from the logbook records of M/V Elspeth during 2008 and 2010 also indicates the highly failed sets for tuna schools as listed in Table 6. According to 369 days at fishing, the total sets made on the free-swimming schools of the combined tropical tuna (skipjack and yellowfin, mainly for skipjack) were recorded to be 268, of which 38% led to unsuccessful events. This contribution to the log schools was 96% of the total sets. Average catch per set for the free-swimming schools was 25 tones as compared to around 43 tones for the log schools. The potential problem of the highly failed sets is thought to be decreased by modification in the construction of the present purse seine nets.

2. Materials and methods

In order to test the effect of large-meshed panels and netting materials on the sinking depth of the net, some alternatives of the new designs of the prototype drawn by the relevant program tool. Panels with 381 and 508 mm mesh sizes, each made of both polyamide (PA) and polyester (PES) materials were used for the 254 mm mesh size of the prototype net in the main body section. This modified section does not include the salvages and the bunt part with some adjacent panels having smaller mesh sizes (Fig. 32). For simplicity, the nets were named in abbreviated form. For example, PA-381mm denotes a net of 381mm mesh size at the main section with netting material of polyamide. In length and depth, the main dimensions of the new designs were the same as those of the prototype, along with the same buoyancy and sinking weight. The twine diameters were calculated according to the condition of equal

total strength (Fridman, 1973), considering that the breaking strength of polyamide is 20% larger than that of polyester, which is given as

$$C_d = C_v \sqrt{\frac{C_n C_a C_l C_{u_1}}{C_\sigma C_{u_2}}} \quad 4.1$$

where C_d is the scaling factor for the twine diameters of the new gear and prototype. For the other components the scaling factors are described as C_v , the relative velocity, C_σ , the breaking stress, C_n , the safety margin, C_a , the mesh size, C_l , the linear dimension of two gears, and C_{u_1} and C_{u_2} , the primarily and secondary hanging ratios, respectively. Table 7 indicates the twine parameters of the different drawing plans.

Table 6. Preliminary data on tuna catch of the Korean purse seiner during 2008 and 2010 from Elspeth vessel.

School type	Day		Catch	set			CPUE/set	
	Days at	Days		Successful	Failed	Total	Succes	Total
Free swimming			6685	102	166	268	65.5	24.9
Log school			3500	79	3	82	44.3	42.7
Total	416	369	10185	181	169	350	56.3	29.1

Table 7. Twine parameters for net of different designs used in the simulation method.

Design type	Material	Mesh size	Twine size	R tex	Twine diameter (mm)
		(mm)			
Prototype	Polyamide	203	23× 6× 16	2428	2.2
New design	Polyamide	381	23× 8× 16	3238	2.7
		508	23× 12 × 16	4857	3.1
		381	28× 10 × 16	4928	3
	Polyester	381	28× 10 × 16	4928	3
		508	28× 15 × 16	7392	3.5

3. Results

Fig. 33 shows the simulated sinking depth of the lead line as the net starts to submerge to the maximum operating depth for the prototype made from PA, with a mesh size of 254 mm in the main body section; and new drawings of the gear, with large-meshed panels of 381mm and 508mm, each consisting netting materials of PA and PES, for the same three successive positions as in Figs. 20 and 32. The nets were simulated at a pursuing speed of $1.3\text{m}^{-\text{s}}$ and current velocities of 0.1, 0.15 and $0.31\text{ m}^{-\text{s}}$ for layers 1 to 3 respectively. The recorded depths for the prototype and the new designs of the gear are given in Table 8. The difference in sinking depth between the prototype and the new designs is noticeable as the mesh size is increased. The increase in net depth is much more pronounced when the heavier PES material is used for netting. For F, for example, the sinking depth of the prototype 6 min after sinking is recorded as 113 m, as compared to values of 115 m, 117 m, 128 m, and 129 m for designs of PA-381 mm, PA-508 mm, PES-381mm and PES-508 mm, respectively. The difference in depth between the prototype and new designs is more noticeable when comparing the middle, M, and end, E, parts of the nets. The maximum operable depth for the prototype is measured at 148 m 21 min after submerging, as opposed to 150 m, 155 m, 168 m and 171 m for the PA-381 mm, PA-508 mm, PES-381 mm and PES-508 mm nets respectively.

There is a definite difference in slope of the calculated average sinking speed between the different cases from surface to maximum depth for the first few minutes; this difference becomes smaller with elapsed time as the vertical netting strips stretch out at depth (Fig. 34). A considerable difference is indicated at the M and E positions of the nets. For the M position, the prototype sinks at a speed of $0.45\text{ m}^{-\text{s}}$ two minutes after sinking compared to speeds of

0.46 m^s, 0.49 m^s, 0.52 m^s and 0.54 m^s for the improved PA-381 mm, PA-508 mm, PES-381 mm and PES-508 mm nets, respectively. Reduction in sinking speed by depth is shown in Fig. 35. The decrease speed is more obvious in the first, F, position.

The changes in tension at both ends of the purse line of the different purse seine drawing plans during the pursing process are summarized in Fig. 36, which corresponds to a pursing speed of 1.3 m^s. In all cases, at the beginning of the pursing the tension in the purse line increases rather sharply until it reaches its maximum value at the instant when the weight of the lower part of the net and of all the riggings is transmitted to the purse line as the netting moves in depth towards the center of the circular area. As the pursing process continues and the lead line moves upward, the tension increases again until it exhibits a reduction at the end of the course when the seine is pulled to the side of the vessel and all the rings are closed together as shown in Fig. 36. Accordingly, the tension of the purse line in the prototype drops from around 43000 kgf at the peak to 33000 kgf at the end of pursing, with the corresponding values of 38000 kgf to 29 000 kgf for the PA-381 mm version, 36000 kgf to 27000 kgf for PA-508 mm, 42000 kgf to 36000 kgf for PES-381 mm, and 41000 kgf to 35000 kgf for the PES-508 mm nets. Even when the new drawing plan features gear constructed of PES material with a density of 1.38 g/cm³, and the thickness of the twines is somewhat increased, a smaller tension is exerted on the gears as compared to the case for the prototype with polyamide netting material of density 1.14 g/cm³. The average values in tension difference between the prototype and the improved nets were greater for the net made of PA-508 mm, which showed 14% less tension than did the prototype (Fig. 37). For the net of PES-508 mm, the average tension was recorded as 97% of the prototype.

A comparative analysis of the netting material volume of the prototype and that of the new different designs is represented in Fig. 38. As with tensile force, the net constructed from PA-381 mm panels was calculated to yield less netting volume, accounting for 70% of that of the conventional seine with the same operational dimensions. The netting volume is reduced to 80% of the prototype when the main section of the net is made up of PES-508 mm panels, in which the increased sinking depth yielded the highest values. A comparison of the economics of net construction is shown in Fig. 39. The trend in cost is proportional to the netting weight; it would be possible to save at least 84% of the netting construction cost when the purse seine with PA-381 mm webbings in the main body of the prototype is used. Inversely, the net with PES-381 mm panels represents an increase in cost of net building of 110% of the prototype. While the cost for the design with PES-508 mm panels increases to 115% of the prototype.

Table 8. Comparison of sinking depth of the prototype and the new designs of the purse seine gear with different mesh sizes in the main body for different measurement positions on the lead line as represented in Fig.32.

Position	Design type	Time (Min)						
		3	6	9	12	15	18	21
F	Prototype	75	113	127	136	144	146	140
	PA- 381 mm	80	115	128	138	145	148	143
	PA- 508 mm	83	117	130	140	147	151	147
	PES- 381mm	93	128	141	151	159	163	160
	PES- 508 mm	95	129	143	153	161	166	162
M	Prototype	62	105	120	129	136	143	148
	PA- 381 mm	70	110	124	134	140	148	150
	PA- 508 mm	80	114	128	137	143	151	155
	PES- 381mm	85	123	137	146	153	161	168
	PES- 508 mm	94	127	140	149	156	165	171
E	Prototype	63	86	97	107	108	99	87
	PA- 381 mm	65	91	103	114	112	101	89
	PA- 508 mm	68	95	106	116	114	105	93
	PES- 381mm	74	104	116	126	124	114	108
	PES- 508 mm	78	108	121	130	126	117	112

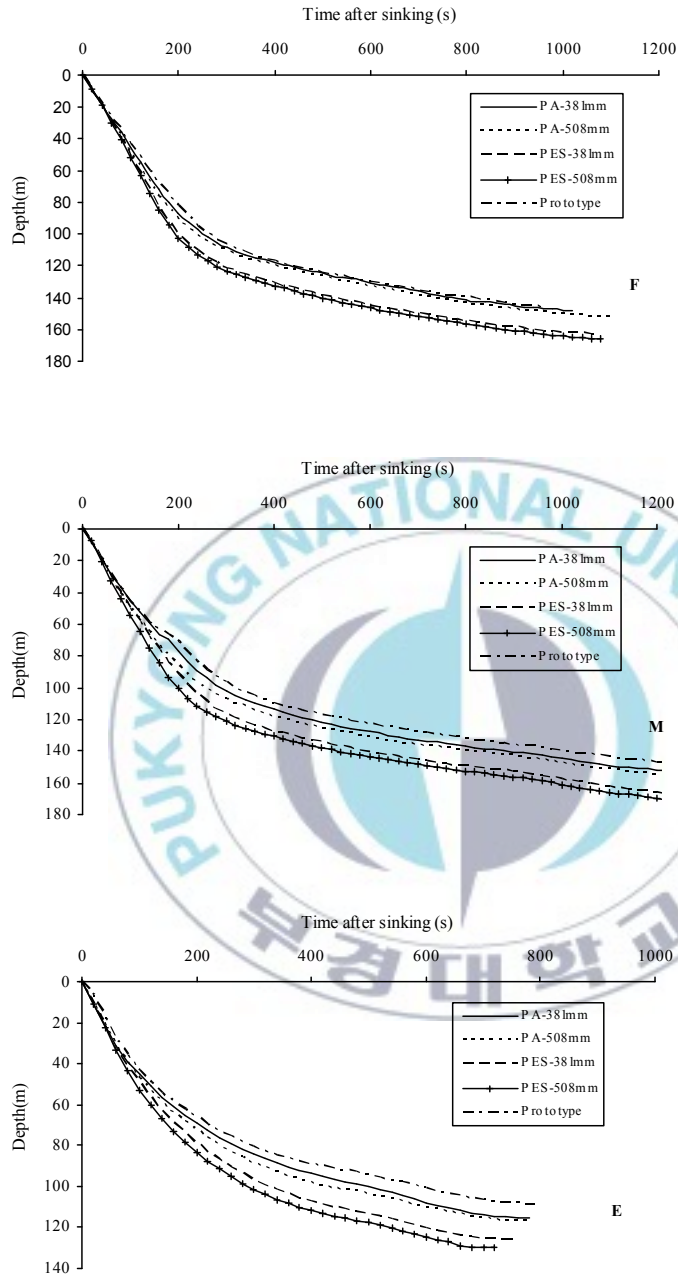


Fig.33. Comparison of the simulated sinking depth of the lead line for the prototype and the different new designs of the main body of the prototype at the same three positions (for detailed explanation, see text).

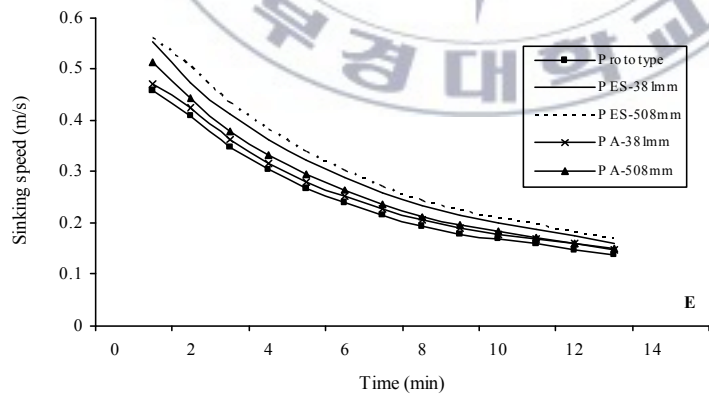
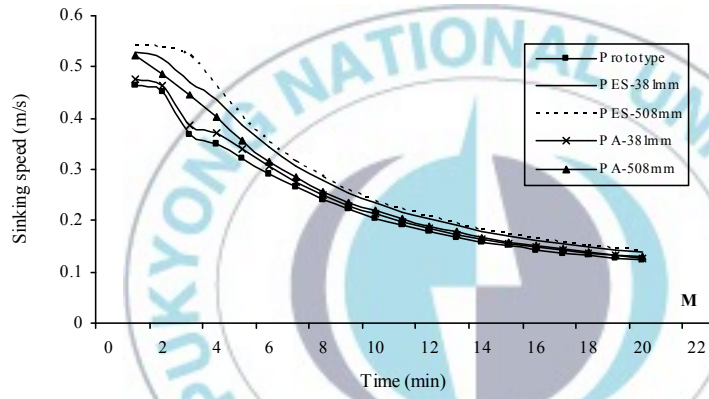
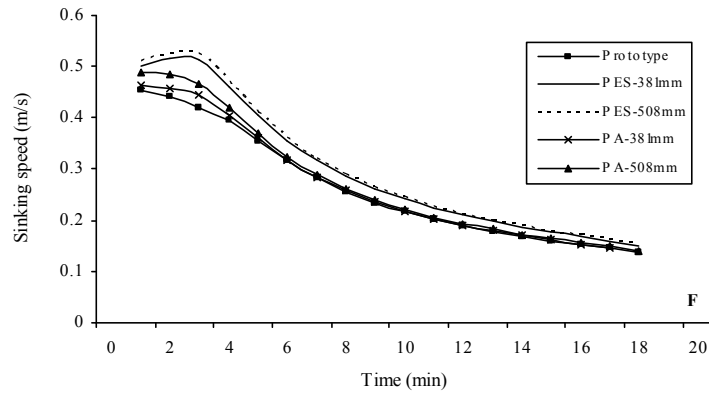


Fig.34. Simulation results for mean sinking speeds by time for the lead line of the purse seine for the prototype and the new designs at the same three positions as in Fig. 33.

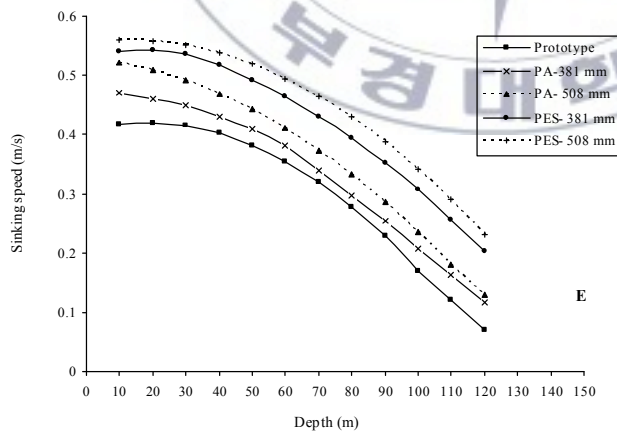
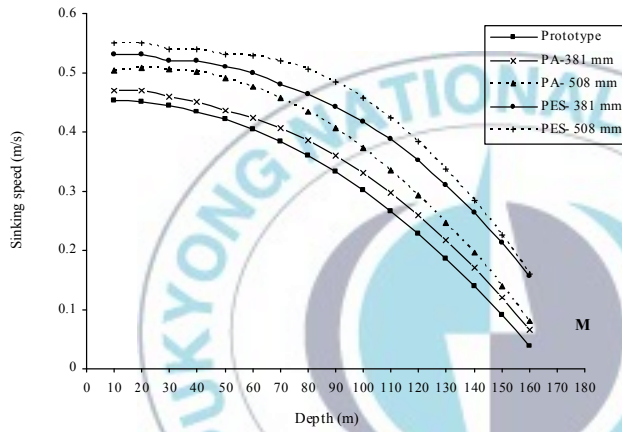
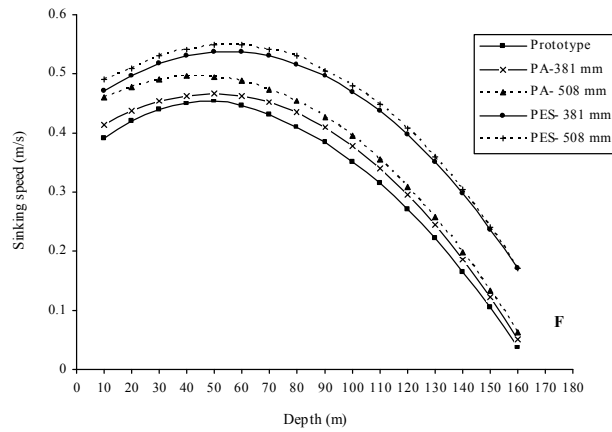


Fig.35. Simulation results for mean sinking speeds by depth of the lead line of the purse seine for prototype and the new designs at the same three positions as in Fig. 33 with the same simulation conditions.

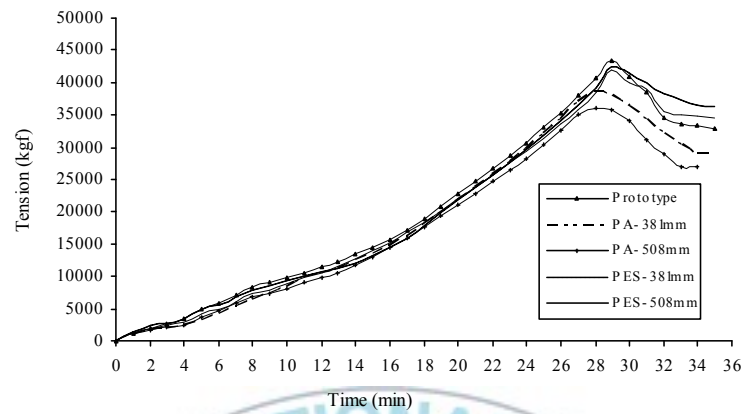


Fig. 36. The trend of tension in the purse line at both ends for the prototype and the new designs, simulated at a pursing speed of $1.3 \text{ m}^{-\text{s}}$.

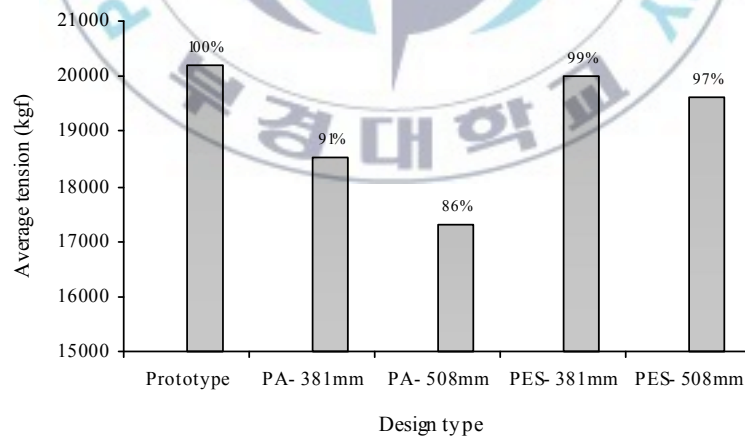


Fig.37. Average tension values of the purse line at both ends for the prototype and the new designs simulated by the same situation as in Fig. 36.

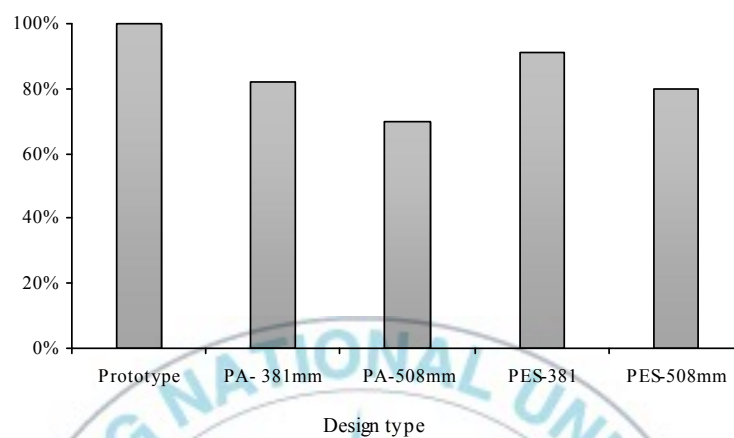


Fig.38. Netting material volume comparison for the prototype and the new designs of the net.

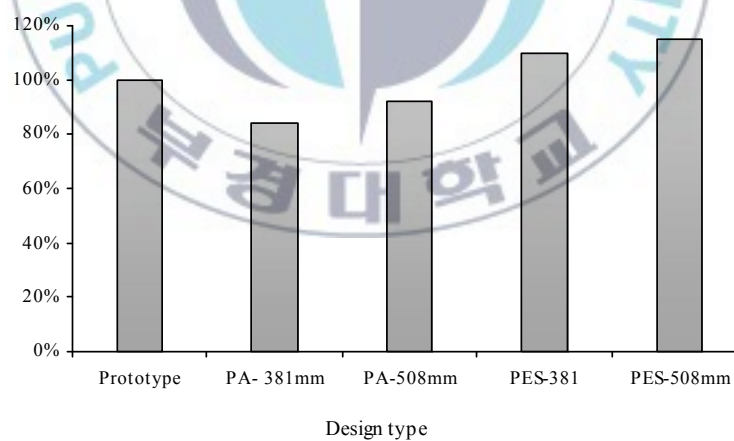
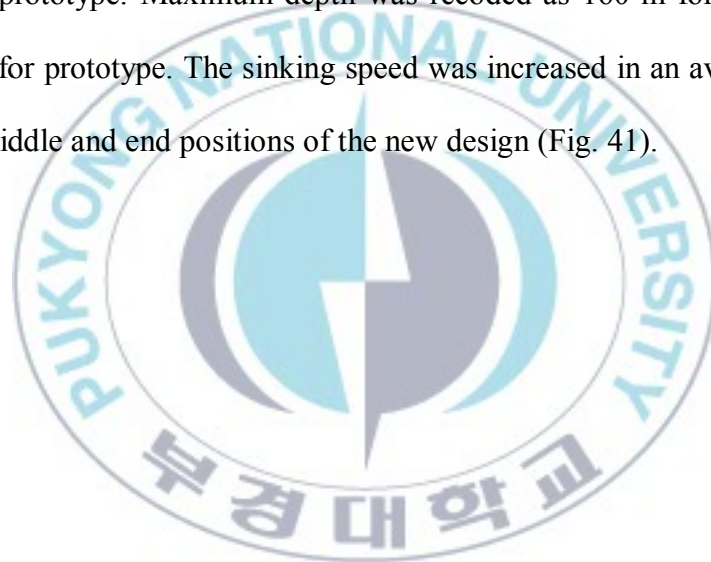


Fig.39. Comparative analysis of the net construction costs of prototype and new designs of the net.

III. Effect of sinking weight on the sinking depth

To investigate the effect of sinking weight of the lead line on the sinking depth, the prototype gear rigged by an increasing ballast of 20000 kg (more than 33% heavier than the prototype) on the lower part was simulated under the current speeds of 0.1, 0.12 and 0.28 m^s for layers 1 to 3, respectively, and a pursuing speed of 1.3 m^s. As can be seen from Fig.40 the sinking depth remarkably increased for the recorded data at three positions. The new design of the gear 5 minutes after sinking attains a depth of 116, 114 and 93 m as compared to 99, 94 and 70 m for the prototype. Maximum depth was recoded as 160 m for the new gear m in contrast of 135 m for prototype. The sinking speed was increased in an average of 14, 21 and 22% in the first, middle and end positions of the new design (Fig. 41).



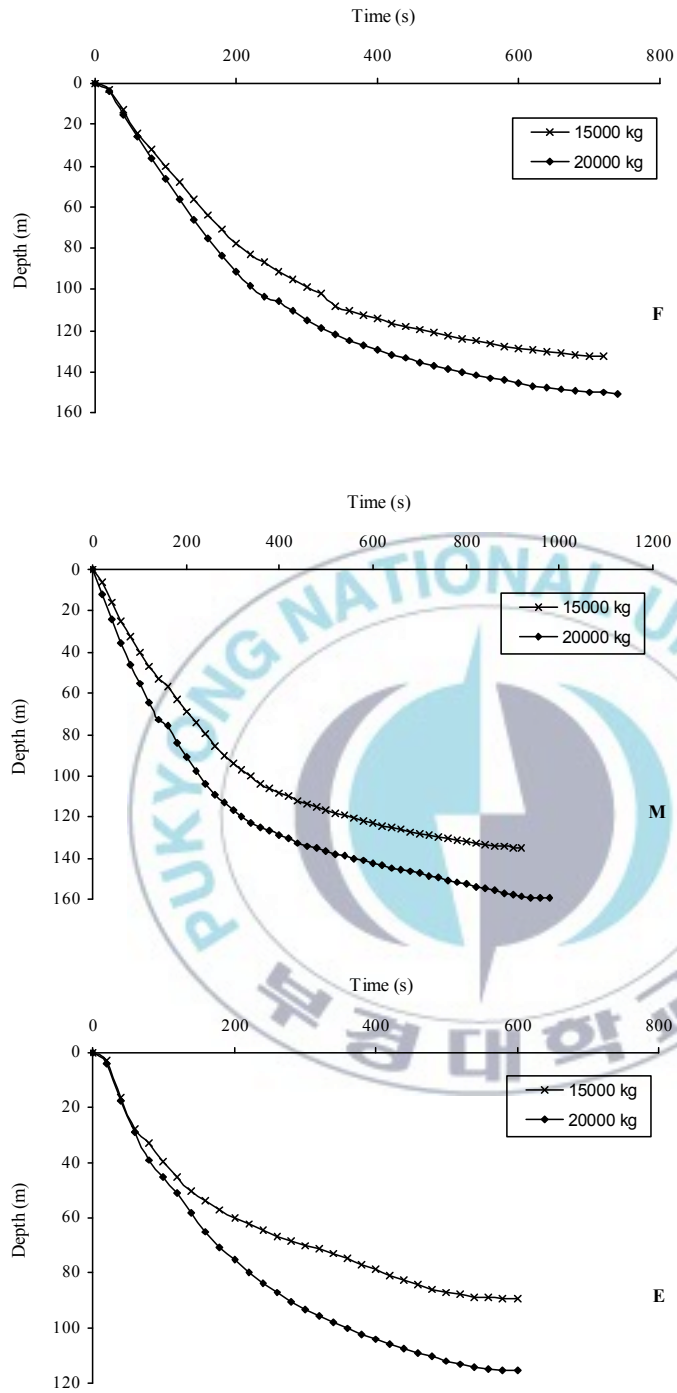


Fig.40. The simulated sinking depth of the prototype gear rigged with different sinking weights of lead line for the same three positions as in Fig. 20 (for simulation conditions, see text).

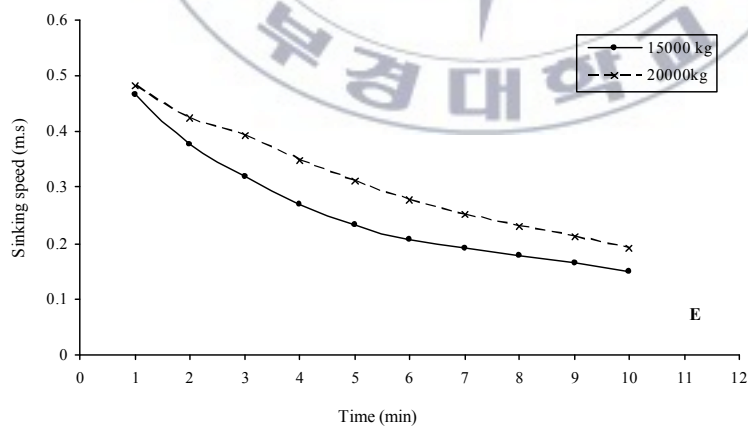
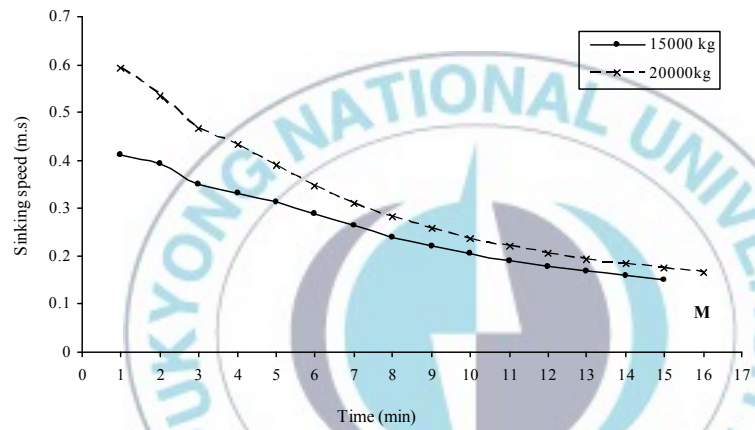
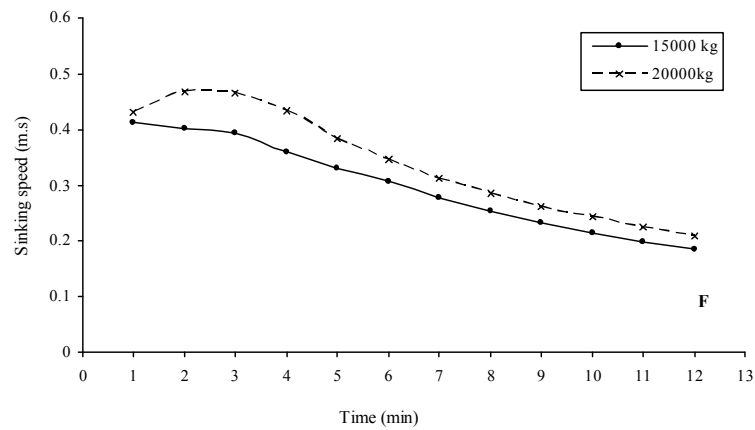


Fig.41. Average sinking speed of the prototype gear rigged with different sinking weights as simulated with conditions in Fig. 42.

IV. Effect of pursing speed on the purse seine gear performance

Pursing operation is a very complicated process and different changes are involved in the shape of the seine and its parts. Different points of the seine move at different speeds and in different directions. A considerable step forward in the study of this gear is made by the aid of the simulation. As an example of the application of this method, we give the results of an investigation of the operation of the prototype gear at pursing speeds of $1.3 \text{ m}^{-\text{s}}$ and $1.7 \text{ m}^{-\text{s}}$. The gear was simulated under the current speeds of 0.12, 0.13 and $0.27 \text{ m}^{-\text{s}}$ for the three layers of water, respectively. Fig. 42 shows the time after pursing against the depth of the central part of the lead line and the float line under the different pursing speeds. The solid lines with filled symbols show the trajectory of the lead lines for the two cases of pursing speeds, while the dotted lines with empty symbols represent the track of the float lines of the two conditions. In the case of pursing speed $1.3 \text{ m}^{-\text{s}}$, the float line moves along the surface as the operation goes forward, and there is an excess buoyancy force so that the force submerging the float line does not exceed the buoyancy one. The force applied to the entire seine increases gradually which equals a maximum value of 43000 kgf acting on the purse line (Fig. 43). As for pursing speed $1.7 \text{ m}^{-\text{s}}$, the float line is submerged 15 min after pursing and reaches to a depth of around 10 m in 7 min. At this time, the tension of purse line is measured at 46000 kgf. The line floats to surface after 1 min when there is enough buoyancy force to hold the float line at surface. This coincides with a reduction in tension as recorded to 44000 kgf. Comparison of the average tension between the two cases of pursing speeds indicates an increase value of 13% when we use the pursing speed of $1.7 \text{ m}^{-\text{s}}$ (Fig. 44).

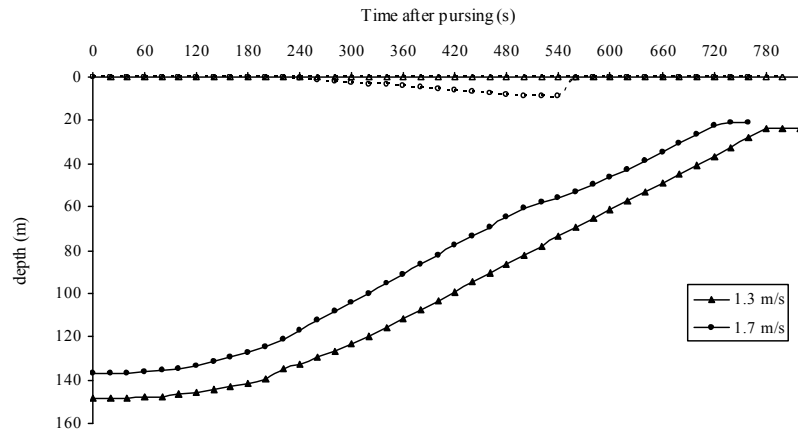


Fig.42. Positions in depth of the central part of the lead line (solid lines with filed symbols) and the float line (dotted lines with empty symbols) of the prototype when simulated under different pursing speeds.

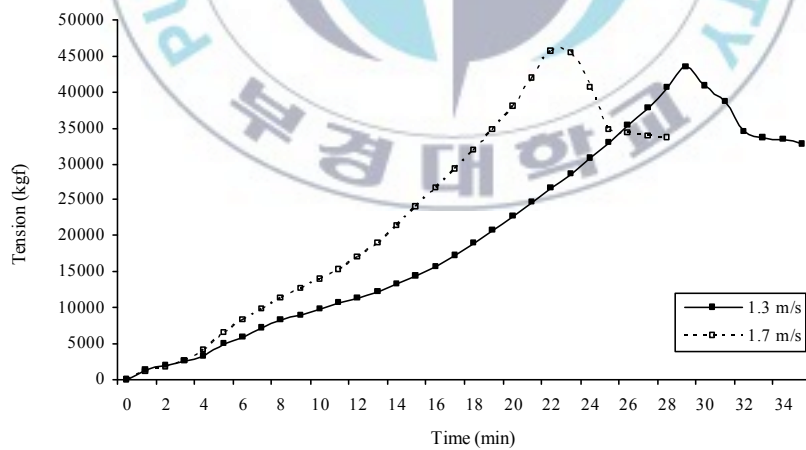


Fig.43. The trend of tension for the prototype gear recorded by the numerical method at different pursing speeds the same as in Fig. 42.

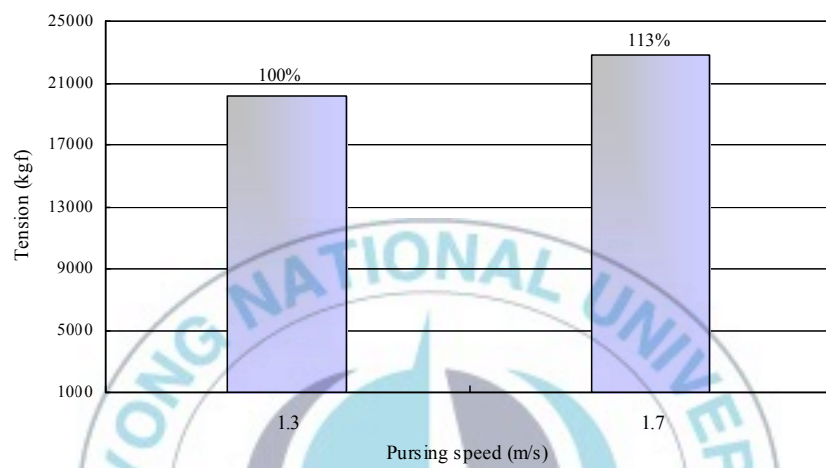


Fig.44. Comparison of the average tension values for the prototype gear simulated under the conditions in Fig. 43.

V. Discussion

Comparing the sinking depth associated with different net designs, we see that nets with larger meshed-panels of polyester netting are superior in two ways; higher sinking speed and less tension resulting from the lower resistance force.

Results from simulation on sinking depth of different new purse seine designs show that the mesh size and netting material together considerably influence on the operating depth of the net. Our results show that a purse seine of 381mm-meshed panels composed of polyester material attains a maximum depth approximately 14% greater than that attained by the comparable prototype. The comparable value for the design of PES-508 mm net is 16%, say, no significant difference is observed between the two new designs for sinking depth. Such an increased depth was recorded at 1% and 5% for the new designs of PA-381 mm and PA-508 mm respectively.

Although higher sinking speed of the larger mesh sizes would be an advantage, such an issue of escaping the fish through the meshes is another strategy to be considered when selecting any appropriate mesh size. Such a risk can be more emphasized during pursuing, as the fish schools are expected to escape away the net when they encounter the netting wall being shot.

It appears that it is also possible to increase lead weights accordingly, if any new design of the net is operated under the same tensile condition with that of prototype. Using a seine with a higher sinking speed would lessen the need to wait to begin pursuing to ensure that the net has settled adequately and would reduce the possibility of fish escaping under the lead line (Iitaka, 1964). Even so, seines using webbing of low resistance with heavy materials show fairly good sinking speeds under the current conditions (Kanagaya, 1971b). It is advisable that

the netting between both the lead lines be positioned under the school as quickly as possible to close the gap from below, through which the school is more likely to escape under the vessel. The use of large meshes that act as herding net in the last part near the lead line is therefore advantageous (Misund, 1992). There is an evidence of bigger catches of tuna purse seine when the net sinks at higher hanging depth (Inada *et al.*, 1997).

Improvement in sinking depth of the purse seine can also be obtained by a change in mesh geometry as argued by Beltestad (1981) during experiments with hexagonal meshes (H-net) in which the H-net had higher sinking speed compared with the conventional net of rhombic meshes (F-net).

The sudden change in tension in the purse line during the early stage of pursing is undesirable and leads to entanglement. This disadvantage can be somewhat lessened by using nets with large-meshed panels. The decreased bulk and weight of the large-meshed sections of net require less powerful purse winches and smaller power blocks, and the seine maintains a good operative shape even during high tidal currents (Beltestad, 1981). Under the same conditions of tension as with the prototype, larger nets can be used to increase the efficiency of the catches considering the space from the netting volume required on the aft part of the vessel deck for stacking the net. If we use the seine of PES-381 mm netting, longer net can be used, considering that this kind of net occupy approximately 90% of the netting space on the deck in comparison to that of prototype, regardless to the comparative analysis of tensile force.

The proposed designs provide some alternatives to the potential problem of failed sets that frequently occurs with the present design. A favorable design is involved in the subjective decision by the designers. It can be chosen by considering the desirable results from the

sinking depth and from the retaining of the catch properties by the large-meshed panels, although economic issue as net building cost can be regarded as an optional parameter.

The numerical method outlined here has been shown to be suitable for evaluating changes purse seine gear and should meet the demands of the designers for prejudgment of newly designed nets before their use in actual fishing operations. Further improvement of the numerical method is currently being pursued.

The pattern of changes in net tension is somewhat different from that described by Fridman (1973) and Machii and Nose (1990b); these authors mention a fairly flat trend in tension of the purse line for some time after equilibrium is reached between the resistance of the seine, the tension of the purse line and the weight of the lead line. The translatory motion occurs before the tension attains its peak and is simultaneous with deformation of the whole wall of the net and the attainment of a curvilinear shape as the seine moves to the center of the encircled area. The results of measurements of the pursing speed V and winch power N (Fig. 45) carried out at five times are described by linear reduction for pursing speed in the second phase when the pull S is almost constant and the purse line attains equilibrium. At the end, when the force in the purse line S strongly increases, pursing velocity continues to decrease and the winch power remains constant due to a balance between the tension and pursing speed.

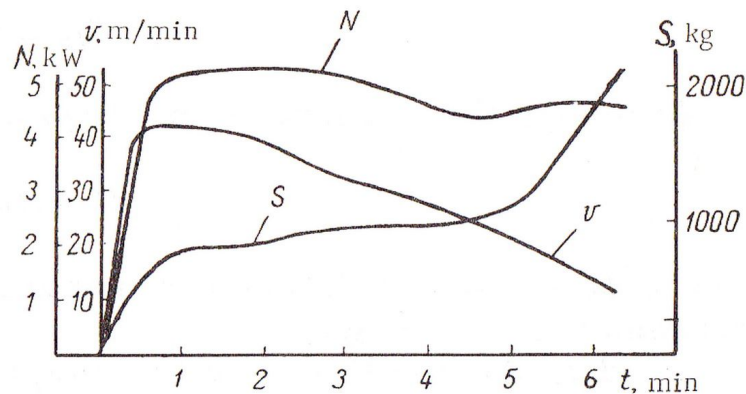


Fig.45. Mean values of tension S in the purse line, speed of its movement V and power winch N during pursing. Measurements carried out at five times from a typical anchovy purse seine of 400×75 m (after Fridman, 1973).

Since the sinking speed of the seine is proportional to the square root of the apparent lead line weight (Iitaka, 1971), it would be appropriate to use higher values of the weight to sink the seine as quickly as possible to its full depth in preventing the fish escape. But this advantage is limited by the gear damage, strain on the hauling equipment and other handling problems. Accordingly, measurements of the tension by the simulation enable us to decide upon any magnitude of the sinking weight to be proper to the operational condition.

The results from Fig. 42 make it possible to draw conclusion on the relationship between the forces exerted on the net:

1. if a change in the type of netting corresponds to a change in the resistance R by n times, and if the tracks of the float line and lead line during pursing are expected to remain

invariable, the tension of the purse line as well as the weight applied to the lead line and the buoyancy of the floats have to be increased n times. Such a change in all the forces in same ratio is equivalent to a change of the scale factor of the forces and does not follow any change in the net configuration.

2. If a change in the pursing speed v_l is in concord with a change in the resistance of the seine by m times (based on the formula $R = kAv_l^2$), no changes in the trajectory of the main lines are introduced, providing that the lead line weight and the buoyancy of the floats are changed by the same ratio of m .

It follows from the above that if there is knowledge of the arrangement of a purse seine and its satisfactory performance under given conditions, it can be used as a prototype in the design of the other purse seines.

The trajectory of the lead line also confirms the conclusion that the depth of the seine can be fully utilized only if the seine being pursed slowly and cautiously. It may be useful after shooting the net to wait some time so that the seine can sink to its full depth without entanglement of the webbing to the purse line with consideration to the fact that the seine is experienced by less tension for the lower pursing speed. In practice, however, the main intention is to accelerate the progress to prevent the encircled school from escaping. As a consequence, the seine sweeps a smaller volume of water than that corresponds to its dimensions.

Chapter 5

A preliminary research on behaviour of tuna fish schools

to purse seining process

I. Introduction

Purse seine as an active fishing is the most effective fishing gear among the other pelagic seines so that the swimming behaviour of the schools is reflected by the gear designed to the particular species. In this respect, the purse seine structure in terms of dimensional, material and rigging properties required to conform to the salient features of the swimming behaviour of the fish school; its possible movements in horizontal and vertical routs in relation to the relative distance to the purse seine.

The purse seine with longer and deeper dimension is designed properly to catch the faster swimming schools. When the net setting ends we must ensure the timely vertical sinking speed of the net to prevent escape of the school from the encircled area.

The active response of the foraging schools of pelagic fish such as swimming speed and movement pattern to various stimulants is one of the main factors to be considered when conducting purse seining. In this regard, tuna with fast -swimming speed is of major importance. With their swimming speed, they can escape the fencing net under the lead line or changing their direction.

Information on the swimming behaviour of tuna schools during purse seining process is rarely found as the lack of the insufficient observation instruments and the difficulties in recording the required data. Recently, mutli-beam, true motion sonars are deployed on board purse seiners to display the horizontal movements of the schools as distinct high intensity spots. The units are identified clearly with definite extent and rather higher densities, when

the schools exhibit synchronized swimming and they can be distinguished in numbers (Misund, 1993). When the schools are not uniform in structure, they are scattered on visually.

The purpose of the chapter is to describe the findings from a short research on the swimming behaviour of skipjack fish schools in reaction to vessel and operating gear as stimuli.

II. Field observation

During sinking depth measurements of the experimental purse seine, there has been an opportunity to record the horizontal positions of the skipjack schools from some possible sets with the purpose of preliminary report on the reaction of fish schools to the net.

Recording was made from scanning sonar (Furuno-FSV24) on board the vessel. The movement of the school was tracked in relative to the heading of the vessel in 1 min. To do this, the horizontal positions of the central schools were measured by the sonar radius circle on a sheet of transparency film and then they converted from the relative coordinates into the real horizontal positions.

The school size (visually approximated by the fishing master) per set differed considerably, ranging from 30 tons to around 100 tons, with majority being approximately 20-30 tons as shown in Table 9. From the 8 settings, the results revealed that around 4 sets (50%) led to failed catch owing to the escape of capture under the net during shooting or pursing operation, but mostly came from shooting. Fig. 46 indicates representatives of the escape under the lead line for both shooting and pursing operations. The average distance of the school center to the vessel was 240 ± 120 m with mean swimming speed of 1.83 ± 0.28 m^s.

It is evident in the figure (Fig. 46a), that during shooting the school avoided the vessel with swimming out under the lead line approximately in opposite direction to the vessel. As for pursing case (Fig. 46b), the school swims nearly parallel to the vessel heading during shooting, but when pursing starts the fish performs scaring behaviour and come in contact with the netting wall. The school escaped the capture as the fish fled under the lead line. Fig. 47 shows capture situation of the skipjack school during pursing. The swimming speed for the setting was estimated to be $1.5 \text{ m} \cdot \text{s}^{-1}$ with a distance of 383 m from the school to the vessel.



Table 9: Characteristics of catch of the skipjack school as observed in capture and escape status (the catch size visually approximated by the fishing master).

Type	Shooting course	Shooting period	Location (Lat & Long)	Catch (ton)	Remarks
Captured	170°	11:20 – 11:30 am	01:40 N , 141:20 E	100	
	190 °	14:30 – 14:36 pm	00:39 N , 146:18 E	30	
	335 °	10:30 – 10: 34 am	00:46 N , 146:18 E	30	
	245 °	13:20 – 13: 27 pm	01:16 N , 140:39 E	50	
Escape	210 °	16:45 – 16: 53 pm	01:07 N , 142:30 E	50	During pursuing
	50 °	15:20 – 15: 27 pm	01:24 N , 140:42 E	30	During shooting under the net
	115 °	17:15 – 17: 21 pm	01:42 N , 141:22 E	30	During shooting under the net
	130 °	11:00 – 11:07 am	01:15 N , 140:40 E	100	During shooting avoiding the vessel



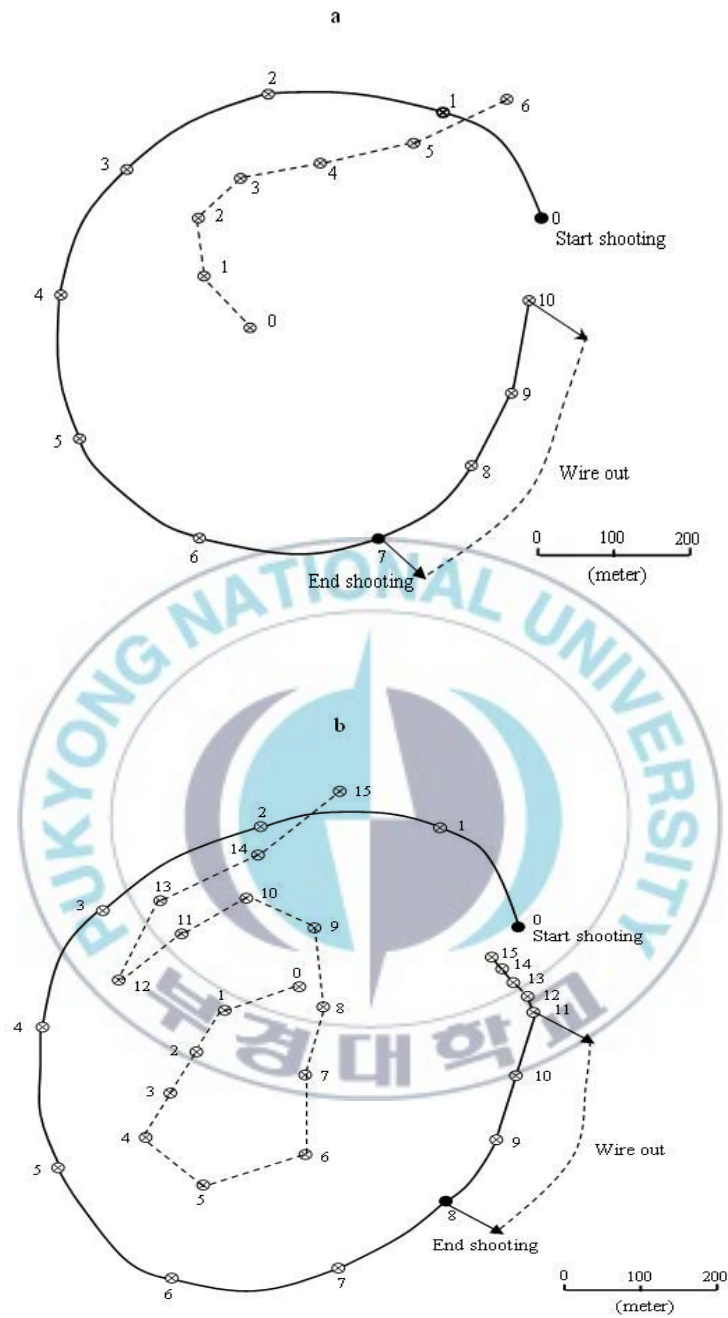


Fig.46. Horizontal movement of skipjack as centers of school in purse seine capture situations. School of 30 t escape under the lead line (circle and dotted line) in relation to net setting (circle and solid line) during shooting (a). School of 50 t escape under lead line during pursing (b). Similar numbers refer to the track of the school and vessel simultaneously.

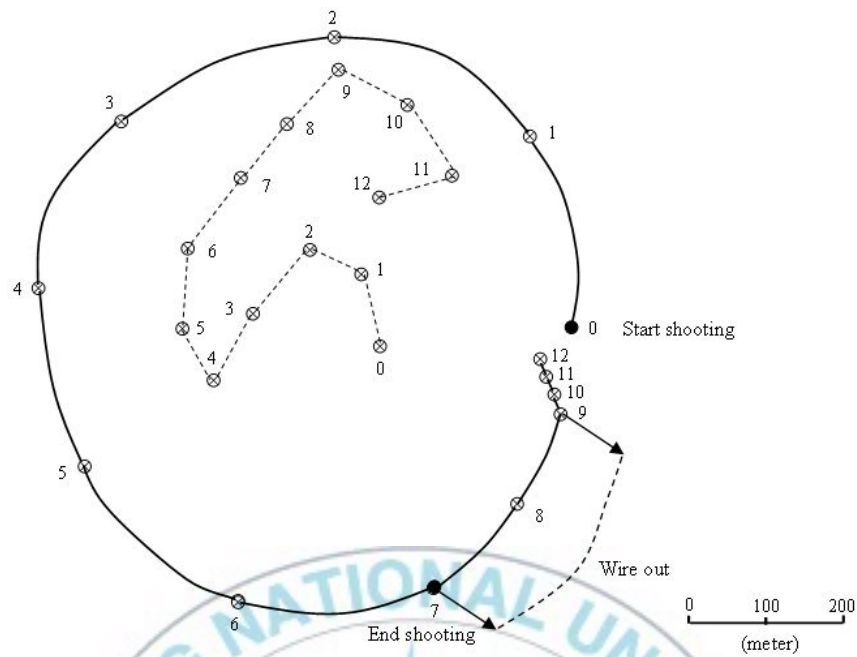


Fig.47. Horizontal movement of skipjack as centers of school in purse seine capture situations when school of 50 t captured (circle and dotted line) in relation to net setting (circle and solid line) during pursing. Similar numbers refer to the track of the school and vessel simultaneously.

III. Discussion

Successful purse seining is very dependent on a “friendly” fish behaviour so that the fish must be calm, not moving at high speed, and must remain in a dense school near the surface. In that case the seine is set parallel to the direction of the fish movement and fairly far ahead of the school. Scaring behavior of the fish school during purse seining process may be involved in both visual and hearing stimuli from the vessel and the seine (Olsen, 1971).

There are frequent examples of temporary scaring of fish school in reaction to the noise from the seiner in which there is a short time interval between a scared condition and apparent relaxation in a fish school. The reactive behavior of the fish is critical in the low frequency components of vessel as it corresponds closely to the rather narrow hearing range of the teleost fishes (Olsen, 1971).

Various contributing sources are responsible for the noise pattern from the vessel, depending on the operation mode, such as changes in engine revolutions, in the pitch of the propeller and the rudder position. Such a case can be observed frequently in purse seine operation where the vessels sudden change in its pitch and speed of propeller when starting to shoot the purse seine which probably explains the avoidance behaviour of the fish schools during shooting. By above consideration, many fishermen have improved their net setting strategy by changing the propeller and to keep the pitch as constant as practical.

The vessel-generated sound seems to be directive while lobes of higher intensity are produced to the sides with sound of minimum intensity in the front of the vessel (Urlick, 1967. In: Fernö and Olsen, 1994). Such forward-sideways-forward movements of the schools in purse seine and pelagic trawling are apparently explained by the fact that very low frequencies (< 50 Hz)

dominated ahead of the vessel and the schools direct themselves into the position with lower sound stimulation, while distribution of the medium frequencies (50-100 Hz) dominated athwartships makes the schools to behave the sideways avoidance (Engås, 1991. In: Fernö and Olsen, 1994). There is clearly evidence of reaction of fish schools to the circling purse seiners. In a situation where the schools are surrounded during pursuing they are guided in an inner and get closed to the net due to the quit steep sound from the side of the seiner (Maniwa, 1971).

The noise field around the net may be generated when the leads are run overboard and by the purse line as it freely runs through the purse rings. The tendency of the school away from the seine and to descend the water during shooting may be explained by such sudden changes in field noise (Misund, 1992). Rapid swimming schools like tuna are difficult to encircle and some times the attempts failed by escaping the schools under the sinking net wall (Olsen, 1971). In situation where the schools are encircled the consequence of the purse sine capture relied on the swimming behaviour of the schools during pursuing process. During the process, as the netting wall is being closed, the fish may be herded to the lower part of purse seine (Misund, 1993). Often a school, which has descended below the seine, avoids it and appears on the surface again. On some occasions, however, the schools may escape under the noisy vessel as the lead line rises to the surface (Misund, 1993). Escape of capture under the noisy vessel during pursuing seems to be explained strongly by the visual stimulus from the gear than the vessel-and gear-generated sound stimuli (Wardle, 1983, 1993. In: Fernö and Olsen, 1994). Swimming behaviour of the enclosed schools depends on the fishing ground situation. Panic behaviour of the schools to the surface may happen as early as the pursuing operation starts or

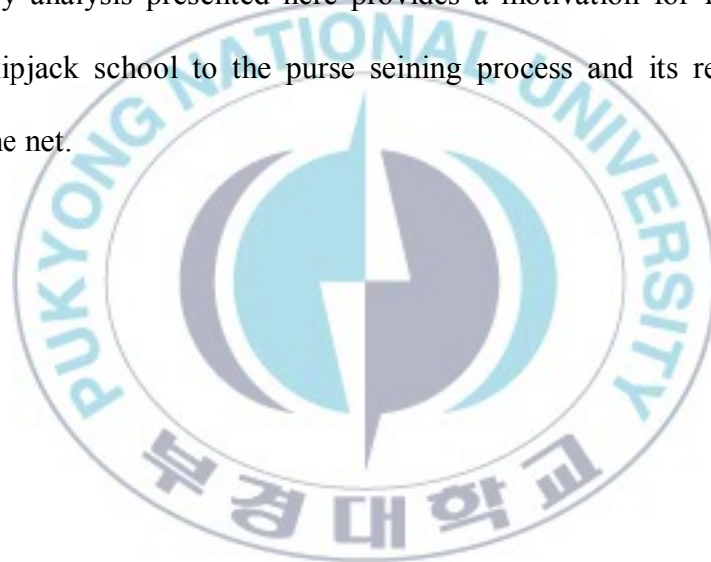
at the end of the operation when they milled around the net. This kind of behaviour may be due to the presence of predator or the hearing or visual stimuli from the net.

In our study, the avoidance behaviour of the skipjack school during pursing may be due to the idea of propagation of noise in sideways by the intensive vessel manoeuvring. It follows from the setting features of the purse seine that the considerable escape from capture that occurs during the setting and pursing process may result from the fairly low sinking speed of the commercial seine, which ranged from 0.2 to 0.6 m/s when operated with more than 200 m in stretched depth. In tagging results, the sinking speed of skipjack schools has been found to be at least 2.3 m^s during natural diving movements (Schaefer and Fuller, 2007). Success in catch for skipjack purse seining was recorded to be 50% at daytime (Shimozaki *et al.*, 1975). Kim (2007) reported the mean swimming speed of 1.7 ± 0.7 m^s for caught schools and 2.2 ± 0.8 m^s for escaped schools of skipjack, but no significantly difference observed between them. According to this, the mean distance from the edge of the skipjack school to the net was 119 ± 76 m for captured schools and 117 ± 120 m for escaped schools, but still not varied significantly. The author argued that the absence of variations between the distance of the skipjack schools to the net and swimming speed or the swimming direction is because of complex behaviour of the species. Prevailing condition such as feeding without the risk from the predators was one of the reasons was expressed. However, the maximum aerobic swimming speed of skipjack was reported to be 4.6 body lengths (BL/s) while maximum burst swimming speed is about 20 BL/s (Kim *et al.*, 2008).

The available evidence clearly suggests that the knowledge about the fish school behaviour in response to the visual and hearing stimulus from purse seine net and the vessel is

crucial and many complicated parameter are involved. From this aspect, the characteristics and usual sources of the stimulus, and also the fish school capacities in detection of the scaring sources with their reactive behaviour are precisely needed for any simulation attempts to mimic their response to the impressive parameters and to predict efficiently the capture-escape ratio for improvement in the fishing efficiency. Detailed field observations of the swimming behavior of the fish schools can help provide a better understanding of the fish responses as they encounter the netting wall.

The preliminary analysis presented here provides a motivation for further study on the reaction of the skipjack school to the purse seining process and its relationship with the sinking speed of the net.



References

- Baranov, F.I., 1976. Selected works on fishing gear. Vol. 1. Israel Program for scientific Translation, Jerusalem. pp. 456-483.
- Beltestad, A.K., 1981. Purse seines with hexagonal mesh. Southwest Fisheries Center Admin. Rep. LJ-81-12, p. 60, NOAA/NMFS, La Jolla.
- Bessonneau, J. S., Marichal, D., 1998. Study on the dynamics of submerged supple nets (application to trawls). Ocean Eng. 25 (7), 563–583.
- Delmer, T.N., Stephens, T.C., 1981. Development of a numerical simulation of purse seine fishing. Southwest Fisheries Center Admin. Rep. LJ-81 (13C), p. 126, NOAA/NMFS, La Jolla.
- Dickson, W.D., 1980. Trawl drag area and netting geometry. Institute of Fisheries Technology Research Report, Bergen, 31 pp.
- Fernö, A., Olsen, S., 1994. Marine fish behaviour in capture and abundance estimation. Fishing News Books. Ltd, Oxford. pp. 84-106.
- Fredheim, A., Faltinsen, O.M., 2003. Hydroelastic Analysis of a Fishing Net in Steady Inflow Conditions. Hydroelastic in Marine Technology, Oxford, UK, pp. 1–10.
- Fridman, A.L., 1973. Theory and design of commercial fishing gear. Israel Program for Scientific Translation, Jerusalem, pp. 145-146.
- Fridman, A.L., 1986. Calculations for fishing gear designs. Fishing News Books Ltd.
- Hue, F., Matuda, K., Tokai, T., Haruyuki, K., 1995. Dynamic analysis of midwater trawl system by a two-dimensional lumped mass method. Fish Sci. 61, 229-233

- Imai, T., 1986. Fundamental studies of the fluid dynamical resistance on the plan netting. Memories of the faculty of fisheries, Kagoshima University 35 (2), 169-253 (in Japanese).
- Inada, H., Sekine, J., Kim, H. S., Nemoto, M., Takeuchi, S., Kagoshi, Y., Yabuki, K., 1997. The influence of environmental condition on fish catches during purse seining operations for Skipjack *Katsuwonus Pelamis* and Yellowfin Tuna *Thunnus Albacares* in the western tropical pacific fishing grounds. J. Tokyo Univ. Fish. 83 (1.2), 129-138.
- Iitaka, Y., 1964. Studies on the mechanical characteristics of purse seine in relation to its fishing efficiency. PhD dissertation. Memories of the faculty of Agriculture of Kinki Univ. 2.
- Iitaka, Y., 1971. Purse seine design and construction in relation to the fish behaviour and fishing conditions. In: H. Kristjonsson (Editor), Modern Fishing Gear of the World: 3. Fishing News (Books), London, pp. 253-256.
- Konagaya, T., 1971a. Studies on the Purse Seine-III. On the Effect of Sinkers on the Performance of a Purse Seine. Bull. Jap. Soc. Scient. Fish., 37 (9), 861-865 (in Japanese).
- Konagaya, T., 1971b. Studies on the Purse Seine-V. Effects of the "Waiting Time" and the Under Water Current on the Pursing Operation. Bull. Jap. Soc. Scient. Fish., 37 (10), 939-942(in Japanese).
- Kim, S. J., Imai, T., Park., J. S., 1995. Characteristics on the Motion of the Purse Seine (1)-The Sinking behaviour of Model Purse Seine by different Netting Material. Bull. Kor. Soc. Fish. Tech., 31(4), 362-371 (in Korean).
- Kim, D.A., 1995. Flow resistance and modeling rule of fishing nets. 1. Analysis of flow resistance of bag nets. J. Koran Fish. Soc., 28 (2), 194-201 (in Korean).

- Kim, H.Y., Lee, C.W., Shin, J.K., Kim, H.S., Cha, B.J., Lee, G.H., 2007. Dynamics simulation of the behaviour of purse seine gear and sea-trial verification. *Fish. Res.* 88, 109–119.
- Kim, S. J., Imai, T., Park, J. S., 1995. Characteristics on the Motion of Purse Seine (1)- The Sinking Behaviour of the Model Purse Seine by Different Netting Material. *Bull. Korean Soc. Fish. Tech.* 31 (4), 362-371 (in Korean).
- Kim, S.J., 2004. An analysis of the sinking resistance of a purse seine. (2). In the case of a model purse seine with different netting material and sinker. *Bull. Korean Soc. Fish. Tech.* 40 (1), 29–36 (in Korean).
- Kim, Y.H., 2000. Geometry of model purse seine in relation to enclosed volume during hauling operation. *J. Fish. Sci. Tech.* 3(2), 156-162.
- Kim, Y.H., 2007. Complex Movements of Skipjack schools Based on Sonar Observations during Pelagic Purse seining. *J. Fish. Sci. Tech.* 10 (2), 220-225.
- Kim, Y.H., Park, M. C., Ha, S. W., 2008. Simulation and Three-dimensional Animations of skipjack behaviour as Capture Process during Purse seining. *J. Fish. Sci. technol.* 11 (2), 113-123.
- Kim, Y.H., Park, M.C., 2009. The simulation of the geometry of a tuna purse seine under current and drift of purse seiner. *Ocean Eng.* 36, 1080–1088.
- Lader, P.F., Enerhaug, B., Fredheim K. A., 2003. Modeling of 3D Net structures exposed to Waves and current, hydroelasticity in Marine Technology, Oxford, Uk.
- Lee, C.W., Lee, J.H., Cha, B.J., Kim, H.Y., Lee, J.H., 2005a. Physical modeling for underwater flexible systems dynamic simulation. *Ocean Eng.* 32, 331–347.

- Lee, C.W., Kim, Y. B., Lee, G.H., Choe, M.Y., Lee, M.K., Koo, K.Y 2008. Dynamic simulation of a fish cage system subjected to currents and waves. *Ocean Eng.* 35, 1521–1532.
- Lee, J.H., Lee, C.W., Cha, B.J., 2005b. Dynamic simulation of long tuna long line gear using numerical methods. *Fish Sci.* 71, 1287–1294.
- Lee, M. K., L, C. W., Song, D. H., 2007. Experiments on the hydrodynamic coefficients of netting in relation to mesh grouping. *DEMAT' 07, Contribution on the theory of fishing gears and related marine systems*, 5, 35- 44.
- Machii, T., Nose, Y., 1990a. Mechanical properties of a rectangular purse seine in a special operation. *Nippon Suisan Gakkaishi*. 56 (4), 557–562.
- Machii, T., Nose, Y., 1990b. Determination of Mechanical Properties of a Peruvian Small Purse Seine. *Nippon Suisan Gakkaishi*. 56 (4), 563–567.
- Machii, T., Nose, Y., 1992. Mechanical properties of a rectangular purse seine in ideal conditions. *Fish. Res.* 14, 261–271.
- Maniwa, Y., 1971. Effects of vessel noise in purse seining. In: H. Kristjonsson (Editor), *Modern Fishing Gear of the World: 3*. Fishing News (Books), London, pp. 294-296.
- Misund, O.A., Dickson, W., Beltestad, A.K., 1992. Optimization of purse seines by large-meshed sections and low lead weight. Theoretical considerations, sinking speed measurements and fishing trials. *Fish. Res.* 14. 305-317.
- Misund, O.A., 1992. Predictable swimming behaviour of schools in purse seine capture situations. *Fish. Res.* 14, 319-328.

- Misund, O.A., 1993. Avoidance behaviour of herring (*Clupea harengus*) and mackerel (*Scomber scombrus*) in purse seine capture situations. Fish. Res. 16. 179-194.
- Newman, J. N., 1977. Marine Hydrodynamics. MIT Press, Cambridge, MA.
- Niedzwiedz, G., Hopp, M., 1998. Rope and net calculations applied to problems in marine engineering and fisheries research. Archive of Fishery and Marine Research. 46 (2), 125-138.
- Olsen, K., 1971. influence of vessel noise on the behaviour of herring: In: H. Kristjonsson (Editor), Modern Fishing Gear of the World: 3. Fishing News (Books), London, pp. 291-294.
- Paschen, M., Winkel, H.J., 2002. Wind tunnel tests for fishing gear development-methods and limits, DEMAT 01, Contributions on the Theory of Fishing Gears and related Marine Systems, vol. 2, 29-41.
- Schaefer, k.M., Fuller, D.W., 2007. Vertical movement pattern of skipjack tuna (*Katsuwonus pelamis*) in the eastern equatorial Pacific Ocean, as revealed with archival tags. Fish. Bull., 105, 379-989.
- She, H., 1994. Calculation and configuration of the gill net. National Fishing Academic Treatises 8, 1-7, (in Chinese).
- Schlichting, H., 1968. Boundary-Layer Theory. McGraw-Hill, New York.
- Steven, C.C., Raymond, P.C., 1998. Numerical method for engineering: With programming and Software Applications. WCD/McGraw-Hill, pp. 719-744.

- Takagi, T., Shimizu, T., Suzuki, K., Hiraishi, T., Yamamoto, K., Nashimoto, K., 2004. Validity and layout of “NaLA” : a net configuration and loading analysis system. Fish. Res. 66, 235-243.
- Tsukrov, I., Eroshkin, O., Fredriksson, ., Swift, M. R., Celikkol, B., 2003. Finite element modeling of net panels using a consistent net element. Ocean Eng. 30 , 251–271.
- Vincent, B., 1999. A new generation of tools for trawls dynamic numerical solution. In Proc. Of the International workshop “DEMat 99” Rostock, Germany.
- Wan, R., Huang, W. Q., Song, X. F., Hu, F. X., Tokai, T., 2004. Statics of a gillnet placed in a uniform current. Ocean Eng. 31, 1725–1740.
- Yun-pong, Z., Yu-cheng, L., (2007). Numerical simulation of the effects of weight system on the hydrodynamic behaviour of 3-d net of gravity cage in current. J. Hydrodynamic. 19 (4), 442-452.